www.sciencemag.org/cgi/content/full/science.1258361/DC1

Supplementary Materials for

Casting inorganic structures with DNA molds

Wei Sun, Etienne Boulais, Yera Hakobyan, Wei Li Wang, Amy Guan, Mark Bathe,* Peng Yin*

*Corresponding author. E-mail: py@hms.harvard.edu (P.Y.); mark.bathe@mit.edu (M.B.)

Published 9 October 2014 on *Science* Express
DOI: 10.1126/science.1258361

This PDF file includes:

Supplementary Material I

Casting Inorganic Structures with DNA Molds

Wei Sun[1,2] Etienne Boulais[3] Yera Hakobyan[3] Wei Li Wang[1,2] Amy Guan[1] Mark Bathe[3*] Peng Yin[1,2*]

Wyss Institute for Biologically Inspired Engineering, Harvard University, Boston, MA[1]
Department of Systems Biology, Harvard Medical School, Boston, MA[2]
Department of Biological Engineering, Massachusetts Institute of Technology, Cambridge, MA[3]

E-mail address*: py@hms.harvard.edu; mark.bathe@mit.edu

Contents

List of Figures

List of Tables

S1 Summary figure

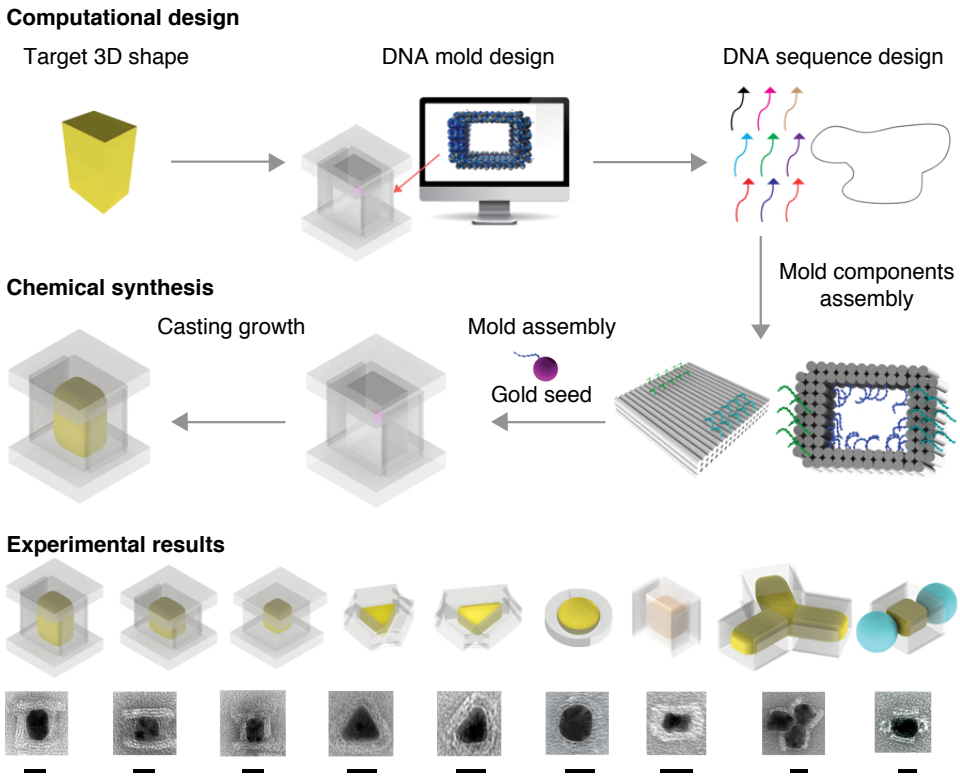

Fig. S1: **Casting metal particles with prescribed three-dimensional (3D) shapes using programmable DNA nanostructure molds.** Top, computational shape-by-design framework to encode the user-specified 3D shape of an inorganic particle in the linear sequences of DNA Middle, assembly of the mold and casting growth of the metal particle. Bottom, experimental characterization of the cast products. Top row, schematics; bottom row, TEM images. Scale bars, 20 nm.

S2 Materials and experimental methods

S2.1 DNA-decoration onto 5-nm Au seeds

Conjugation of thiolated DNA onto 5-nm gold (Au) seeds was achieved following previous reported protocol (*64*). In a typical experiment, 20 μL 2.5 μM phosphine-coated 5-nm Au seed was mixed with 0.5 μL 2 M $NaNO_3$ and 0.65 μL 100 μM thiolated DNA in 0.25$\times$ TBE buffer. The reaction solution was incubated at room temperature for 36 hours in dark. After that, the reaction solution was loaded into 1% agarose gel containing 0.5$\times$ TBE buffer. The electrophoresis was running at 95 V for 1 hour in a gel box on an ice-water bath. The purple band was recovered by pestle crushing, followed by centrifugation for 3 min at 10,000 rpm at room temperature using "Freeze 'N Squeeze" DNA gel extraction spin columns (Bio-Rad). Recovered DNA-decorated Au seeds were stored at 4 °C in dark for further use. The sequence for the thiolated DNA was: TATGAGAAGTTAGGAATGTTA-TTTTT-Thiol. Note that thiol group was modified at the 3' end of anti-handle sequence TATGAGAAGTTAGGAATGTTA via a TTTTT spacer.

S2.2 DNA mold folding

Assembly of DNA-origami molds was accomplished following previous reported protocol (*22, 23*). In a one-pot reaction, 50 nM scaffold strands (mutated P8064) derived from M13 bacteriophage was mixed with 250 nM of every staple strands (Bioneer Inc. or IDTDNA Inc.) in a buffer including 5 mM Tris, 1 mM EDTA, 16 mM $MgCl_2$ (pH 8), and subjected to a thermal-annealing ramp that cooled from 80 °C to 65 °C over 75 minutes and then cooled from 64 °C to 24 °C over 70 hours.

S2.3 Gel purification

40 μL of folding products were mixed with 10 μL of glycerol, and loaded into 1.5% agarose gel pre-stained with Sybr Safe containing 0.5$\times$ TBE and 10 mM $Mg(NO_3)_2$. The electrophoresis was running at 75 V for three hours in a gel box incubated in an

ice-water bath. Monomer band was excised and origami was recovered by pestle crushing, followed by centrifugation for 3 min at 6000 rpm at room temperature using "Freeze 'N Squeeze" DNA gel extraction spin columns (Bio-Rad). Recovered DNA molds were stored at 4 °C for further use.

S2.4 Seed decoration

Purified DNA molds were mixed with 50 mM $NaNO_3$ and 10 nM purified 5-nm Au-DNA conjugates, and incubating at 35 °C for 16 hours, followed by slowly annealing to 24 °C over 3 hours. The reaction buffer was then purified using S300 spin column (GE healthcare) by centrifugation for 2 min at 750 g at room temperature to remove excessive Au-DNA conjugates.

S2.5 Metal growth

For silver (Ag) growth, to 5 μL purified seed-decorated DNA molds, 0.5 μL 14 mM $AgNO_3$ and 0.5 μL 20 mM ascorbic acid were added at room temperature, and pipetted for 30 times for mixing. Then the reaction solution was kept in dark at room temperature for 4 min to 20 min. For Au growth, 0.5 μL 14 mM $HAuCl_4$ and 0.5 μL 20 mM ascorbic acid were added to 5 μL purified seed-decorated DNA molds in 0.5× TB buffer at room temperature, and pipetted for 30 times for mixing. Then the reaction solution was kept in dark at room temperature from 20 min to 2 hours.

S2.6 Transmission electron microscopy

3.5 μL particles were adsorbed onto glow discharged carbon-coated TEM grids for 2 min and then wiped away, followed by staining using 3.5 μL 2% aqueous uranyl formate solution containing 25 mM NaOH for 45 sec. Imaging was performed using a JEOL 1400 operated at 80 kV. High-resolution TEM and electron diffraction were acquired using a JEOL 2010 with FEG operated at 200 kV for unstained nanoparticle (NP) sample deposited onto amorphous carbon film.

S2.7 Electron energy loss spectrum

The low loss electron energy loss spectrum (EELS) data were collected with TEAM I at the Lawrence Berkeley National Lab, a Monochromated TEM operated at 80 kV. The EELS data were collected in the TEM mode under vacuum for an unstained NP sample deposited onto amorphous carbon film.

S3 Mechanical property simulation

S3.1 Methods

S3.1.1 CanDo

The mechanical response of DNA molds is modeled using the finite element method, based on the previously published model CanDo (*31, 32*). Briefly, CanDo treats B-form DNA as a homogeneous elastic rod with isotropic bending stiffness, 0.34 nm rise per base pair and 2.25 nm diameter. Two-node isotropic elastic beam finite elements are used to compute mechanical properties using the experimentally measured bending stiffness of B-form DNA of 230 pN·nm^2, axial stretching stiffness of 1100 pN, and torsional stiffness of 460 pN·nm^2. Single-stranded DNA connecting double-helical domains are modeled as entropic springs using the wormlike chain model and nicks in the backbone of double-stranded DNA are modeled using a local reduction in the bending and torsional stiffness of DNA by a factor of 100. Double-stranded anti-parallel crossovers used to connect neighboring helices are modeled as rigid constraints between neighboring helices. In this approximation, neighboring conjoined helices are still fully free to twist, bend, and stretch or compress.

S3.1.2 Deformation analysis

Mechanical deformations of the DNA molds in response to loading are performed using the commercial finite element software ADINA (ADINA R&D, Inc., Watertown, MA). The ground-state or equilibrium solution structure computed by CanDo is used as the initial configuration. We do not model the specific growth process of the NP itself, which could be incorporated in future work using a chemical physical model that accounts for the solution phase concentration of metal (*69, 70*), but rather investigate two types of loading applying to model distinct types of mechanical loading from the mold onto a given growing NP, namely point contact or distributed contact. In both nonlinear mechanical deformation analyses, the full Newton method is used within nonlinear statics analyses.

Point-contact model

In the first model, termed point-contact model, growing NPs are assumed to contact a single pair of directly opposing points of the DNA mold. In this scenario, equal and opposite point forces are applied to the DNA mold and its nonlinear deformation is computed (fig. S2).

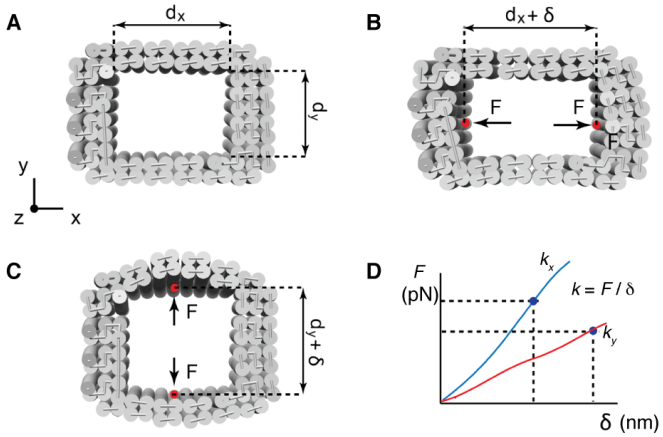

Fig. S2: **Loading via point-contact model to opposing faces of the DNA mold**. (A) Overall inner cavity dimensions are provided by the 3D solution structure computed using CanDo. (B) and (C) two opposite central nodes along a given direction, from inner surfaces of the nanostructure, are chosen as shown. Equal and opposite forces are applied incrementally to the two opposing finite element nodes belonging to inner DNA helices and the resulting deformed structure is simulated. (D) A schematics of a force-deformation response. Here F is the total force acting on one side of the two opposing surfaces and δ is the displacement between the central nodes as shown. The lateral and transverse stiffnesses k were calculated assuming linear response, which was found in all cuboids designed, to be a reasonable approximation to the actual computed nonlinear force-displacement relation, F versus δ, for small values of δ.

Distributed-contact model

In the second model, termed distributed-contact model, growing NPs are assumed to fully fill the mold cavity so that the NP applies a uniformly distributed force along opposing interior walls of the cavity of the mold (fig. S3).

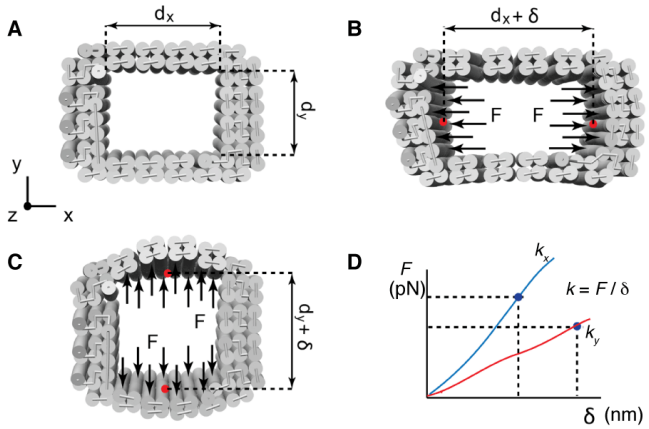

Fig. S3: **Loading via distributed-contact model to opposing faces of the DNA mold**. (A) Overall inner cavity dimensions are provided by the 3D solution structure computed using CanDo. (B) and (C) two opposite central nodes along a given direction, from inner surfaces of the nanostructure, are chosen as shown. Equal and opposite forces are applied incrementally to all opposing in one direction finite element nodes belonging to inner DNA helices and the resulting deformed structure is computed. (D) A schematics of a force-deformation response. Here F is the total force acting on one side of the two opposing surfaces and δ is the displacement between the central nodes as shown. The lateral and transverse stiffnesses k were calculated assuming linear response, which was found in all cuboids designed, to be a reasonable approximation to the actual computed nonlinear force-displacement relation, F versus δ, for small values of δ.

S3.1.3 Normal mode analysis

Normal mode analysis (NMA) is performed extensively in the analysis of protein dynamics to compute their lowest energy modes of deformation (*62, 63*). While each of these NMs is a specific characteristic shape that the molecular structure can adopt, in general, a linear deformation in response to external loading will result in an overall deformation that is a linear combination of a subset of NMs, where lowest NMs are preferred because they require the least amount of mechanical free energy to reach a given state of deformation.

S3.2 Results

S3.2.1 Stiffness of cuboid DNA molds

Point contact	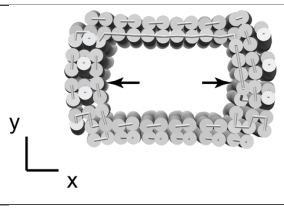	16.9 pN/nm	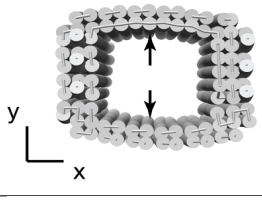	10.2 pN/nm
Distributed contact	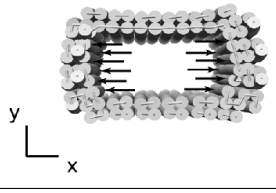	29.8 pN/nm	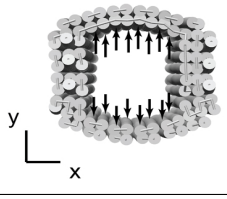	19.1 pN/nm

Table S1: Stiffness values for DNA mold with 21 nm by 16 nm by 30 nm cuboid cavity in Fig. 3B.

Point contact	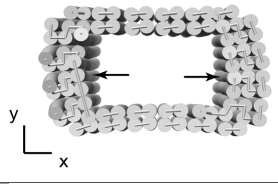	15.1 pN/nm	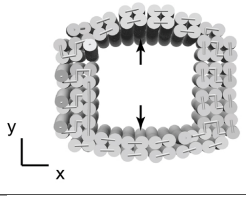	12.4 pN/nm
Distributed contact	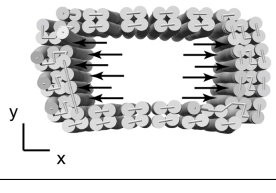	29.4 pN/nm	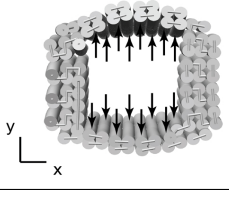	18.6 pN/nm

Table S2: Stiffness values for DNA mold with 21 nm by 16 nm by 20 nm cuboid cavity in Fig. 3C.

Point contact	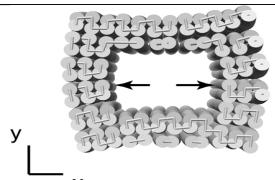	14.1 pN/nm	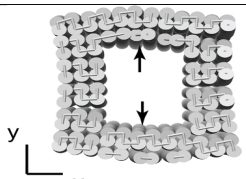	15.9 pN/nm
Distributed contact	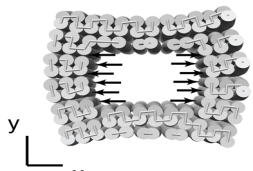	23.7 pN/nm	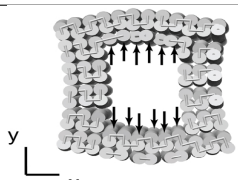	25.0 pN/nm

Table S3: Stiffness values for DNA mold with 16 nm by 16 nm by 20 nm cuboid cavity in Fig. 3D.

Point contact	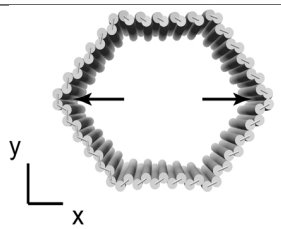	1.83 pN/nm	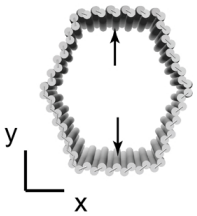	2.01 pN/nm

Table S4: Stiffness values for DNA mold with single layer hexagonal cavity in fig. S67. The force-displacement relation is slightly non-linear here. Displacements considered for stiffness computations are below 4 nm. Stiffness is averaged over the displacement range.

Point contact	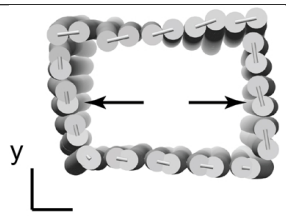	2.48 pN/nm	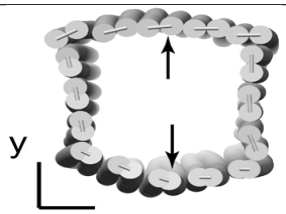	1.93 pN/nm

Table S5: Stiffness values for DNA mold with single layer square cavity of 21 nm by 16 nm by 30 nm. The force-displacement relation is slightly non-linear here. Displacements considered for stiffness computations are below 4 nm. Stiffness is averaged over the displacement range.

S3.2.2 NMA of DNA molds

The simulated lowest energy modes of deformation, obtained by CanDo model, were identified on the experimental TEM images (see fig. S61 for TEM images of NMs for DNA barrel with 21 nm by 16 nm by 30 nm cuboid cavity, and fig. S27 for TEM images of NMs for DNA barrel with 16 nm by 16 nm by 20 nm cuboid cavity).

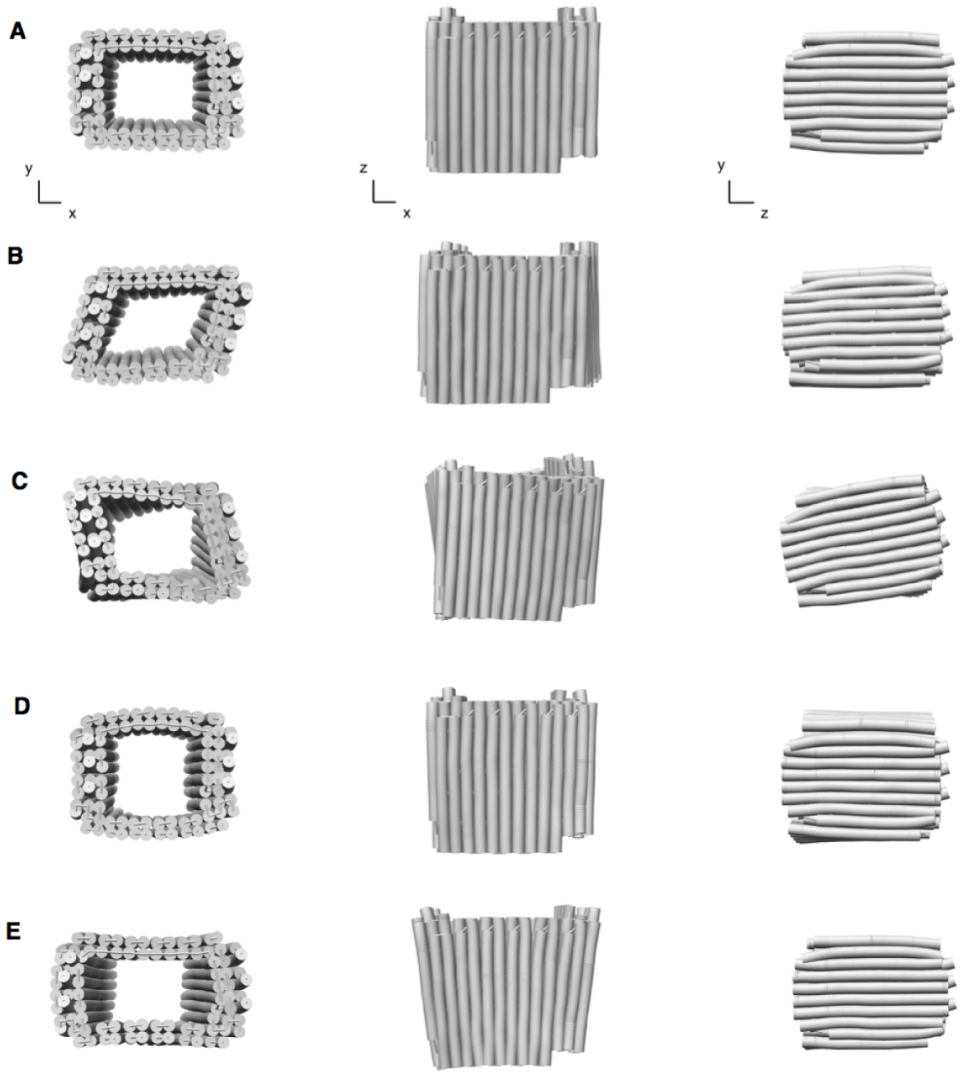

Fig. S4: **NMA for DNA mold with 21 nm by 16 nm by 30 nm cuboid cavity in Fig. 3B**. (A) Ground-state solution conformation and (B)-(E) four lowest energy modes of deformation at room temperature. NM displacements are magnified by a factor of five over their values corresponding to T =298 K.

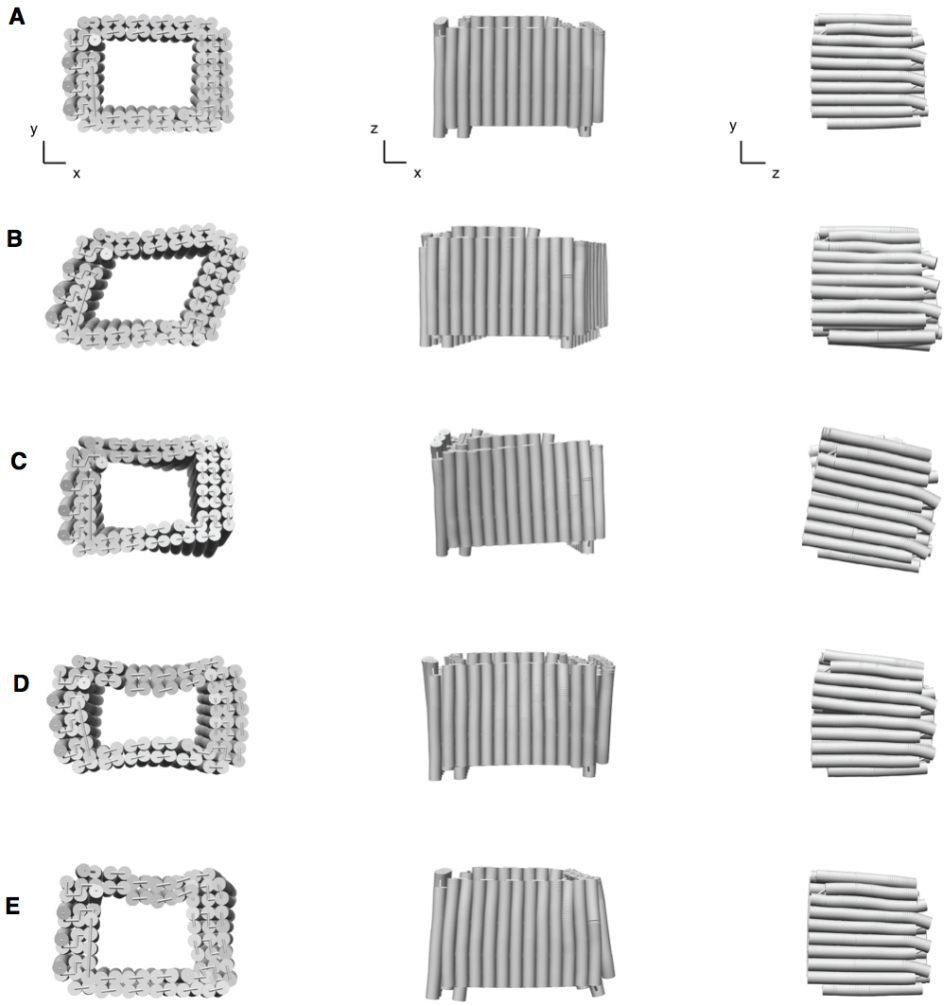

Fig. S5: **NMA for DNA mold with 21 nm by 16 nm by 20 nm cuboid cavity in Fig. 3C**. (A) Ground-state solution conformation and (B)-(E) four lowest energy modes of deformation at room temperature. NM displacements are magnified by a factor of five over their values corresponding to T =298 K.

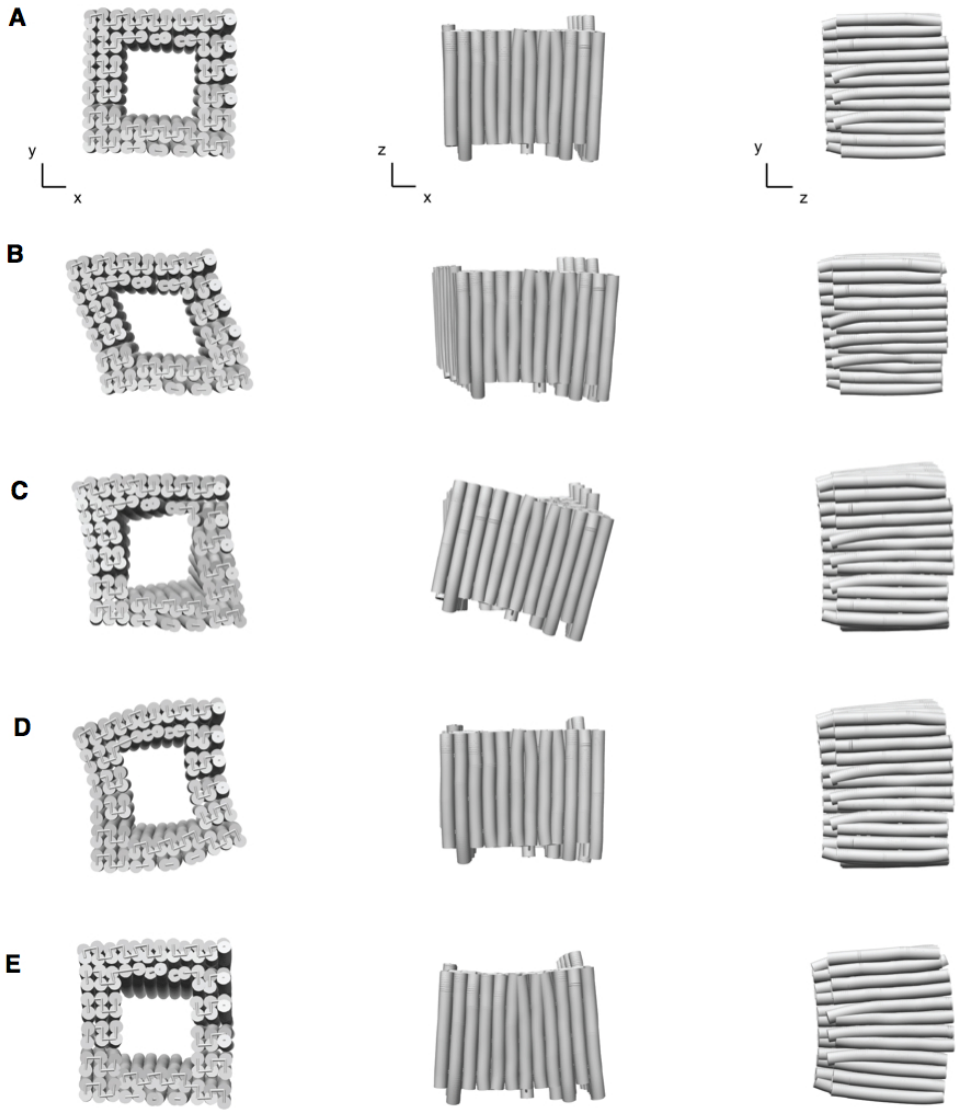

Fig. S6: **NMA for DNA mold with 16 nm by 16 nm by 20 nm cuboid cavity in Fig. 3D**. (A) Ground-state solution conformation and (B)-(E) four lowest energy modes of deformation at room temperature. NM displacements are magnified by a factor of five over their values corresponding to T =298 K.

S3.2.3 Stiffness comparison with viral capsid

In our design framework, we only consider the structural stiffness as the key design parameter. The growing metallic NP produces an outward expansion pressure that deforms the DNA mold until a critical pressure is reached that either (1) inhibits growth entirely for closed molds or (2) constrains NP growth to flow outwards in open molds. Hence, the stiffness of DNA molds needs to be high enough to provide sufficient stability under this expansion pressure. To verify structural stiffness, we compared the simulated stiffness values to the experiment value of a model system, Cowpea chlorotic mottle virus (CCMV) (*34*), which has been reported to successfully confine inorganic material growth within (*35*). Under press condition, the empty CCMV, with a measured stiffness of 150 pN/nm, is observed to be mechanically stable when the diameter distortion is below $\sim$20$\%$ (Figure 3c in CCMV paper (*34*)). However, when subjected to a press force above the threshold value of 600 pN, irreversible non-linear deformation was observed (Table 1 in CCMV paper (*34*)).

To computationally evaluate the mechanical compliance of DNA molds under internal stress, point- and distributed-force loads are applied to the interior of the DNA mold via finite element model. For a multilayered DNA mold, 20$\%$ dimension distortion required a threshold distributed force of 100 pN – 216 pN, which is of the same magnitude as the threshold value of the viral capsids. Additionally, DNA molds were observed to be largely linear up to significant deformations of $\sim$20$\%$ change in dimension prior to significant deformation that would result in the failure of the molds, such as DNA unzipping or dehybridization. These mechanical properties suggest that the mechanical compliance of multi-layer DNA molds is comparable to viral capsids. Alternatively, for a single-layered DNA mold (table S4 and table S5), computation predicts that a similar 20$\%$ distortion required less than 10 pN force, which is two magnitudes smaller than that for CCMV. As such, the single-layered DNA mold is not sufficiently stiff to retain a prescribed shape, which is consistent with our experimental observation (Sect. S10.2.1).

S3.2.4 Discussion on stiffness simulation

To form the box-like DNA molds (Fig. 3(B)-(D)), a rectangular DNA barrel with optimized structural stiffness is hierarchically assembled to three-layer DNA lids using multiple (6 to 16) 16-nt dsDNA connectors (fig. S28). After casting, the lids remain attached (fig. S52, fig. S53 and fig. S54), indicating that these dsDNA connectors between the lids and barrels are stable in the presence of NP growth. Because the lids are ignored in the mechanical deformation simulations, model predictions of the barrel stiffness computed in the x- and y-directions provide lower bounds on the barrel stiffness in a real DNA box, which can only be enhanced by the presence of the lids. Future modeling plus experimentation may be directed to further optimize lid design and elucidate its impact on mold compliance and integrity under NP growth. Notwithstanding, the present simulation results for the lid-free barrels provide a lower-bound on the mold stiffness required to confine a sub-25 nm Ag NP. Further, for the sizes and shapes considered, simulations indicate that the minimum sidewall thickness of two layers requires a threshold stiffness that corresponds to approximately 20$\%$ barrel deformation under a distributed loading of 100 pN.

S4 Plasmonic property simulations

S4.1 EELS simulation methods and results

In EELS, the system is excited by electrons moving at relativistic speed in the vicinity, or through, the structure. This electron creates an excitation field of its own that can be viewed as the electrostatic field of a static point charge in a frame moving at relativistic speed using a Lorentz transform. We use the freely available software MNPBEM, which is provided as a MATLAB toolbox (*65, 66*). This software has been used and referenced in numerous works to calculate EELS and optical spectra of nanomaterials (*71–73*).

Fig. S7 shows the top view of the equilateral 25.2 nm Ag triangle in Fig. 4A with rounded corners with approximately 2.5 nm radii and 8 nm thick DNA mold, estimated from TEM imaging. The thickness of the nanotriangle is assumed to be 10 nm.

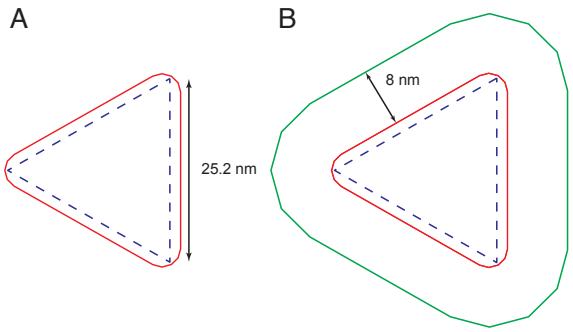

Fig. S7: **Top-view for the equilateral Ag triangle in EELS simulation**. (A) Top view of the rounded equilateral Ag triangle (red) and the idealized straight triangle (dotted blue). (B) In the presence of DNA mold around the rounded equilateral Ag triangle (green).

Fig. S8 shows separately the 3D representation and meshing of the Ag triangle, and DNA mold, along with the surface normal vector. A 3D representation of the total system with the carbon surface is also shown. The entire system is modeled in vacuum.

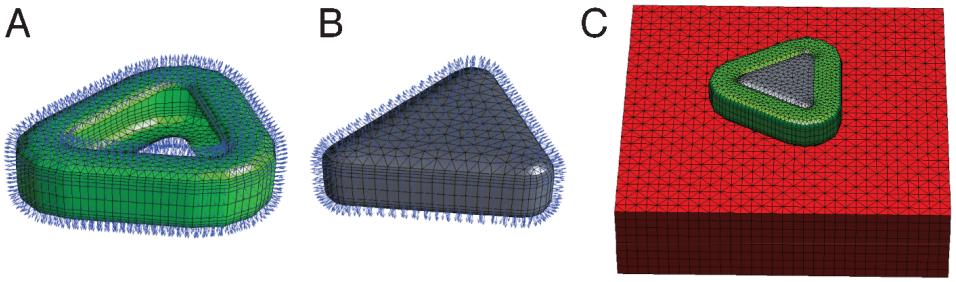

Fig. S8: **3D view for the equilateral Ag triangle within the DNA mold for EELS simulation**. (A) 3D structure, meshing and normal vectors of the DNA mold. (B) 3D structure, meshing and normal vectors of the Ag triangle. (C) 3D structure of the complete system including a 100 nm by 100 nm by 25 nm carbon surface beneath.

The refractive index of the DNA layer is assumed to be 2.1, following Thacker et al. (*74*). The electron beam energy is 80 kV. The refractive index of carbon is 2, following Scholl et al. (*42*). In this simulation, a 1 nm air gap separates the surface from the NP. The Ag refractive index is taken from Palik (*75*). The result is averaged for impact parameters covering a 24 nm radius from the triangle center, to model the electron beam used in the experiment.

For the deposited Ag triangle within DNA mold, simulated results show a strong dipolar mode around 1.95 eV that corresponds to resonance near the corners, red-shifted compared with experiment owing to the uneven carbon film thickness (fig. S9) and the uncertainty on the dielectric function of the DNA mold. In addition, a mode near 3.70 eV, and various modes between 2.45 eV and 3.10 eV, correspond to resonances near the center and edges of the triangle, respectively. A mode at 3.80 eV is also visible corresponding to the bulk Ag plasmon mode. In contrast, the absence of carbon film produces a blue-shifted resonance energy for the dipolar mode, from 1.95 eV to 2.15 eV (fig. S10). Further removing the DNA mold blue-shifted the dipolar mode to 2.75 eV, with fewer resonance modes near the edges only at 3.50 eV (fig. S11).

We also performed similar simulation for a Ag NP with 25 nm circular cross-section (Fig. 4C). The thickness of DNA mold is 8 nm in both the radial and z-directions. A 1 nm air gap is placed to separate the carbon surface from the Ag NP (fig. S12).

Simulation results for the Ag sphere within the DNA mold on a carbon film show a dipolar mode near 2.85 eV at the edge of the NP, in addition to several modes between 3.30 eV to 3.65 eV located near the center of the NP (fig. S13). Removing the carbon film beneath slightly changes the EELS resonance modes and energy (fig. S14); whereas further removal DNA mold produces largely blue-shifted resonance at 3.50 eV at the edge of the NP (fig. S15).

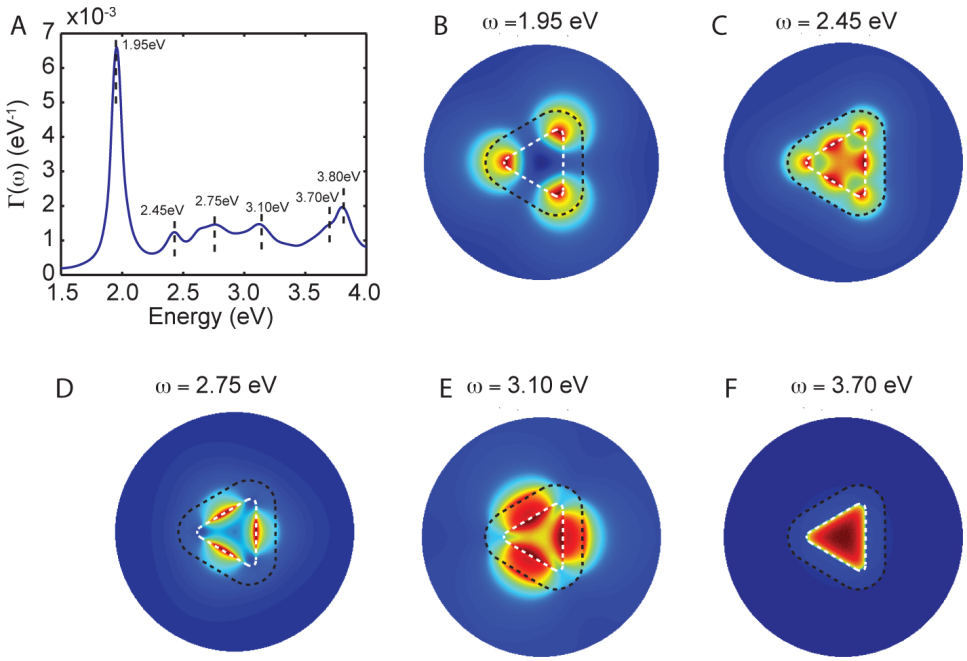

Fig. S9: **Simulations of the EELS result for the equilateral Ag triangle within the DNA mold under experimental measured condition (with carbon film beneath)**. (A) Simulated EELS results from 1.5 eV to 4.0 eV. (B)-(F) The simulated EELS amplitude map for the five major resonant modes present in the simulated spectrum. The white and black dashed lines show the contour of the NP and the DNA mold, respectively.

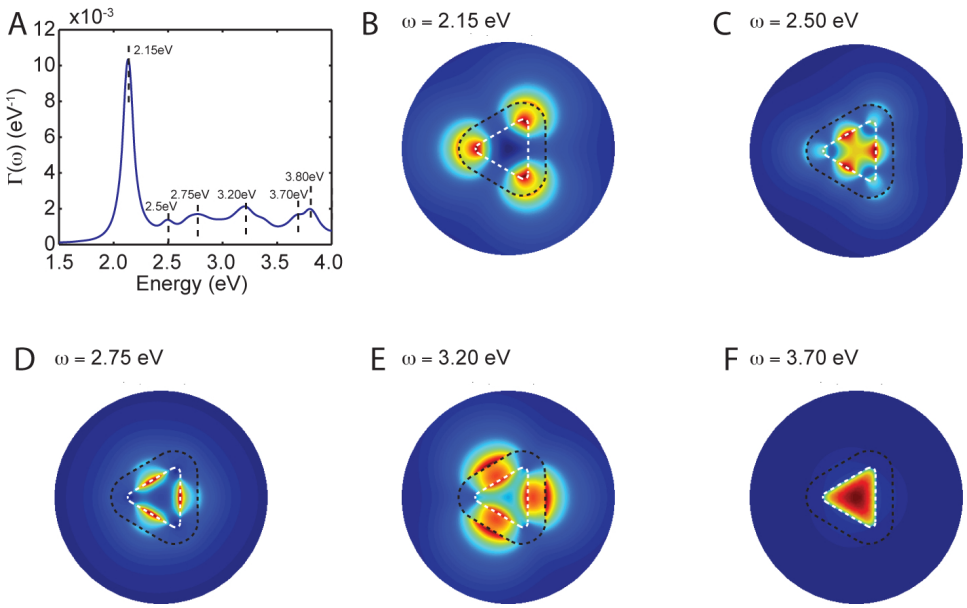

Fig. S10: **Simulations of the EELS result for the equilateral Ag triangle within the DNA mold (without carbon film beneath)**. (A) Simulated EELS results from 1.5 eV to 4.0 eV. (B)-(F) The simulated EELS amplitude map for the five major resonant modes present in the simulated spectrum. The white and black dashed lines show the contour of the NP and the DNA mold, respectively.

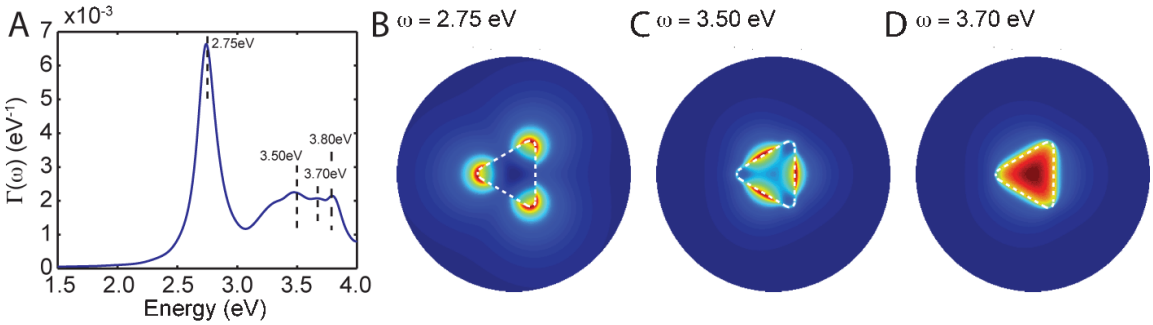

Fig. S11: **Simulations of the EELS result for the equilateral Ag triangle (with no carbon film beneath or DNA mold around)**. (A) Simulated EELS results from 1.5 eV to 4.0 eV. (B)-(D) The simulated EELS amplitude map for the three major resonant modes present in the simulated spectrum. The white dashed lines show the contour of the NP.

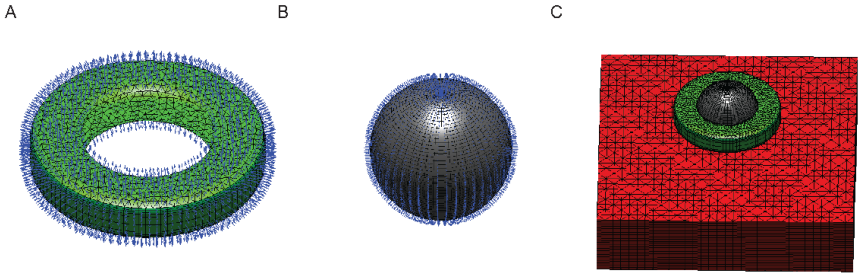

Fig. S12: **3D view for the Ag NP with 25 nm circular cross-section within the DNA mold for EELS simulation**. (A) 3D structure, meshing and normal vectors of the DNA mold. (B) 3D structure, meshing and normal vectors of the Ag sphere. (C) 3D structure of the complete system including a 100 nm by 100 nm by 25nm carbon surface beneath.

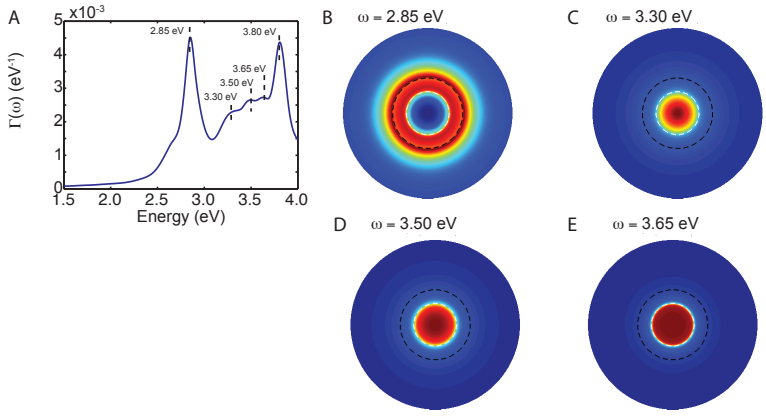

Fig. S13: **Simulations of the EELS result for the spherical Ag NP within the DNA mold under experimental measured condition (with carbon film beneath)**. The Ag sphere was placed on top of a carbon film in vacuum. (A) Simulated EELS results from 1.5 eV to 4.0 eV. (B)-(E) The simulated EELS amplitude map for the four major resonant modes present in the simulated spectrum. The white and black dashed lines show the contour of the NP and the DNA mold, respectively.

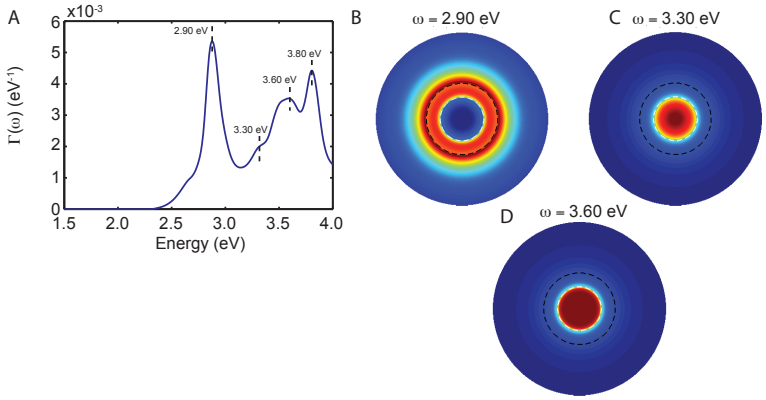

Fig. S14: **Simulations of the EELS result for the spherical Ag NP within the DNA mold (without carbon film beneath)**. (A) Simulated EELS results from 1.5 eV to 4.0 eV. (B)-(E) The simulated EELS amplitude map for three major resonant modes present in the simulated spectrum. The white and black dashed lines show the contour of the NP and the DNA mold, respectively.

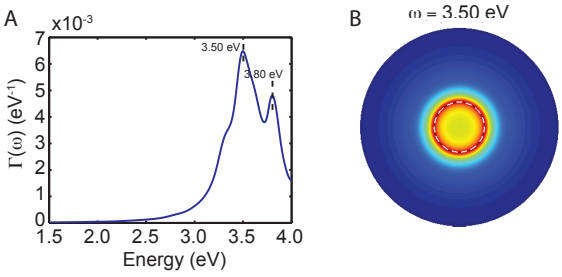

Fig. S15: **Simulations of the EELS result for the 25 nm spherical Ag NP (with no carbon film beneath or DNA mold around)**. (A) Simulated EELS results from 1.5 eV to 4.0 eV. (B) The simulated EELS amplitude map for the main resonant mode present in the simulated spectrum. The white dashed lines show the contour of the NP.

S4.2 Optical simulation methods

While a 3D analytical solution for the interaction of an electromagnetic (EM) field with a dielectric or metallic NP exists for highly regular and symmetric geometries such as spheres (*76*), the calculation of the interaction for NPs of arbitrary, more complex geometries rely on the use of numerical procedures. A popular choice is the discrete dipole approximation, where the dielectric or metallic domain is divided into individual dipoles that interact with each others (*77*). In this work, we use the finite-element method to solve directly the full continuum Helmholtz equation in three dimensional space (*67, 68*).

Eq. 1: $\bigtriangledown\times\bigtriangledown\times\mathbf{E} - {\kappa_0}^2\varepsilon_r\mathbf{E} = 0$

In Eq. 1, $\mathbf{E}$ is the 3D electric vector field, assumed time-harmonic, κ_0 is the wavenumber of free-space and ε_r is the complex relative permittivity of the material. The magnetic response of the material is assumed negligible. From the electric field distribution, the absorption (σ_{abs}), scattering (σ_{scatt}) and extinction (σ_{ext}) cross-sections are calculated (*78*).

Eq. 2: $\sigma_{\text{abs}} = \frac{1}{2}\frac{\int \omega\varepsilon'' |\mathbf{E}|^2 dV}{I_0}$

Eq. 3: $\sigma_{\text{scatt}} = \frac{1}{2}\frac{R_e[\oint(\mathbf{E}_{scatt}\times\mathbf{H}_{scatt}{}^*)\cdot dS]}{I_0}$

Eq. 4: $\sigma_{\text{ext}} = \sigma_{\text{abs}} + \sigma_{\text{scatt}}$

In Eq. 2 and 3, ω is the frequency of light, ε'' is the imaginary part of the permittivity, I_0 is the incident light power density (intensity) and $\mathbf{H}$ is the vector magnetic field, which is calculated from the vector electric field $\mathbf{E}$ and Maxwell's equations. The volume integral of Eq. 2 is performed on the NP domain, whereas the surface integral of Eq. 3 is performed on a surface that surrounds completely the NP.

Eq. 1 is solved using the commercial software COMSOL (COMSOL Inc., Burlington, MA) assuming plane-wave excitation. The NP is placed in a cubic water box of sides 250 nm (ε_r = 1.77). This box is surrounded by perfectly matched layers (PML), which are absorbing boundaries that efficiently emulate an infinite domain. Tetrahedral quadratic vector finite elements are used. Because the water/NP boundary is the most sensitive area, elements sizes are constrained below 2 nm at the boundary for the mesh generation. The integral for the calculation of σ_{scatt} is performed on a sphere of diameter 200 nm surrounding the NP. We use the complex permittivity of Au tabulated by Johnson and Christy (*79*), and Ag tabulated by Palik (*75*).

The electric field distribution $\mathbf{E}$ is calculated every 10 nm for wavelengths ranging from 250 nm to 1000 nm. Note that the cross-sections depend on the direction and polarization of the incident plane wave. Therefore, in order to obtain averaged results accounting for the isotropic distribution present in a solution, the field distribution $\mathbf{E}$ is calculated for all orientations and polarizations of the incident plane wave with an angular resolution of 30 degrees. NP symmetry was used to speed up the preceding calculation, where, for example, the prism contains three axes of symmetry that enable averaging results only over the first octant.

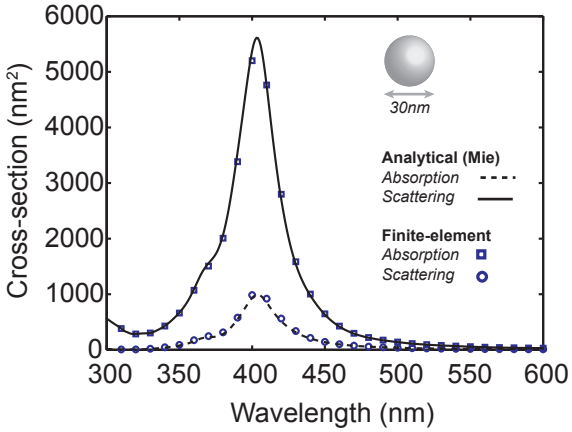

Fig. S16: **Validation of the finite-element procedure**. Numerical results on the scattering and absorption spectrum are compared with the analytical solution of Mie for a homogeneous 30 nm Ag sphere in water.

S4.3 Optical simulation results

To validate our procedure, we calculated σ_{scatt} and σ_{abs} for a Ag nanosphere of 30 nm diameter in a water medium and compared our result with the solution obtained with the Mie procedure, and found similar wavelength-dependent cross-sections for both methods, indicating the accuracy of our method (fig. S16).

We calculated the optical properties for the three Ag cuboids present in the paper, the Ag triangles with distinct dimensions, and the Au cuboid. Sizes of the simulated NPs are approximated from TEM measurement of the NPs presented in the paper. Thicknesses for the metal NP in Fig. 4A, B, and D are estimated from the thicknesses of DNA molds.

Extinction cross-sections for the various structures exhibit highly distinct peaks with numbers, positions, and amplitudes that are strongly dependent on the specific NP shape (fig. S17). Energy absorption represents the principal contribution to the extinction

in each case, due to the small size of the NP (*80*).

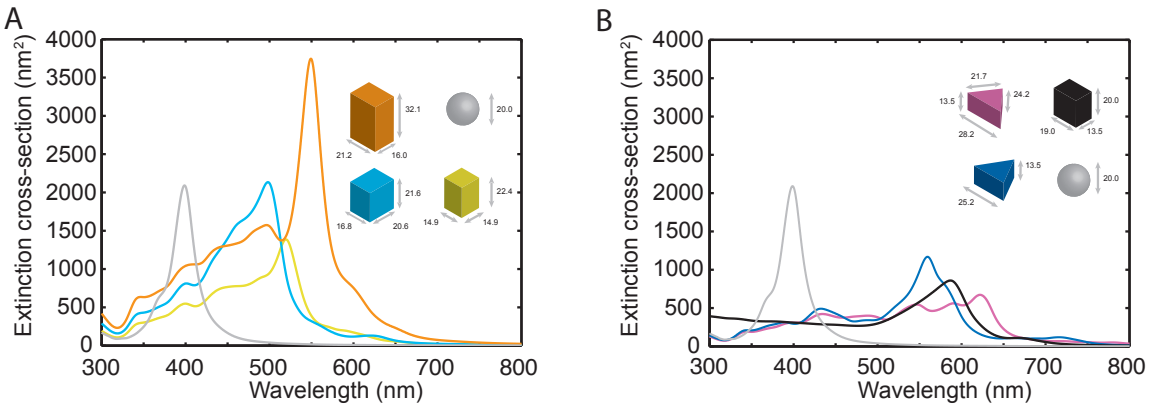

Fig. S17: **Simulated extinction cross-sections for the cast metal NPs with sharp corners**. (A) Extinction cross-section of Ag cuboids with distinct dimensions in Fig. 3B-D and a single Ag sphere as reference. (B) Extinction cross-section of metal NPs with prescribed cross-sections in Fig. 4A, B, D, and a single Ag sphere as reference.

Creating angular and high-aspect ratio shapes yield extinction peaks that are red-shifted (∼500-560 nm) compared to the sphere dipolar mode (∼400 nm). For the cuboids, the more intense plasmon mode is longitudinal (fig. S18). The rich spectrum in the 350-500 nm region is associated with the numerous planes of symmetry that are inherent to the cuboid geometry (*81*).

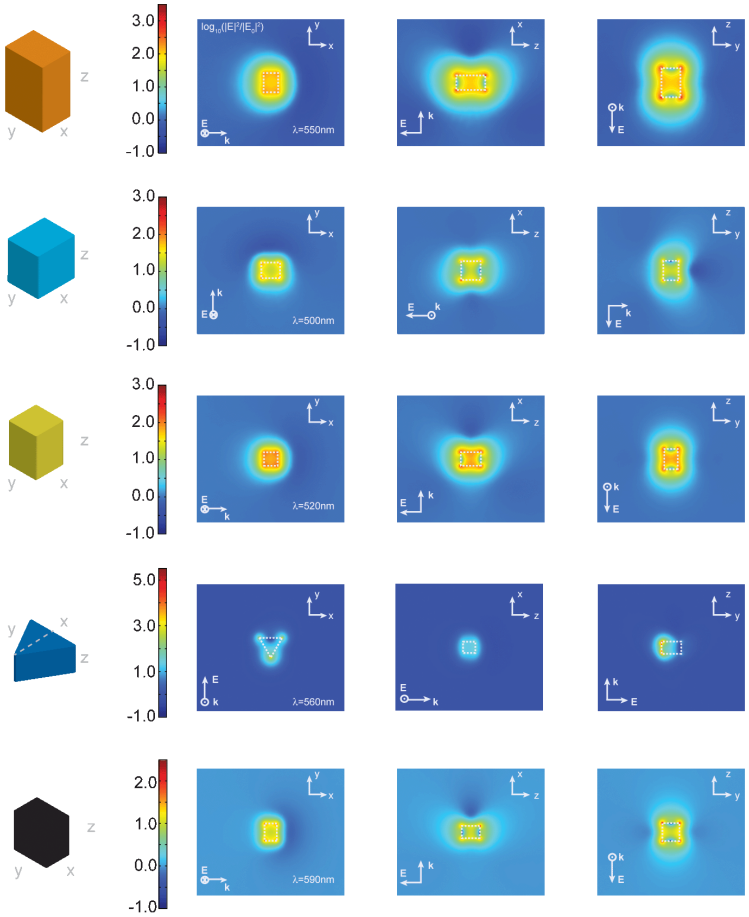

Fig. S18: **Simulated electric field intensity enhancement at the longitudinal (cuboids) and in-plane (triangle) plasmon modes for the target geometries with sharp corners**.

TEM imaging shows that the structures synthesized using the DNA mold technique in reality deviates from the idealized geometries studied above. In particular, cast structures have rounded corners. We performed similar simulations on similar geometries for which sharp corners were replaced with a sphere or cylinder to assess the influence of these slightly rounded geometries on

their optical properties. The corner radii were measured from TEM images.

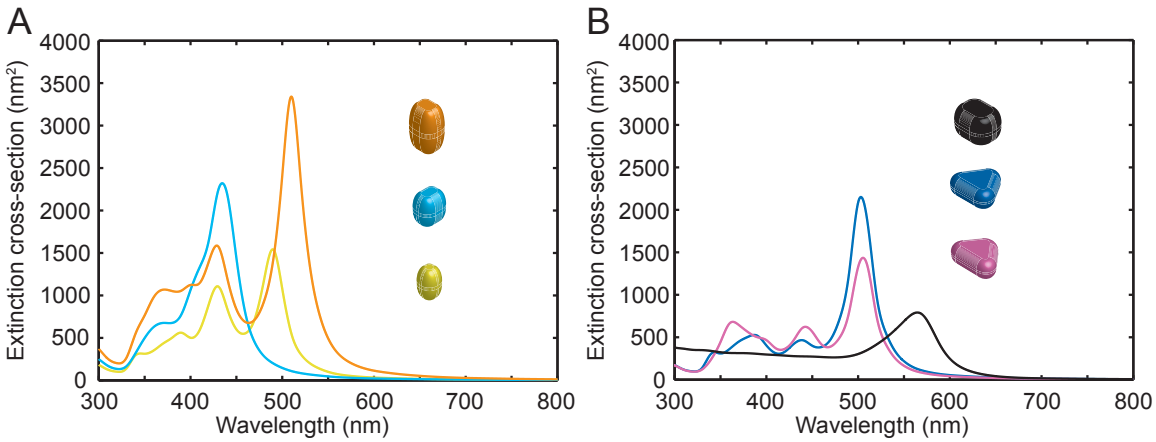

Fig. S19: **Simulated extinction cross-sections for the cast metal NPs with rounded corners, as measured from TEM images**. (A) Extinction cross-section of Ag cuboids with distinct dimensions in Fig. 3B-D. (B) Extinction cross-section of metal NPs with prescribed cross-sections and compositions in Fig. 4A, B, and D.

Interestingly, significant spectral tunability remains in spite of the presence of rounded corners (fig. S19). However, a slight blue-shift of the plasmon resonance is observed for all structures. This demonstrates the importance of precisely controlling the corners geometry when a specific optical response is desired, although the aspect ratio also greatly influences the position of the peak. The richness of the spectrum in the 350-500 nm is also modulated because of the shape symmetry transition towards a more spherical geometry. The distribution of the electric field shows that the modes differ significantly from those of the target geometries (fig. S19 and fig. S20). Importantly, the localization and magnitude of the near-field enhancement is considerably reduced, which can be significant for applications that rely on linear and non-linear field absorption such as fluorescence enhancement, SERS and cell nanosurgery, amongst others.

Additionally this plasmon resonance was slightly affected by the structural thickness. In the case of the equilateral triangle, increasing the thickness from 7 nm to 13.5 nm blue-shifted the plasmon resonance from 575 nm to 505 nm (fig. S21). Based on the TEM images, the experimentally determined thicknesses are in the range of 10-13 nm.

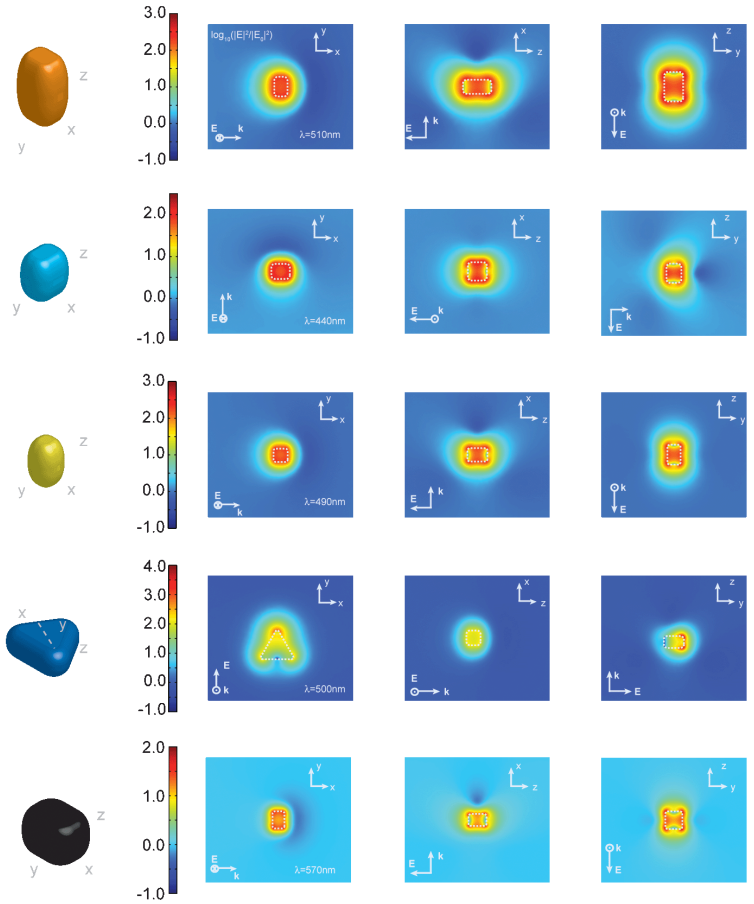

Fig. S20: **Simulated electric field intensity at the longitudinal (cuboids) and in-plane (triangle) plasmon modes for the target geometries with rounded corners (measured from TEM images).**

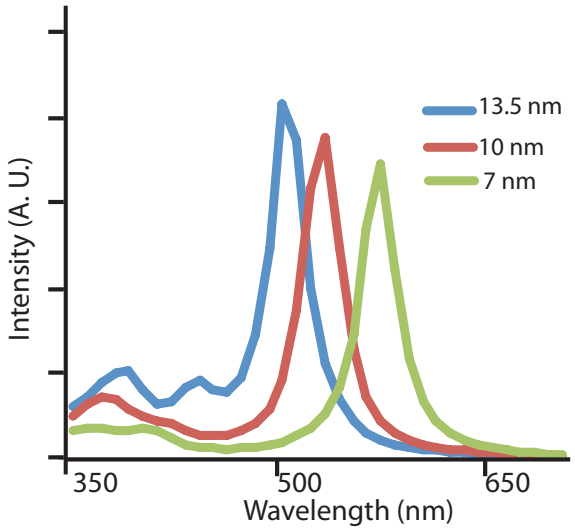

Fig. S21: **Simulated extinction spectrum of Ag triangle with a 25 nm equilateral triangle cross-section at different thicknesses.**

S5 Yield analysis

S5.1 Overview

Reaction yields for each step in Fig. 1A are listed in table S6.

Casting yield from step 4 was determined to be the ratio between the number of NPs with designed projection shapes and the total number of seed carrying boxes for closed boxes (with both lids well attached, see Sect. S5.5), or the ratio between the number of NPs with expected shapes confined in the DNA barrels and the total number of seed-decorated DNA barrels for open-ended barrels (see Sect. S5.6 for details), in the TEM image. It represented the conversion yield from a well-formed DNA mold to a metal NP with designed projectional shape. The criteria for well formed NPs is discussed in Sect. S9.2 for the closed boxes and Sect. S9.6 for open-ended barrels.

The casting yield is acquired through direct counting of NP with prescribed shapes and dimensions from each of the three projection views. We note that although such TEM based counting method is the general standard to acquire the yield for the synthesis of shape-specific NPs, it likely results in over-estimation (for this work as well as for others): the NP morphology in the projection orthogonal to the observing plane is not visualized, and thus defects could be missed, resulting in potential over-estimation.

For each individual design of closed DNA box, the barrel formation yield from step 1a (Fig. 1) was determined from agarose gel, and was measured as the ratio between the molar quantity of target structure (determined by comparing the SYBR Safe stained target band intensity and the intensity of a standard DNA marker with known molar quantity) and the molar quantity of the initial scaffold strand used in the experiment (for more details, see Sect. S5.2). Lid formation yield of step 1b was similarly defined and measured. Seed decoration yield from step 2 was determined as the ratio of the number of barrels with at least one seed attached to the interior surface and the total number of seed-decorated barrels in the TEM image (Sect. S5.3). Box closure yield from step 3 was measured as the ratio of the number of seed-decorated barrels with both lids well attached and the total number of seed-decorated barrels in the TEM image (Sect. S5.4).

For each individual design of open-ended DNA mold, the yields for each step were listed in table S6. As lids were not used, the folding yield (Yield 1b) and box closure yield (Yield 3) are not applicable. The barrel formation yield from step 1a (Fig. 1) was determined from agarose gel, and was measured as the ratio between the molar quantity of target structure (determined by comparing the SYBR Safe stained target band intensity and the intensity of a standard DNA marker with known molar quantity) and the molar quantity of the initial scaffold strand used in the experiment (for more details, see Sect. S5.2). Seed decoration yield from step 2 was determined as the ratio of the number of barrels with at least one seed attached to the interior surface and the total number of seed-decorated barrels in the TEM image (Sect. S5.3).

Procedure	Mold Construction				Nano-Casting
	Step 1a	Step 1b	Step 2	Step 3	Step 4
Yields	Barrel formation yield	Lid formation yield	Seed decoration yield	Box closure yield	Casting yield
Ag cuboid 1	20%	12%	86%	31%	40%
Ag cuboid 2	13%	12%	74%	13%	33%
Ag cuboid 3	5%	12%	91%	21%	39%
Ag triangle 1	10%	NA	75%	NA	10%
Ag triangle 2	8%	NA	60%	NA	14%
Ag sphere	5%	NA	65%	NA	18%
Au cuboid	20%	NA	86%	NA	6%
Ag Y-shape	5%	NA	80%	NA	10%
Quantum dot (QD)-Ag-QD	88%	NA	86%	NA	31%

Table S6: Reaction yields for each step in Fig. 1A. Gel electrophoresis was used to measure the formation yield of both the barrels (Yield 1a) and the lids (Yield 1b). TEM images were used to measure the seed decoration, box formation, and casting yields (Yields 2-4). See Sect. S5.1 for a summary and Sect. S5.2-S5.5 for more details.

S5.2 DNA mold folding yield (Yield 1a and 1b in table S6) analysis

Yield was estimated using native agarose gel electrophoresis. The gel was pre-stained with SYBR Safe. After electrophoresis, the gel was scanned using a fluorescent image analyzer Typhoon FLA 9000 (SYBR Safe channel, excitation wavelength: 473 nm; collection filter: $\geq$510 nm). The intensity of the target band and that of a standard sample with known mass value (the double stranded 1500 bp DNA in a 1 kb DNA ladder mixture) were measured using the built-in software ImageQuant TL, where the total intensity of a certain area was the integration of intensity per pixel over all pixels in that area. After background correction ("rubber band" subtraction mode), the mass value of target band was obtained as the ratio between the two intensities, multiplied by the known mass value of the DNA ladder band, i.e.

$$\text{Mass of target band} = \frac{\text{Intensity}_{\text{Target band}}}{\text{Intensity}_{\text{DNA ladder band}}} \times \text{Mass of DNA ladder band}$$

The yield was then calculated as the ratio between the calculated mass of the target band and the expected total mass of the origami structures when 100% scaffold strands were converted into origami structures.

$$\text{Formation Yield} = \frac{\text{Mass}_{\text{Target band}}}{\text{Mass}_{\text{100\% conversion}}}$$

S5.3 Au seed decoration yield (Yield 2 in table S6) analysis

Yield was estimated using TEM images. The yield (termed as TEM yield) was then calculated as the ratio between the number of well-formed DNA barrels decorated with at least one seed on its interior surface and the total number of barrels in the image. At least 100 barrels were measured. In the TEM images, only barrels decorated with seeds and empty barrels were observed, and used for yield calculation.

$$\text{Decoration Yield} = \frac{\text{Number}_{\text{Seed decorated}}}{\text{Number}_{\text{Total barrels}}}$$

S5.4 Formation yield analysis of seed-decorated DNA box closed with lids (Yield 3 in table S6) analysis

Yield was estimated using TEM images. The yield was calculated as the ratio between the number of well-formed boxes decorated with at least one seed and the total number of seed-decorated barrels. In the TEM images, the following objects were observed: (1) well-formed DNA boxes (with both lids appropriately attached to the barrel to form a fully closed box) decorated with at least one seed, (2) well-formed DNA boxes without seed decoration, (3) seed-decorated DNA barrels connected with multiple lids, (4) empty DNA barrels connected with multiple lids, (5) seed-decorated DNA barrels with no lids, and (6) empty DNA barrels with no lids. In our calculation, only (1) was counted as well-formed boxes with seed decoration, and (1), (3), (5) were included when counting the total number of seed decorated barrels. At least 100 barrels were measured to estimate the field.

$$\text{Box Closure Yield} = \frac{\text{Number}_{\text{Well-formed boxes with seed decoration}}}{\text{Number}_{\text{All seed-decorated barrels}}}$$

S5.5 Casting yield (Yield 4 for closed boxes in Fig. 1A) analysis

Yield was estimated using TEM images. The yield was calculated as the ratio between the number of DNA boxes with metal NPs of designed shapes and dimensions and the total number of seed-decorated DNA boxes. At least 50 seed-decorated DNA boxes were measured. In the TEM images, the following objects were observed: (1) a well-formed DNA box (as defined in Sect. S5.4) containing a well-formed metal NP (defined above), (2) a well-formed DNA box that contained an ill formed metal NP (including ungrown seed), (3) a metal NP grown in an ill-formed DNA box (e.g. open barrels with no lids, or open boxes with one lid or multiple lids), (4) a metal NP that was not contained in any DNA structure, and (5) DNA barrels or boxes that contain no NPs or seeds.

The yield was calculated as the ratio between the number of structure (1) and the number of structures (1-2), while structures (3-5) were not considered in the yield calculation.

$$\text{Casting Yield} = \frac{\text{Number}_{\text{Well-formed DNA boxes with metal NPs of designed shape and dimensions}}}{\text{Number}_{\text{Well-formed DNA boxes with seed decoration}}}$$

Also see Sect. S9.2 for example TEM images and more details.

S5.6 Casting yield (Yield 4 for open-ended barrels in Fig. 1A) analysis

Similar with that in Sect. S5.5, casting yield was also estimated using TEM images. The yield was calculated as the ratio between the number of open-ended DNA barrels with metal NPs of designed shapes and dimensions and the total number of seed-decorated open-ended DNA barrels. At least 50 seed-decorated DNA barrels were measured. In the TEM images, the following objects were observed: (1) a well formed barrel containing a well-formed metal NP (defined above), (2) a well formed barrel containing an ill formed metal NP (including ungrown seed or overgrown NP), (3) a DNA barrel containing/attached to a metal NP with exposed *y*-*z* or *x*-*z* DNA mold cross-section, but not the *x*-*y* direction (which would reveal the designed cross-section shape of the mold), (4) a metal NP that was not attached to any DNA structure, and (5) a DNA barrel that contained no NPs or seeds.

The yield was calculated as the ratio between the number of structure (1) and the number of structures (1-2), while structures (3-5) were not considered in the yield calculation.

$$\text{Casting Yield} = \frac{\text{Number}_{\text{A well formed barrel containing a well-formed metal NP}}}{\text{Number}_{\text{Seed-decorated open-ended DNA barrels exposing } x\text{-}y \text{ cross section}}}$$

Also see Sect. S9.5 for example TEM images and more details.

S6 Characterization of DNA molds

S6.1 DNA barrel with 21 nm by 16 nm by 30 nm cuboid cavity

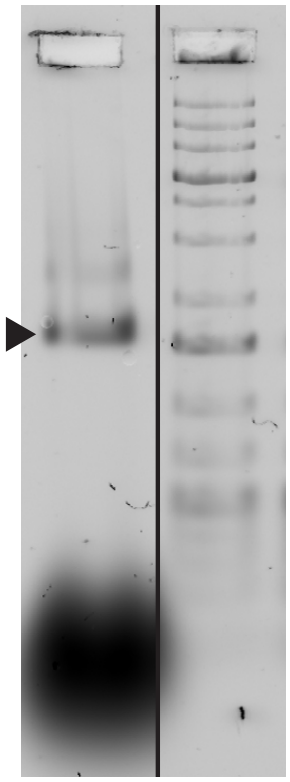

Fig. S22: **Gel image of DNA barrel with 21 nm by 16 nm by 30 nm cuboid cavity.** Left lane shows the result of assembled product. Black triangle indicates the target band. Right lane shows 1 kb ladder. Gel running condition is shown in Sect. S2.3.

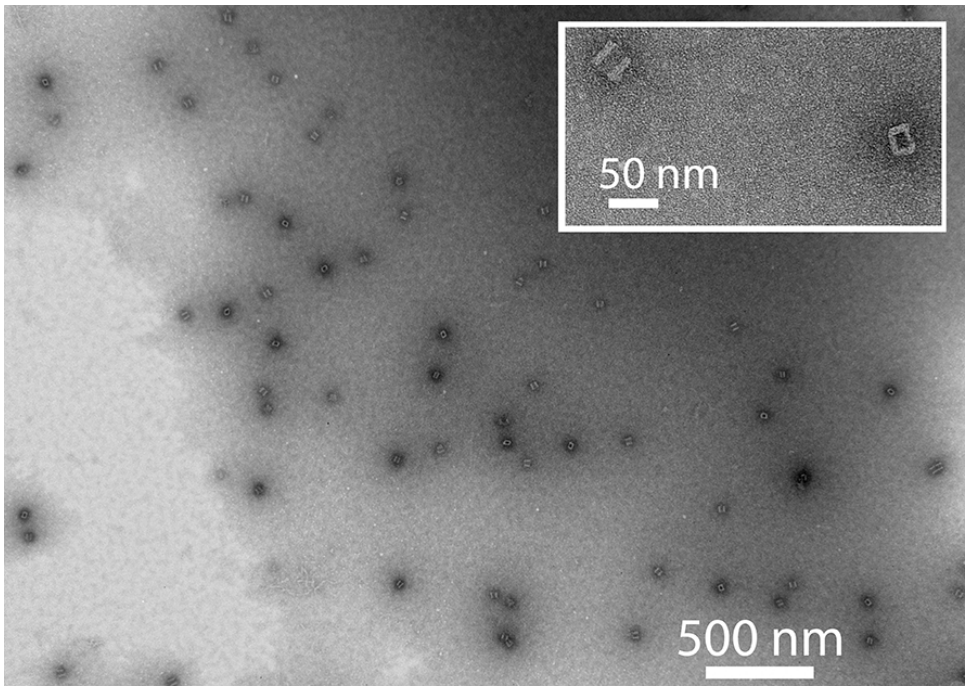

Fig. S23: **TEM image of DNA barrel with 21 nm by 16 nm by 30 nm cuboid cavity.** Inset shows the zoomed-in view of the target structure.

S6.2 DNA barrel with 21 nm by 16 nm by 20 nm cuboid cavity

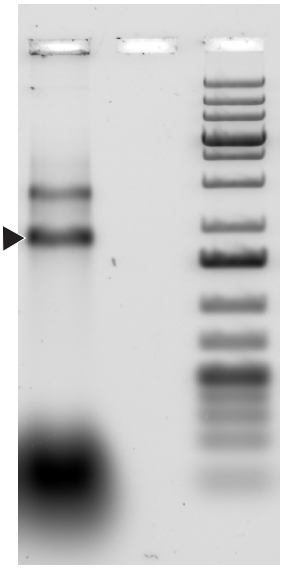

Fig. S24: **Gel image of DNA barrel with 21 nm by 16 nm by 20 nm cuboid cavity**. Left lane shows the result of assembled product. Black triangle indicates the target band. Right lane shows 1 kb ladder. Gel running condition is shown in Sect. S2.3.

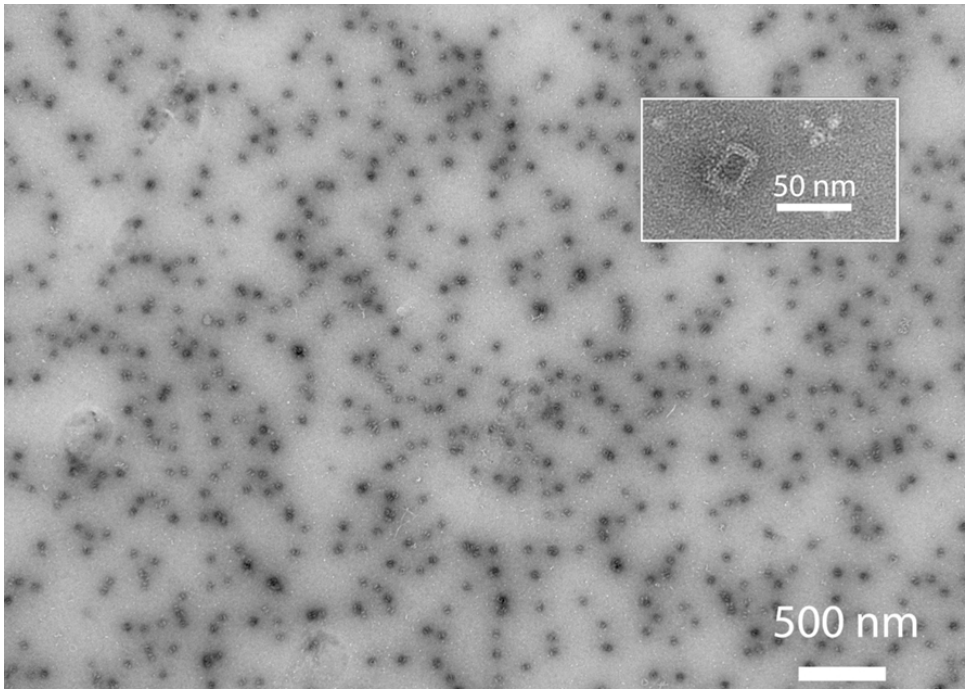

Fig. S25: **TEM image of DNA barrel with 21 nm by 16 nm by 20 nm cuboid cavity**. Inset shows the zoomed-in view of the target structure.

S6.3 DNA barrel with 16 nm by 16 nm by 20 nm cuboid cavity

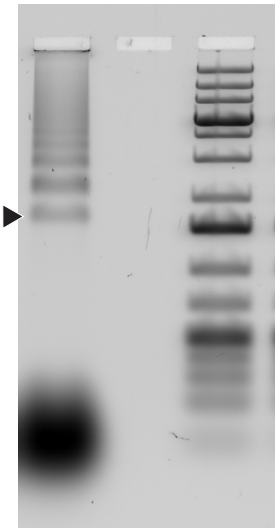

Fig. S26: **Gel image of DNA barrel with 16 nm by 16 nm by 20 nm cuboid cavity**. Left lane shows the result of assembled product. Right lane shows 1 kb ladder. Black triangle indicates the target band. Gel running condition is shown in Sect. S2.3.

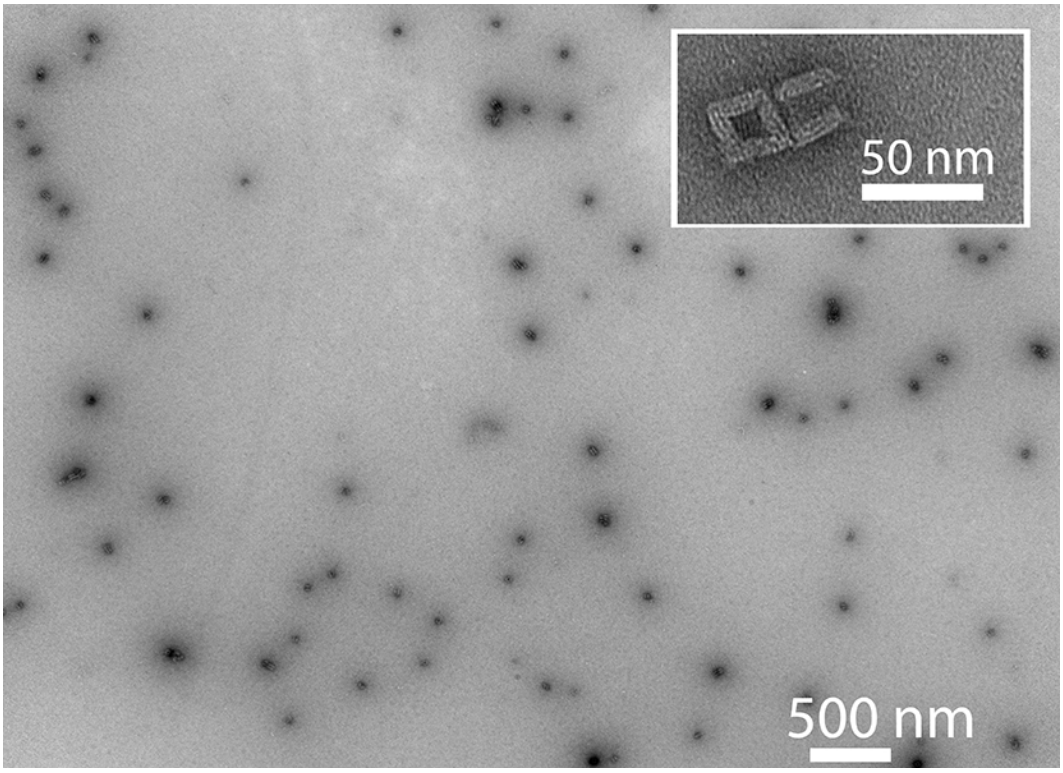

Fig. S27: **TEM image of DNA barrel with 16 nm by 16 nm by 20 nm cuboid cavity.** Inset shows the zoomed-in view of the target structure.

S6.4 Connector design for DNA barrels

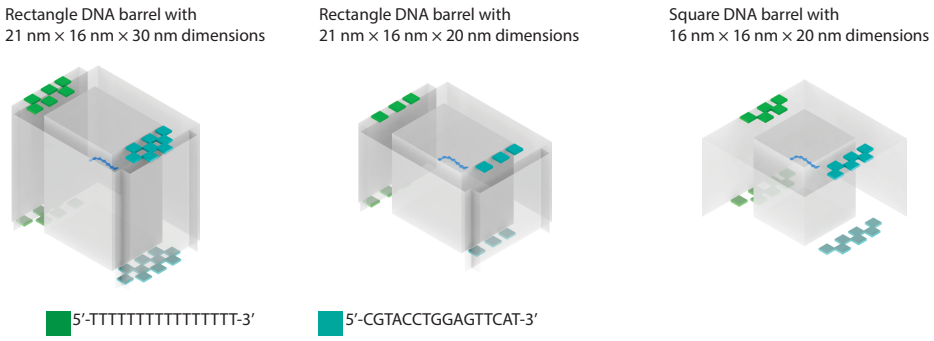

Fig. S28: **Connector design for DNA barrels with different cavities**. Green and cyan dots denote 16-nt connectors with distinct sequences on the DNA barrels. Blue lines denote the handle for Au seed within DNA barrels.

S6.5 DNA lid

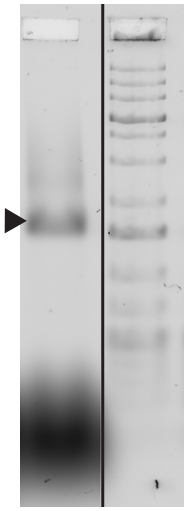

Fig. S29: **Gel image of DNA lid**. Left lane shows the result of assembled product. Black triangle indicates the target band. Right lane shows 1 kb ladder. Gel running condition is shown in Sect. S2.3.

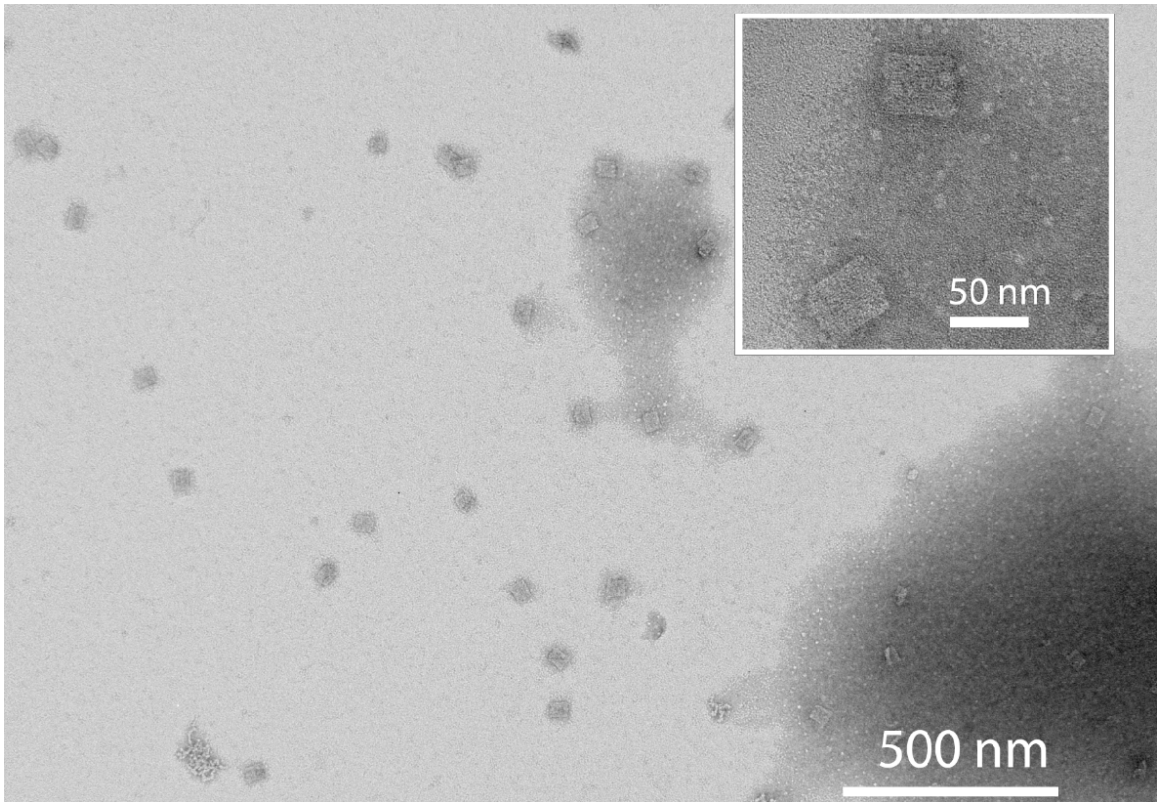

Fig. S30: **TEM image of DNA lid**. Inset shows the zoomed-in view of the target structure.

S6.6 Equilateral triangular DNA barrel with 30 nm by 30 nm by 30 nm cavity

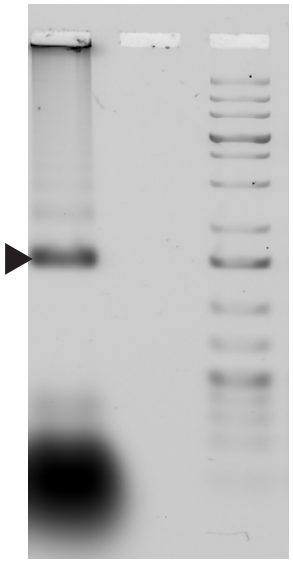

Fig. S31: **Gel image of equilateral triangular DNA barrel with 30 nm by 30 nm by 30 nm cross-section**. Left lane shows the result of assembled product. Black triangle indicates the target band. Right lane shows 1 kb ladder. Gel running condition is shown in Sect. S2.3.

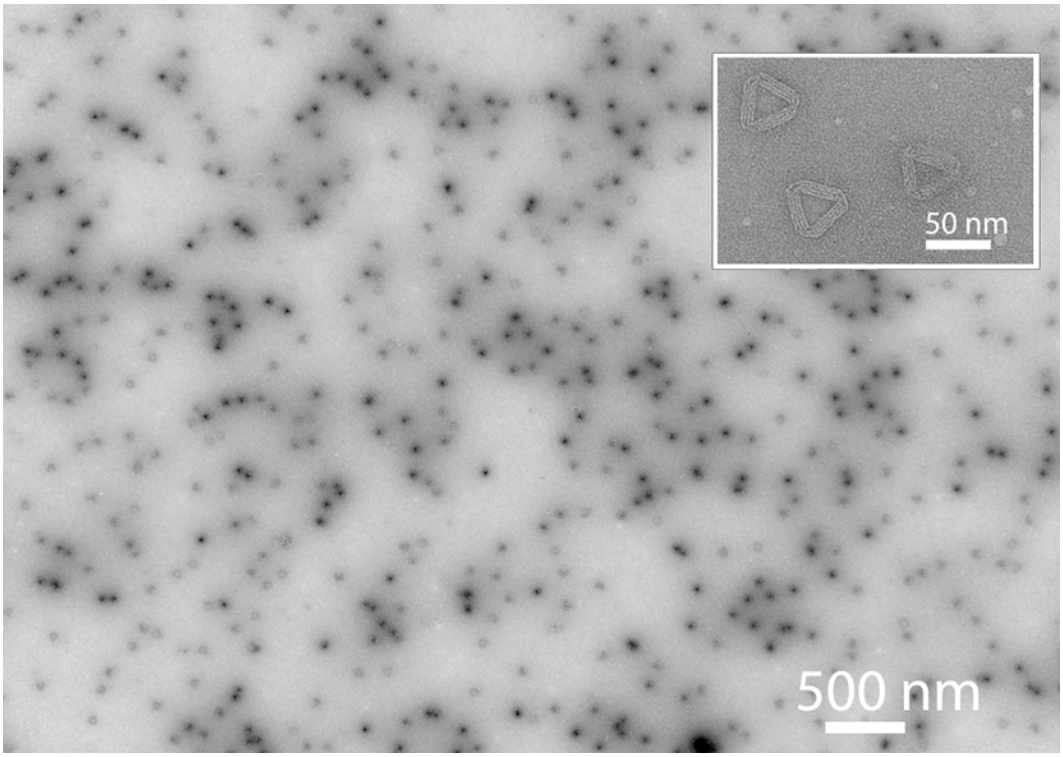

Fig. S32: **TEM image of equilateral triangular DNA barrel with 30 nm by 30 nm by 30 nm cross-section**. Inset shows the zoomed-in view of the target structure.

S6.7 Right triangular DNA barrel with 22 nm by 30 nm by 38 nm cavity

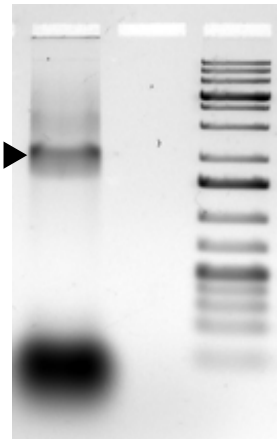

Fig. S33: **Gel image of right triangular DNA barrel with 22 nm by 30 nm by 38 nm cavity**. Left lane shows the result of assembled product. Black triangle indicates the target band. Right lane shows 1 kb ladder. Gel running condition is shown in Sect. S2.3.

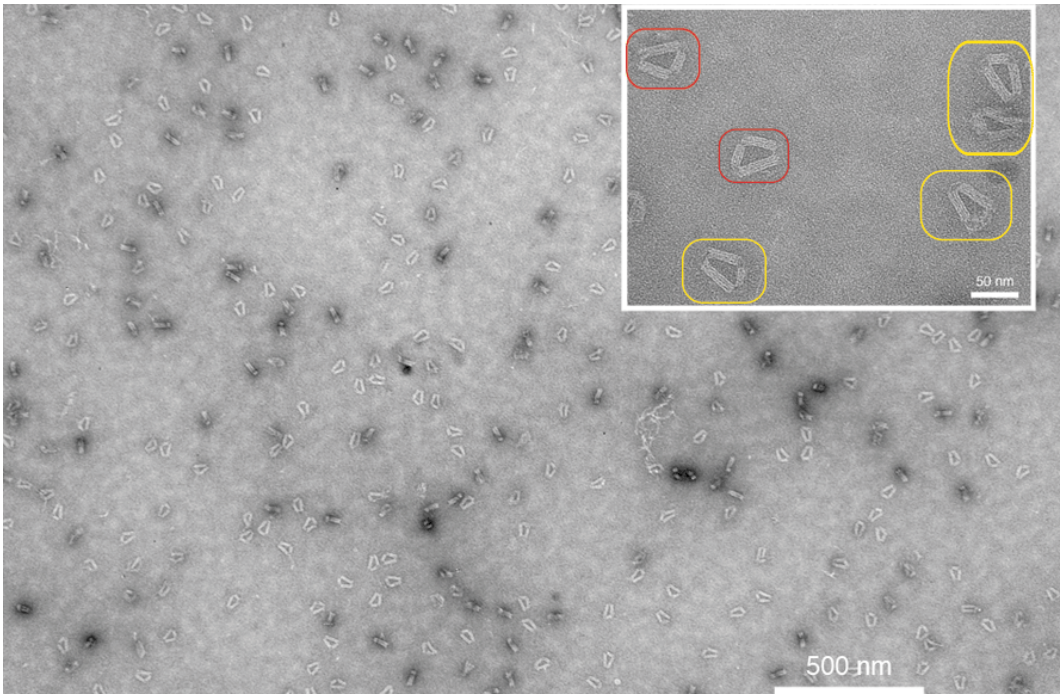

Fig. S34: **TEM image of right triangular DNA barrel with 22 nm by 30 nm by 38 nm cavity**. Inset shows the zoomed-in view of the target structure. To accommodate the right angle requirement for the triangle, multiple flexible single-stranded regions in the scaffold strand. After folding, two populations of the triangle shapes were observed, as denoted by the yellow and red circles in the inset. Red circles indicate triangles with 22 nm by 30 nm by 38 nm cavities. Yellow circles indicate triangles with 17 nm by 34 nm by 40 nm cavities.

S6.8 DNA ring with 25 nm inner diameter

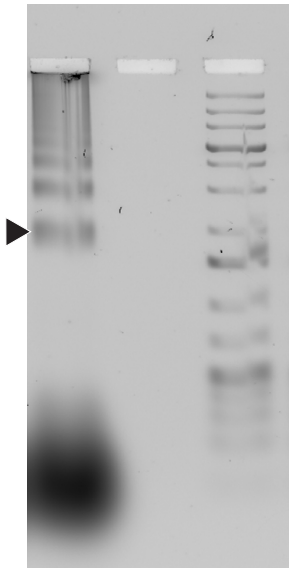

Fig. S35: **Gel image of DNA ring with 25 nm inner diameter**. Left lane shows the result of assembled product. Black triangle indicates the target band. Right lane shows 1 kb ladder. Gel running condition is shown in Sect. S2.3.

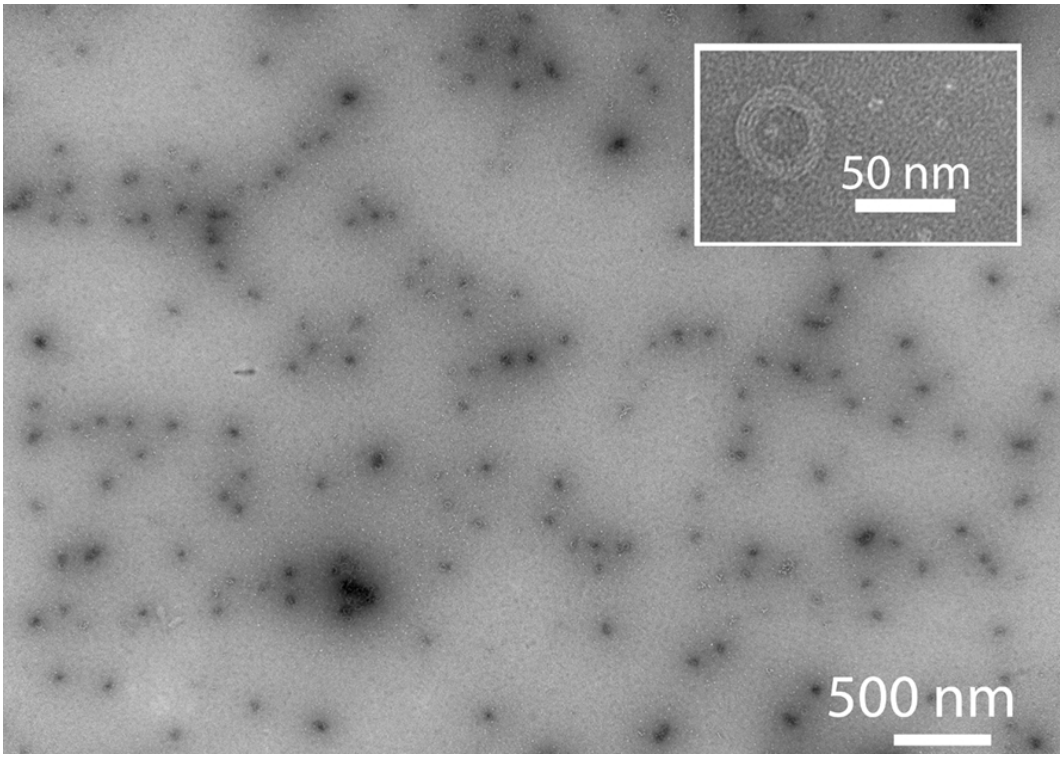

Fig. S36: **TEM image of DNA ring with 25 nm inner diameter**. Inset shows the zoomed-in view of the target structure.

S6.9 Connector design on DNA barrel for Y-shaped DNA mold

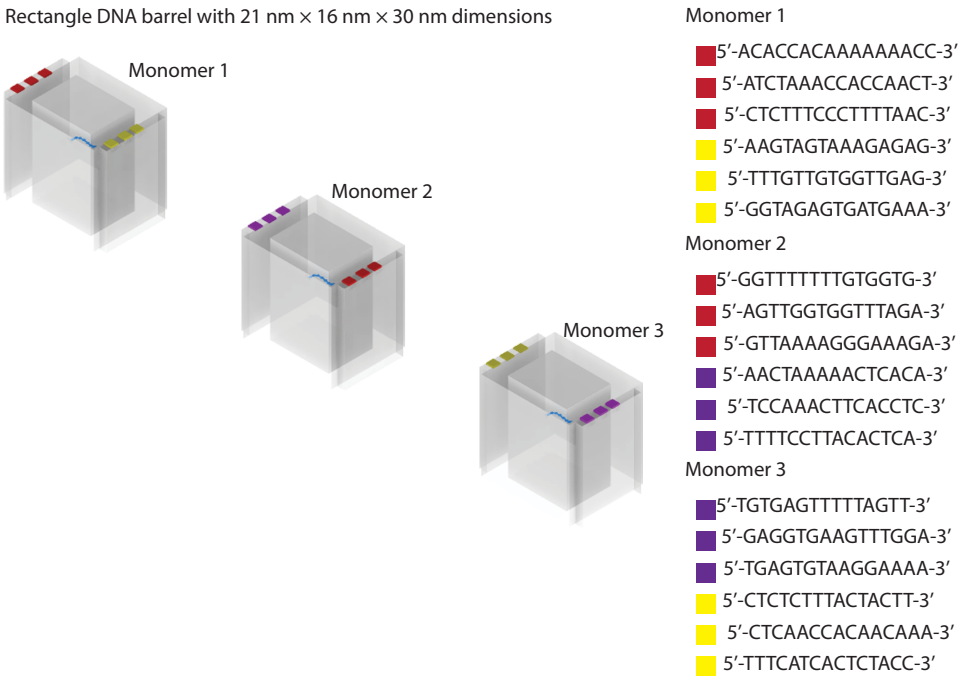

Fig. S37: **Connector design in DNA barrel for Y-shaped DNA mold**. DNA barrels used here exhibit 21 nm by 16 nm by 30 nm cuboid cavity. 15-nt connectors are modified at 3' and 5' ends of selected staple strands. Red, yellow, and purple dots represent the connectors on DNA barrels. Specific colored strands will hybridize to their complementary strands denoted with the same color on a different barrel.

S6.10 Design of DNA barrel with biotinylated ends for QD-DNA-QD composite

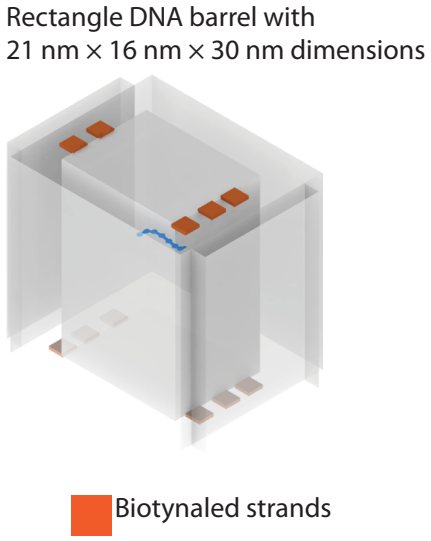

Fig. S38: **Design of DNA barrel with biotinylated ends**. Biotins are modified at 5' ends of selected staple strands via a three-T spacer (TTT). The orange dot denotes the biotynated strands. The blue line represents the handle strand. DNA mold exhibits 21 nm by 16 nm by 30 nm cuboid cavity.

S7 Seed decoration of DNA molds

S7.1 Seed decoration within DNA barrel with 21 nm by 16 nm by 30 nm cuboid cavity

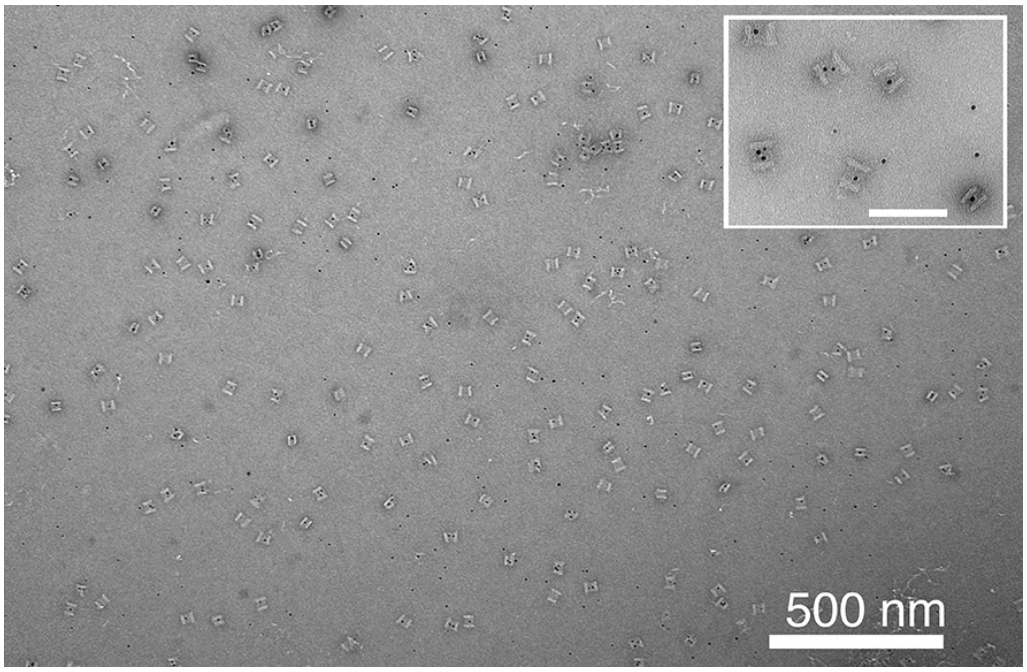

Fig. S39: **Seed decoration within the DNA barrel with 21 nm by 16 nm by 30 nm cuboid cavity**. Inset shows the zoomed-in view of the seed-decorated target structure. Black dots are 5 nm Au seeds.

S7.2 Seed decoration within DNA barrel with 21 nm by 16 nm by 20 nm cuboid cavity

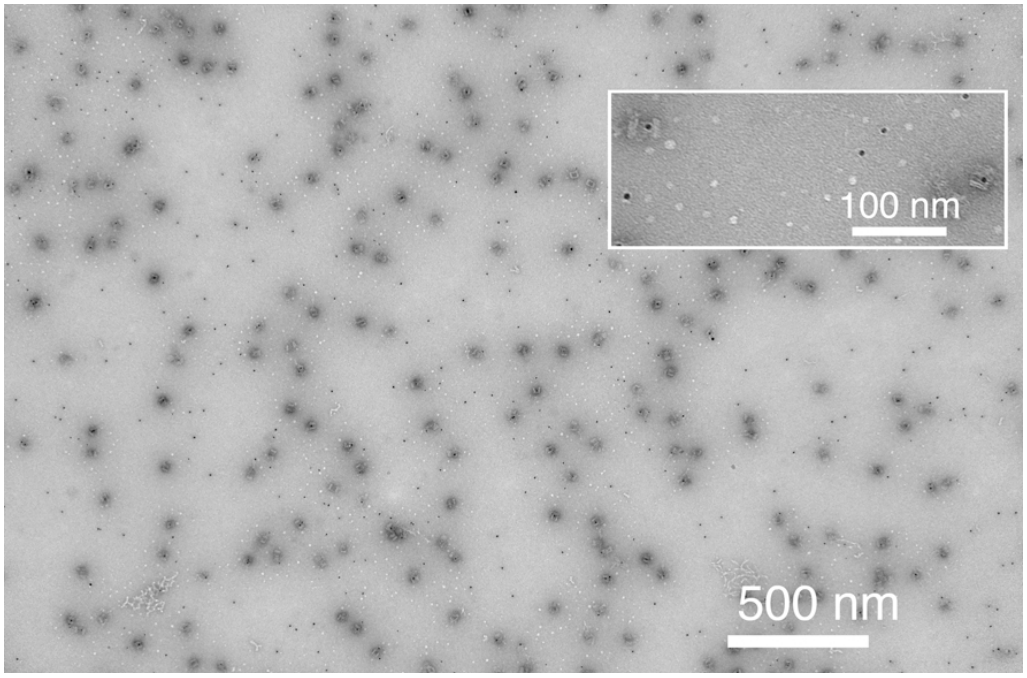

Fig. S40: **Seed decoration within the DNA barrel with 21 nm by 16 nm by 20 nm cuboid cavity**. Inset shows the zoomed-in view of the seed-decorated target structure. Black dots are 5 nm Au seeds.

S7.3 Seed decoration within DNA barrel with 16 nm by 16 nm by 20 nm cuboid cavity

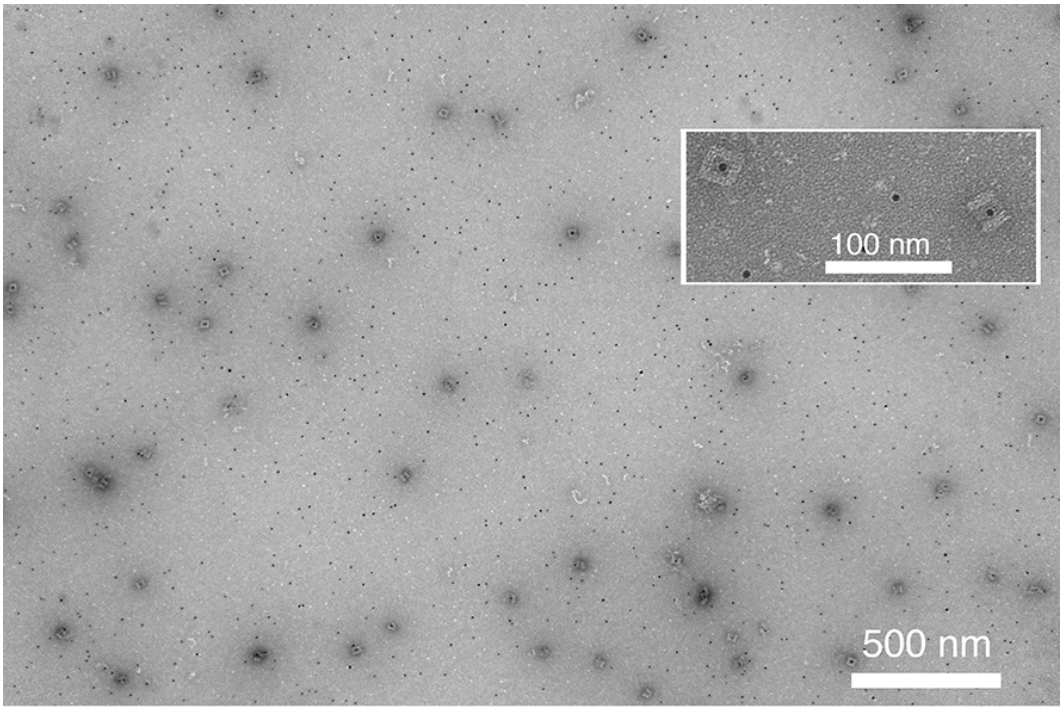

Fig. S41: **Seed decoration within the DNA barrel with 16 nm by 16 nm by 20 nm cuboid cavity**. Inset shows the zoomed-in view of the seed-decorated target structure. Black dots are 5 nm Au seeds.

S7.4 Seed decoration within equilateral triangular DNA barrel with 30 nm by 30 nm by 30 nm cavity

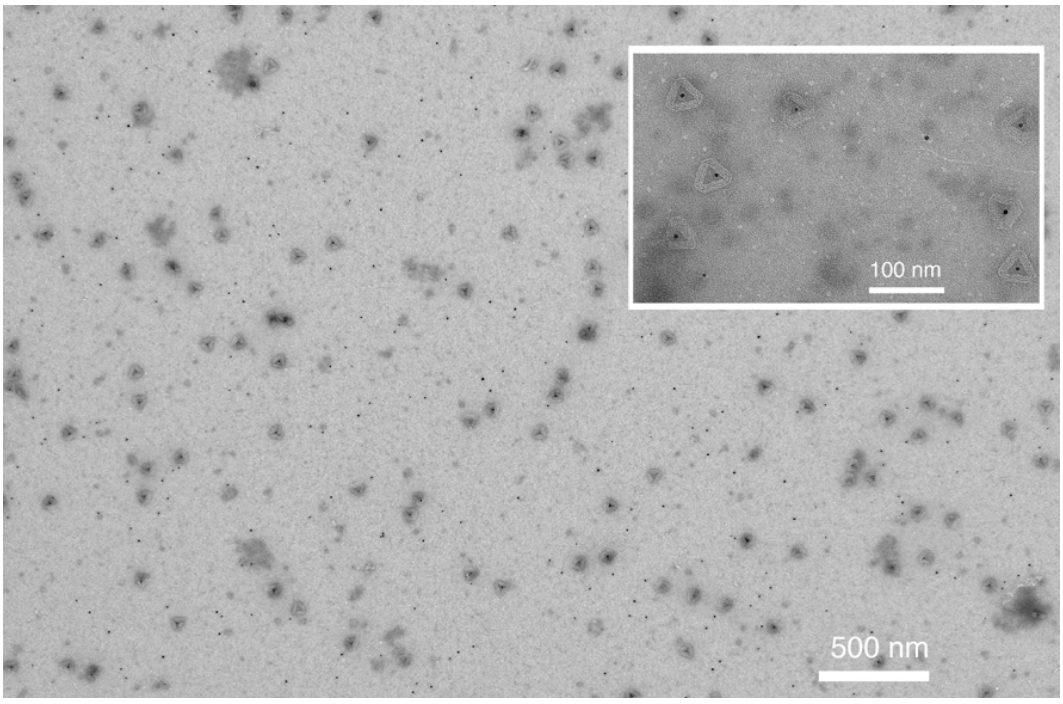

Fig. S42: **Seed decoration within equilateral triangular DNA barrel with 30 nm by 30 nm by 30 nm cavity**. Inset shows the zoomed-in view of the seed-decorated target structure. Black dots are 5 nm Au seeds.

S7.5 Seed decoration within right triangular DNA barrel with 22 nm by 30 nm by 38 nm cavity

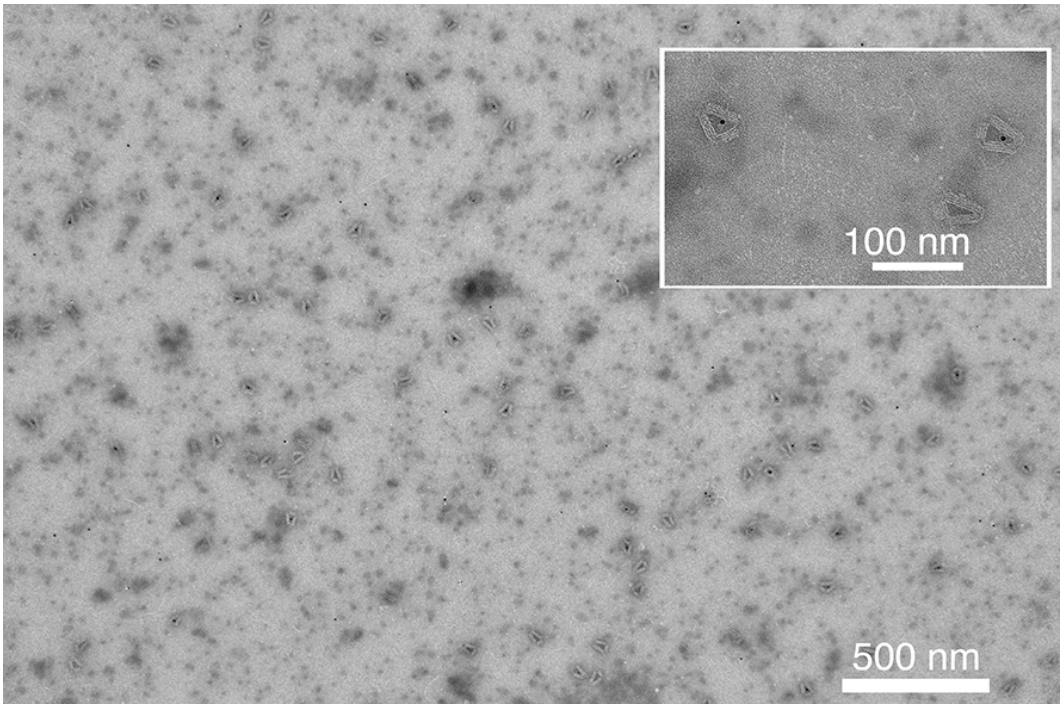

Fig. S43: **Seed decoration within right triangular DNA barrel with 22 nm by 30 nm by 38 nm cavity**. Inset shows the zoomed-in view of the seed-decorated target structure. Black dots are 5 nm Au seeds.

S7.6 Seed decoration within DNA ring with 25 nm inner diameter cavity

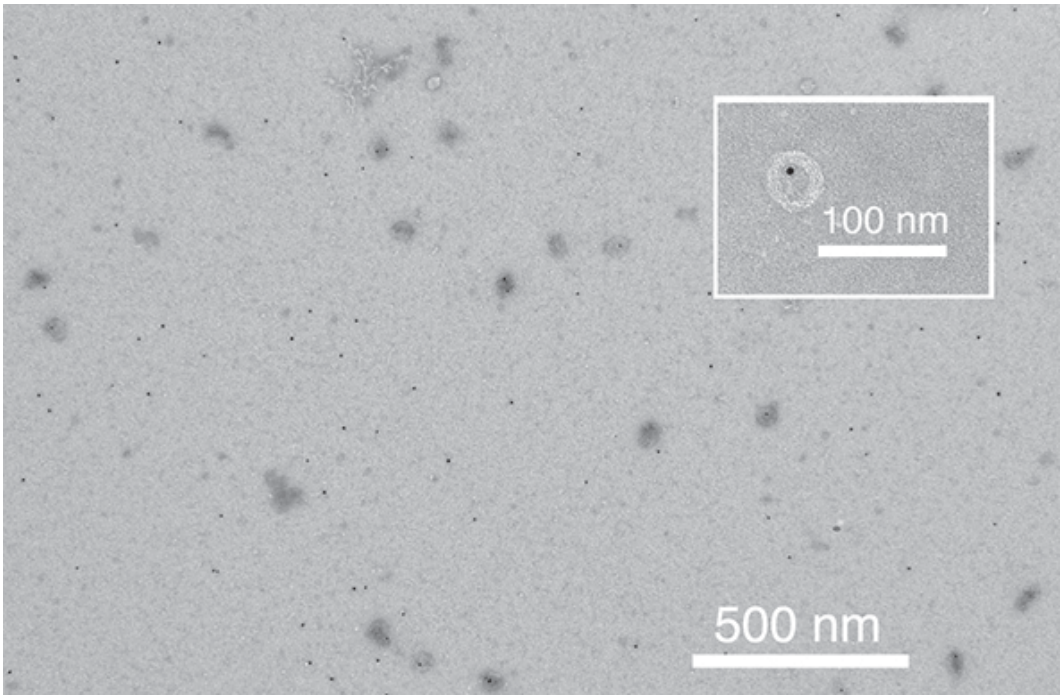

Fig. S44: **Seed decoration within DNA ring with 25 nm inner diameter**. Inset shows the zoomed-in view of the seed-decorated target structure. Black dots are 5 nm Au seeds.

S7.7 Seed decoration within Y-shaped DNA composite

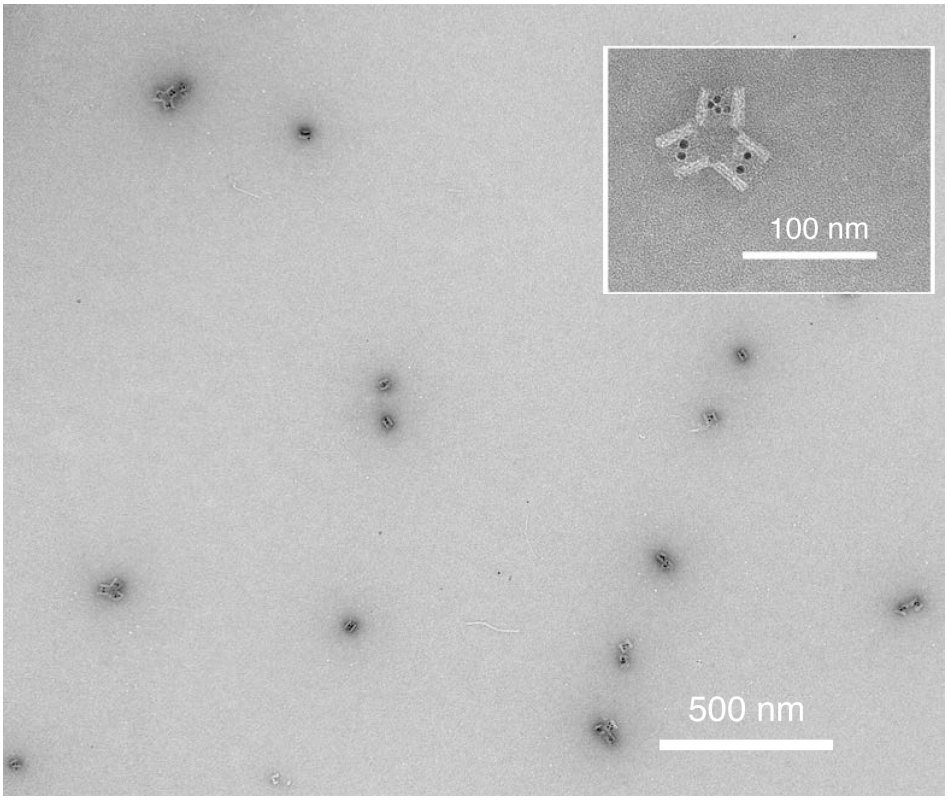

Fig. S45: **Seed decoration within Y-shaped DNA composite, built from three DNA barrels**. Inset shows the zoomed-in view of the seed-decorated target structure. Black dots are 5 nm Au seeds.

S7.8 Seed decoration within QD-DNA-QD composite

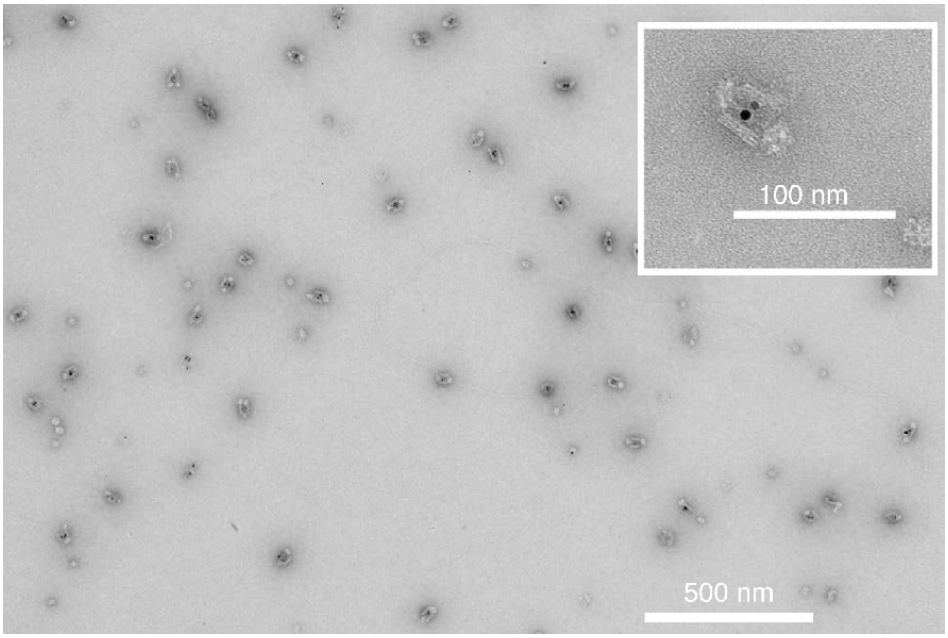

Fig. S46: **Seed decoration within QD-DNA-QD composite**. Each QD-DNA-QD conjugate was assembled from one DNA barrels and two QDs at both open ends. Inset shows the zoomed-in view of the seed-decorated target structure. White spheres in TEM image were ascribed to the stained streptavidin coating layer of QDs. Black dots are 5 nm Au seeds.

S8 Seed-decorated DNA box with closed lids

S8.1 Seed decoration within closed DNA box with 21 nm by 16 nm by 30 nm cavity

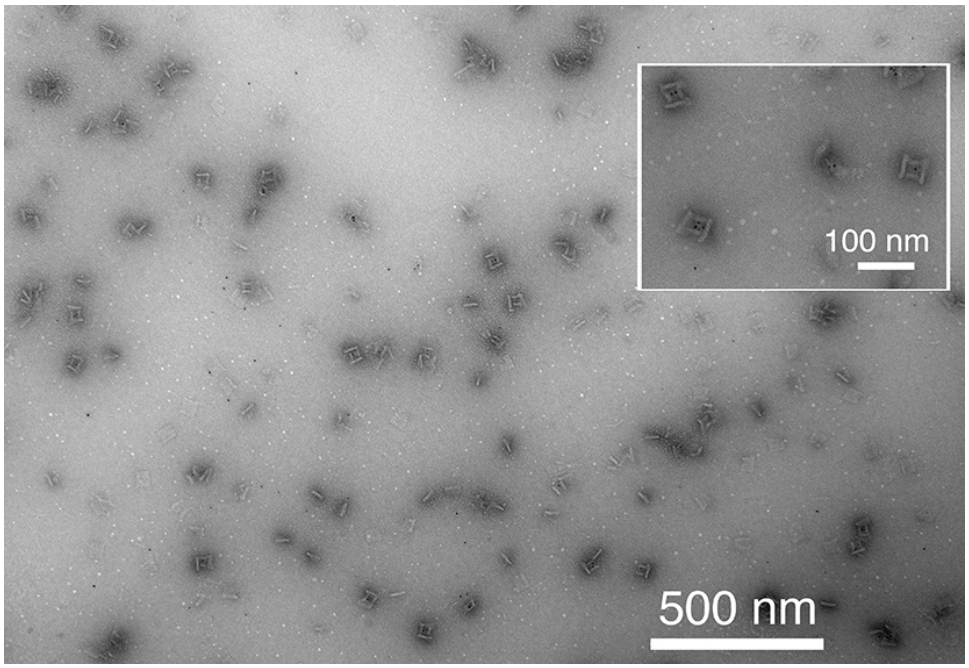

Fig. S47: **Seed decoration within closed DNA box with 21 nm by 16 nm by 30 nm cavity**. Inset shows the zoomed-in view of the seed-decorated target structure. Black dots are 5 nm Au seeds.

S8.2 Seed decoration within closed DNA box with 21 nm by 16 nm by 20 nm cavity

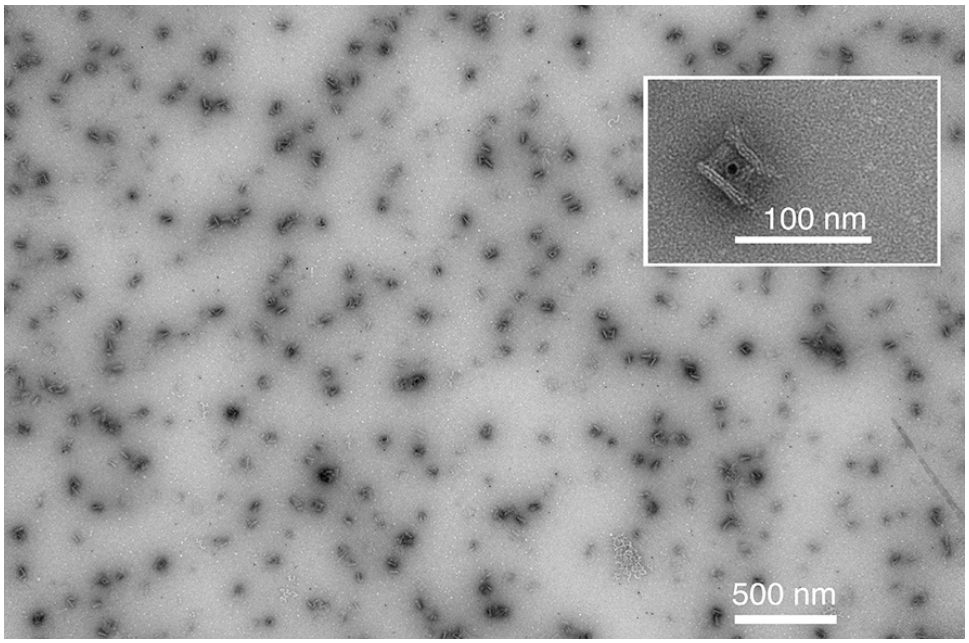

Fig. S48: **Seed decoration within closed DNA box with 21 nm by 16 nm by 20 nm cavity**. Inset shows the zoomed-in view of the seed-decorated target structure. Black dots are 5 nm Au seeds.

S8.3 Seed decoration within closed DNA box with 16 nm by 16 nm by 20 nm cavity

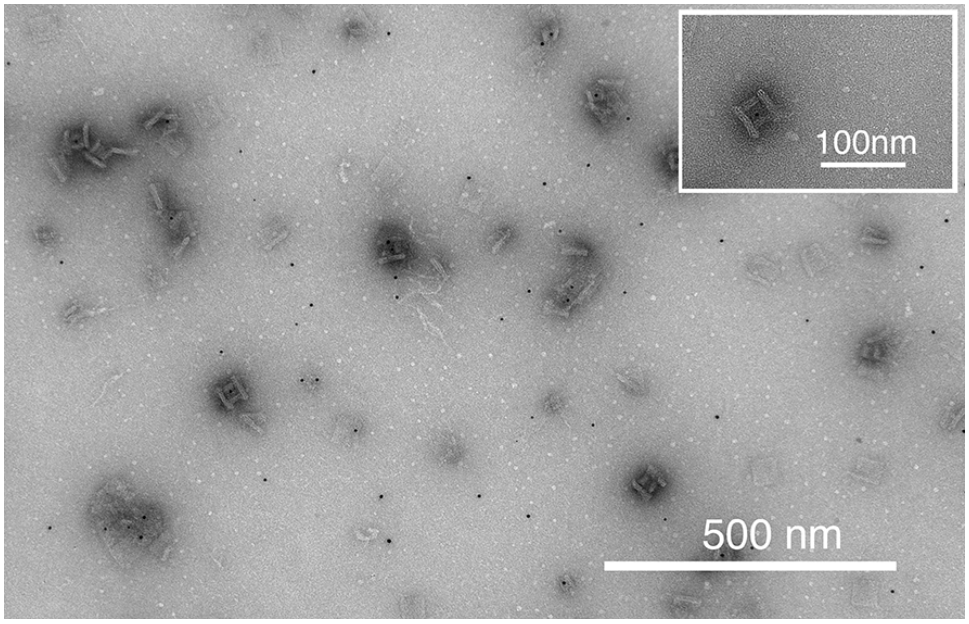

Fig. S49: **Seed decoration within closed DNA box with 16 nm by 16 nm by 20 nm cavity**. Inset shows the zoomed-in view of the seed-decorated target structure. Black dots are 5 nm Au seeds.

S9 Ag NP growth within DNA molds

S9.1 Ag NPs growth in open-ended barrels with 21 nm by 16 nm by 30 nm cuboid cavity

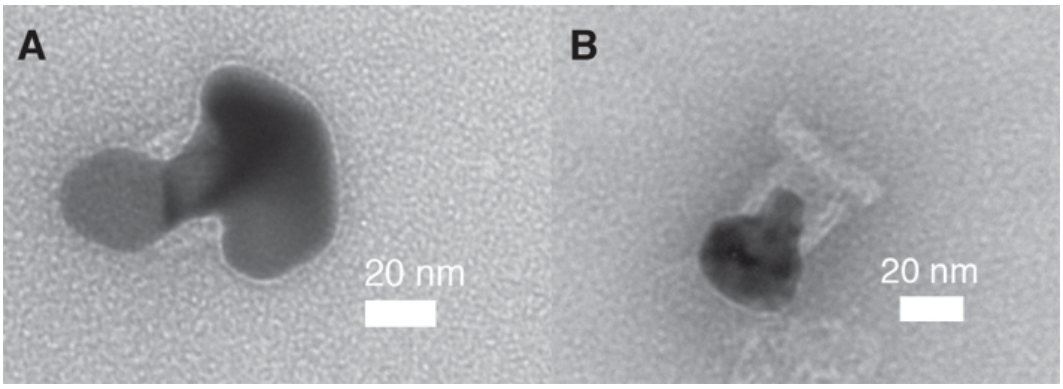

Figure S50. **Ag NPs growth in open-ended DNA barrels with 21 nm by 16 nm by 30 nm cuboid cavity**. (**A**) Ag NP growth in a barrel with both ends open. (**B**) Ag NP growth in a barrel with one open end and one closed end. The reaction condition is shown in Sect. S2.5. Reaction time for both (A) and (B) was 8 min. It is clear from these experiments that the walls of the DNA nanomolds confined the growth of the Ag NP.

S9.2 Ag NP growth within a DNA box with 21 nm by 16 nm by 30 nm cavity

We analyzed the NP growth yield (Yield 4 in Table 1) for the DNA box mold with 21 nm by 16 nm by 30 nm cavity. In Sect. S5.5, when defining the NP growth yield, 5 types of structures were observed in TEM images and Structure Type 1 (a well-formed box containing a well-formed NP) and Structure Type 2 (a well-formed box containing an ill-formed NP) were considered for yield calculation, and Structures (3-5) were uncounted. We describe below the more detailed criteria for determining Structure Type 1 v.s. Structure Type 2 with typical TEM images (fig. S51), and show some typical TEM images for Structure Types 3-5 (Uncounted structures) (fig. S51). Additional large-field-of-view images are shown in fig. S52.

- Structure Type 1: A well-formed NP in a well-formed box

  In addition to the well-formed box (with both lids appropriately attached to the barrel to form a fully closed box), the NP within the box needs to show designed cross-section shape and dimensions in the projection view. For example, in fig. S51, NPs 1, 5, 8, and 10 were denoted as the well-formed structures. They exhibited designed rectangle cross-sections, and occupied the available space in the DNA box.

- Structure Type 2: An ill-formed NP in a well-formed box

  The box mold is well-formed, however, the NP shows cross-section shape or dimensions that deviate from the design, for example, with a shape that only partially fills the mold. In fig. S51, NPs 3, 4, 7, and 9 were denoted as the defect structures. They exhibited either unfilled space in DNA box (NPs 3 and 4, arrows show the unfilled space in DNA box), or larger dimensions than designed (NPs 7 and 9).

- Structure Types 3-5: Uncounted structures

  A Ag NP that was grown in an ill formed box (Type 3) or that was not attached to any DNA barrel or box (Type 4) was not counted in the yield analysis. In fig. S51, NPs 2, 6, 11, 12, 13, 14, 15, and 16 were denoted as the uncounted structures. They were grown either within an open DNA box (NPs 2, 6, and 13) or within an open barrel (NPs 11, 14, and 15) or without surrounding DNA molds (NPs 12 and 16). The open box comes from the unpurified open DNA boxes in Step 3.

  Additionally, Type 5 structures refer to the DNA barrels or (well- or ill-formed) boxes that contained no NPs, e.g. the un-labeled DNA box to the right of structure 7 in fig. S51.

Similar criteria applies to the other two DNA box molds with 21 nm by 16 nm by 20 nm cavity and 16 nm by 16 nm by 20 nm cavity.

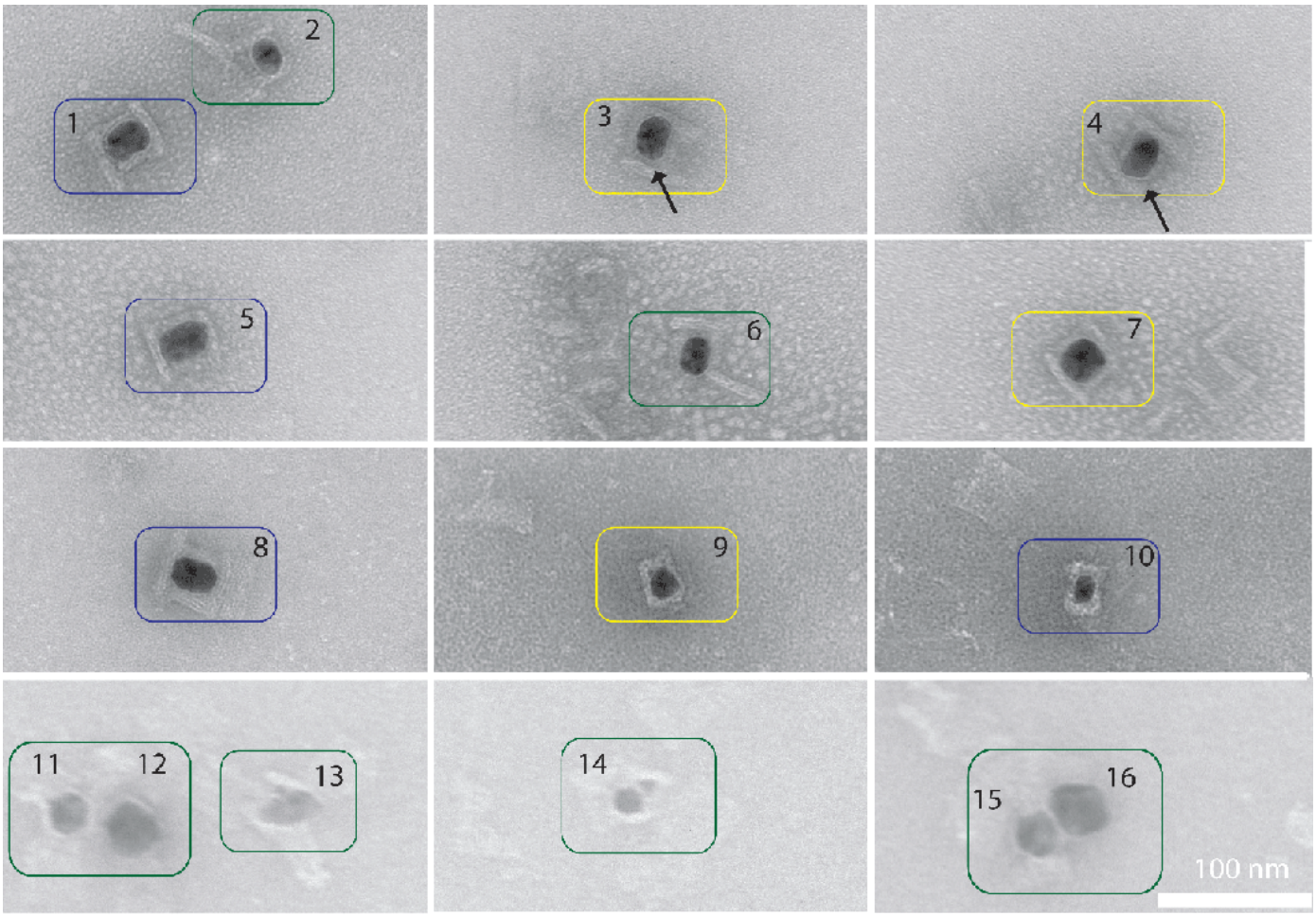

Fig. S51: **Sample images of well-formed, defect, and uncounted Ag NP growth within DNA box with 21 nm by 16 nm by 30 nm cavity**. Blue and yellow circles indicate Type I (well-formed NP in well-formed box) and Type 2 (ill-formed NP in well-formed box) structures, respectively. Green circles indicate the uncounted structures (Types 3, a NP in an ill-formed box; Type 4, a NP that was not attached to any barrel/box), which were not included in the yield analysis. For structures 3 and 4, the arrows point to the defective sites. For example, the bottom right corner of the NP 3 appeared defective.

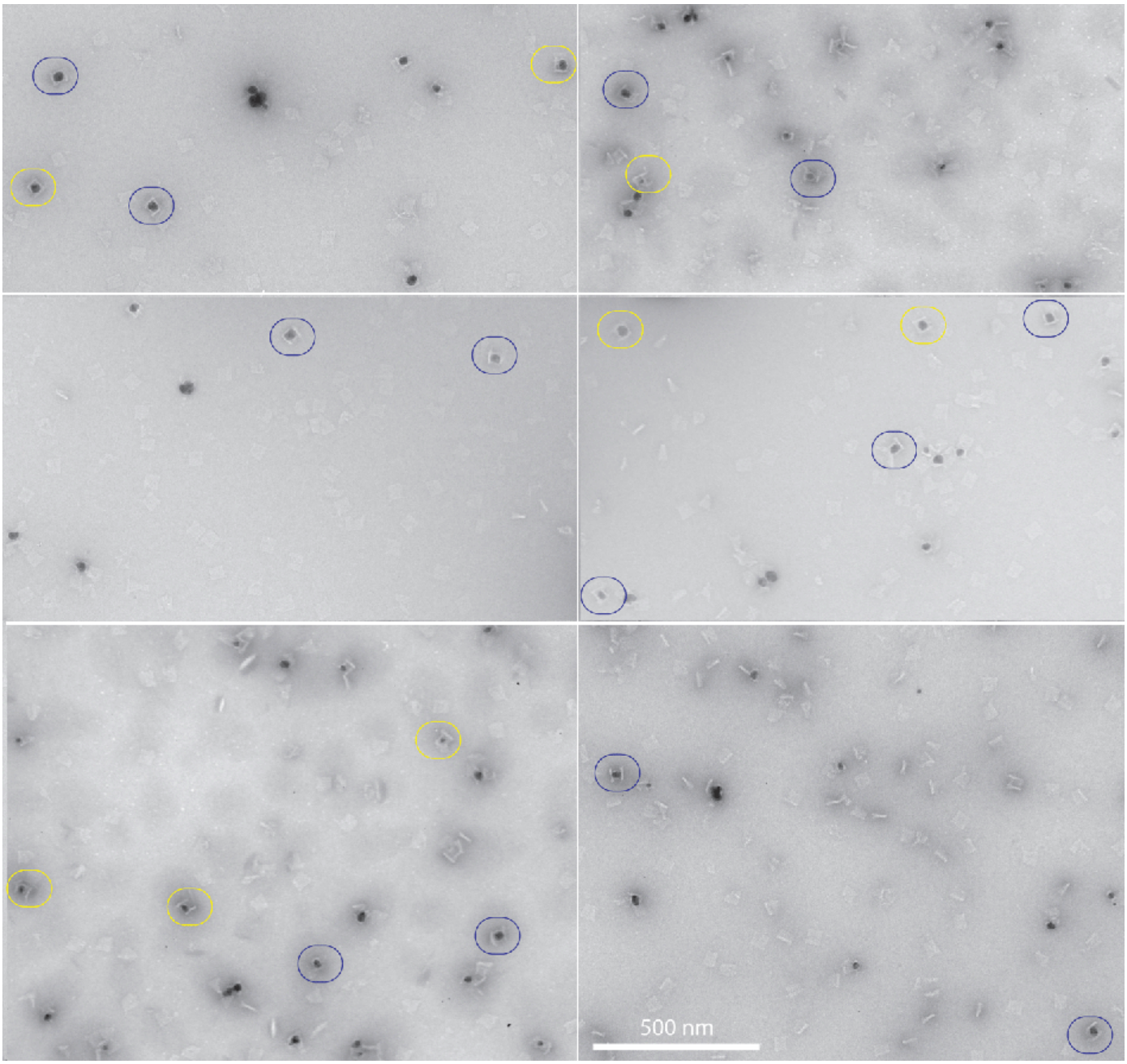

Fig. S52: **Ag NP growth within DNA box with 21 nm by 16 nm by 30 nm cavity**. Blue and yellow circles indicate Type I (well-formed NP in well-formed box) and Type 2 (ill-formed NP in well-formed box) structures, respectively. Only these structures with well-formed box molds were used in determining the NP growth yield (Yield 4). The unlabeled structures were not counted in yield analysis.

S9.3 Ag NP growth within DNA box with 21 nm by 16 nm by 20 nm cavity

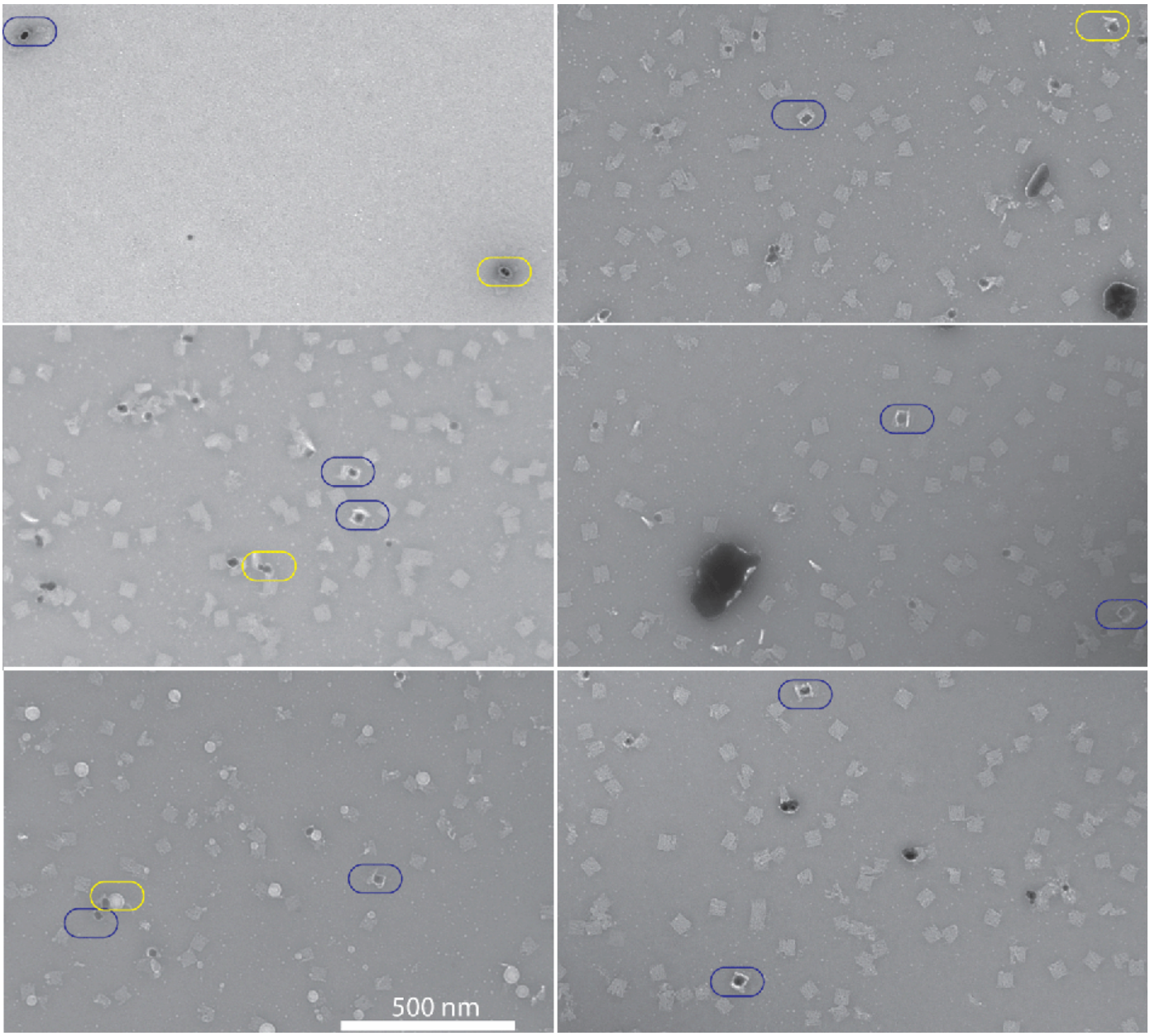

Fig. S53: **Ag NP growth within DNA box with 21 nm by 16 nm by 20 nm cavity**. Blue and yellow circles indicate Type I (well-formed NP in well-formed box) and Type 2 (ill-formed NP in well-formed box) structures, respectively. Only these structures with well-formed box molds were used in determining the NP growth yield (Yield 4). The unlabeled structures were not counted in yield analysis.

S9.4 Ag NP growth within DNA box with 16 nm by 16 nm by 20 nm cavity

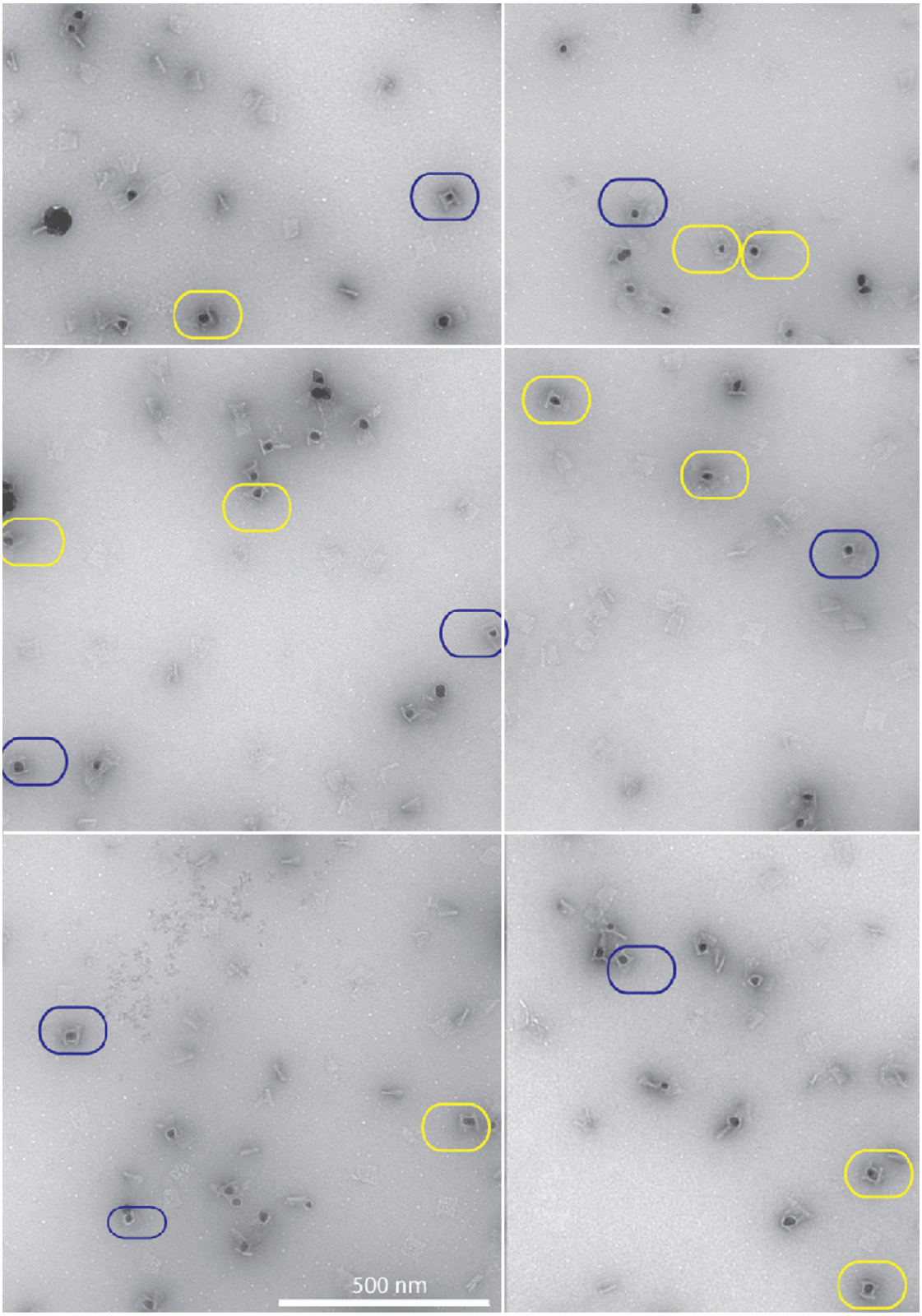

Fig. S54: **Ag NP growth within DNA box with 16 nm by 16 nm by 20 nm cavity.** Blue and yellow circles indicate Type I (well-formed NP in well-formed box) and Type 2 (ill-formed NP in well-formed box) structures, respectively. Only these structures with well-formed box molds were used in determining the NP growth yield (Yield 4). The unlabeled structures were not counted in yield analysis.

S9.5 Ag NP growth within equilateral triangular-shaped DNA barrel with 30 nm by 30 nm by 30 nm cavity

We analyzed the NP growth yield (Yield 4 in Table 1) for the equilateral triangular DNA barrel mold with 30 nm by 30 nm by 30 nm cavity. In Sect. S5.6, when defining the NP growth yield, 5 types of structures were observed in TEM images and Structure Type 1 (a well-formed equilateral triangular barrel containing a well-formed NP) and Structure Type 2 (a well-formed barrel containing an ill-formed NP) were considered for yield calculation, and Structure Types (3-5) were uncounted. We describe below the more detailed criteria for determining Structure Type 1 v.s. Structure Type 2 with typical TEM images (fig. S55), and show some typical TEM images for Structure Types 3-5 (uncounted structures) (fig. S55). Additional large-field-of-view images are shown in fig. S56.

- Type 1: A well-formed NP in a well-formed barrel mold

  A well-formed Ag NP within a DNA-barrel mold is defined as a NP with the designed cross-section shape and dimensions in the projection view. Additionally, the DNA barrels surrounding the Ag NPs must be well-formed. In fig. S55, NPs 1, 3, 8, 9, 14, and 20 were categorized as the well-formed structures. They exhibited designed equilateral triangular cross-sections, and occupied the available space in the DNA barrel molds. Note that rounded corners were observed in all the NPs.

- Type 2: An ill-formed NP in a well-formed barrel mold

  An ill-formed Ag NP within a DNA-barrel mold is defined as a NP that deviated from the designed cross-section shape or dimensions in the projection view. Additionally, the DNA barrels surrounding the Ag NPs must be well-formed. In fig. S55, NPs 2, 7, 12, and 13 were considered as ill-formed. They exhibited either unfilled space in the DNA mold (NP 7), or off-plane growth (NPs 2, 12, and 13).

- Structure Types 3-5: Uncounted structures

  If the *x*-*y* projection view of the triangular mold could not be seen from the structure, such a Ag NP was not considered in yield analysis (Type 3). Similarly a Ag NP that was not attached to any mold was not consider in the yield analysis (Type 4). In fig. S55, NPs 4, 5, 6, 10, 11, 16, 17, 18, 19, and 21 were denoted as the uncounted structures. The *x*-*y* cross section of triangular mold could not be seen in NPs 4, 5, 6, 10, 17, 19, and 21. No DNA mold was observed surrounding NPs 11, 16, and 18.

  Additionally, Type 5 structures refer to empty DNA molds, e.g. the un-labeled DNA mold to the left of structure 19 in fig. S55.

Similar criteria applies to the right angular triangular mold in Sect. S9.6 and DNA ring mold in Sect. S9.7.

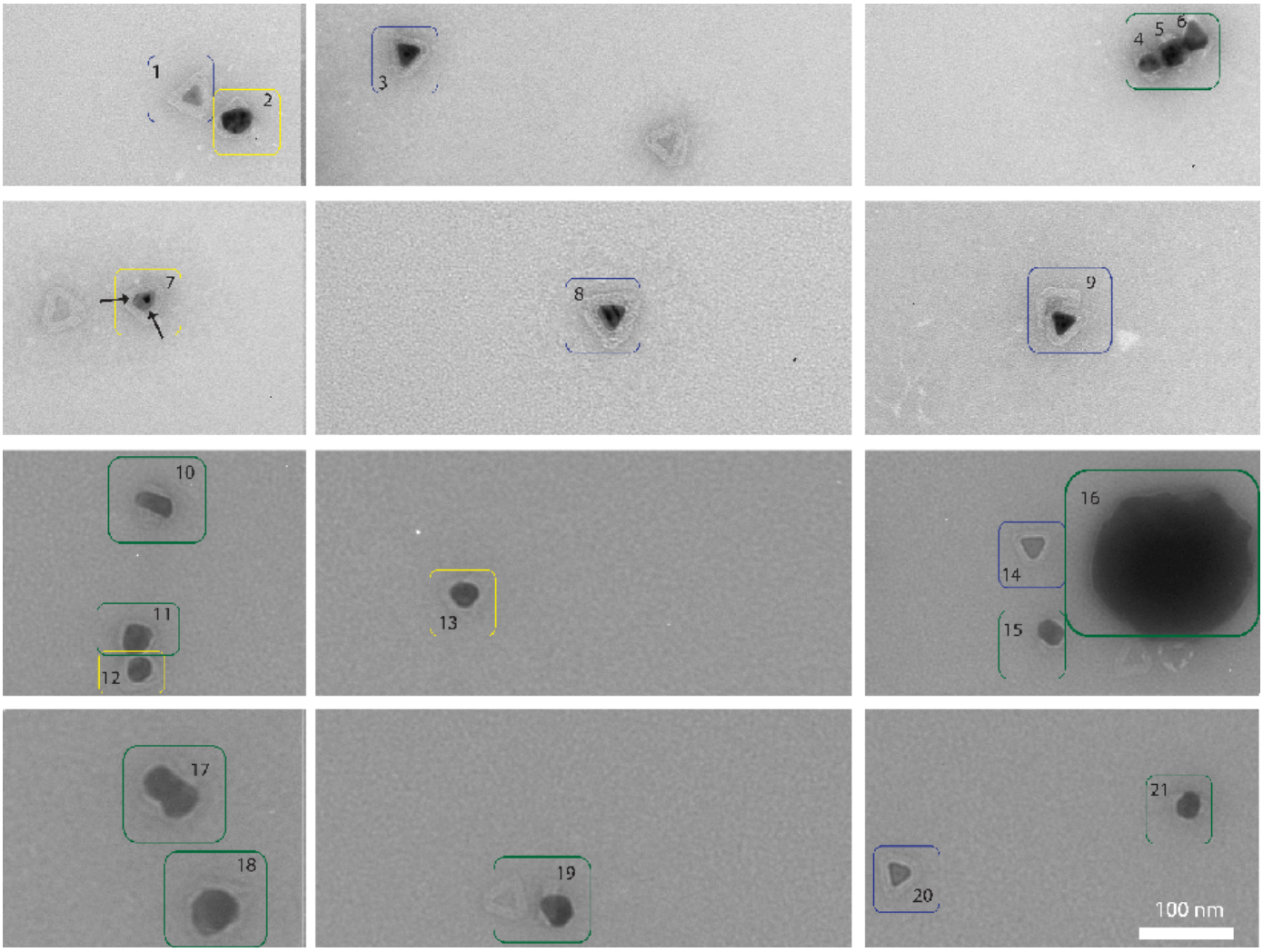

Fig. S55: **Example images of well-formed, defective, and uncounted Ag NPs grown using a DNA barrel mold with a 30 nm by 30 nm by 30 nm triangular cross-section shape**. Blue and yellow circles indicate Type I (well-formed NP in well-formed barrel mold) and Type 2 (ill-formed NP in well-formed barrel) structures, respectively. For structure 7, the arrows point to the defective sites. Green circles indicate the uncounted structures (Types 3, a NP attached to a barrel whose *x*-*y* projection view was not visible; Type 4, a NP that was not attached to any barrel), which were not included in the yield analysis.

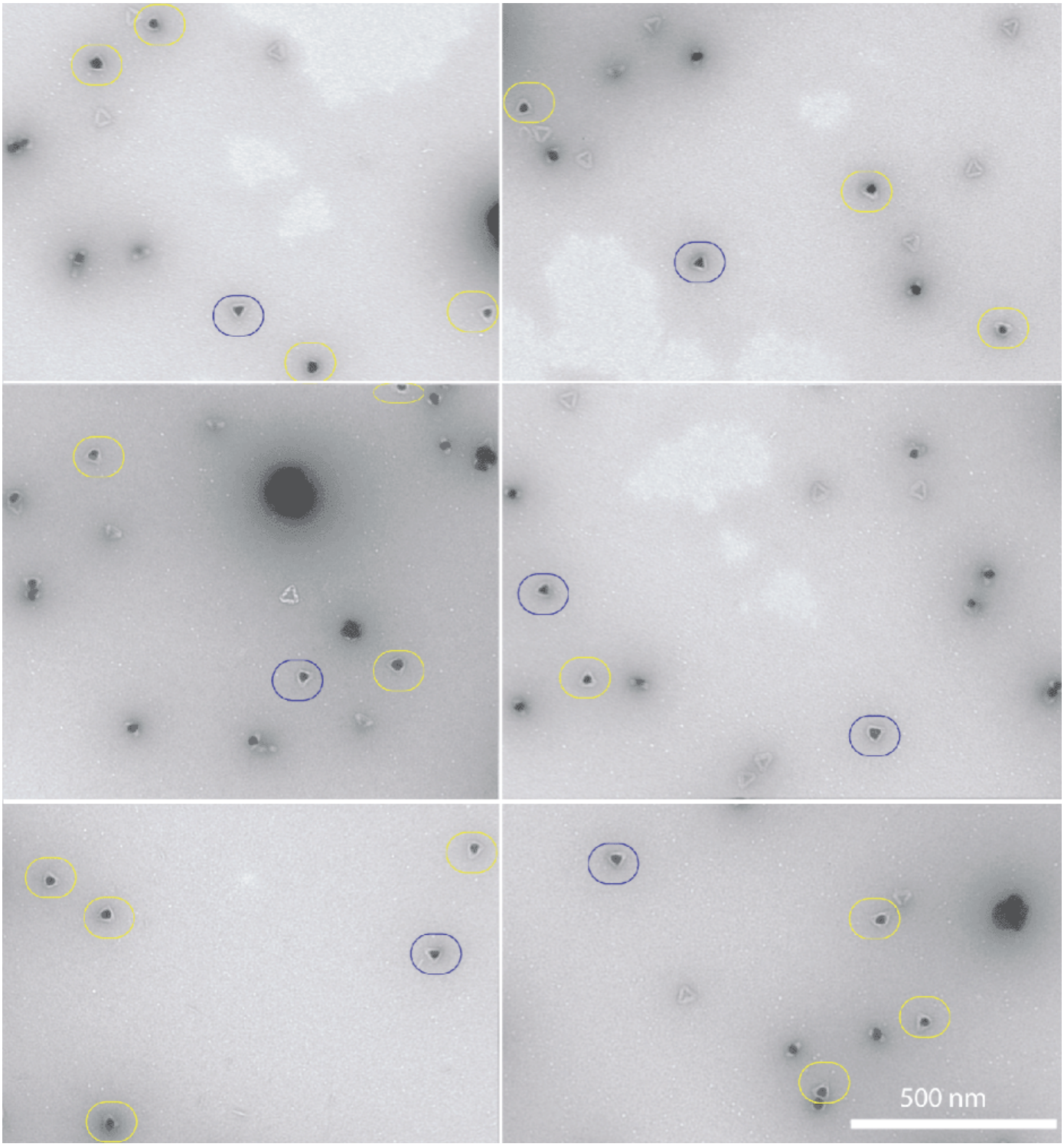

Fig. S56: **Ag NP growth within the equilateral triangular shaped DNA barrel with 30 nm by 30 nm by 30 nm cavity**. Blue circle represents the well-formed Ag NPs. Yellow circle represents the defect structures that are counted in yield analysis. The unlabeled Ag NPs are uncounted in yield analysis.

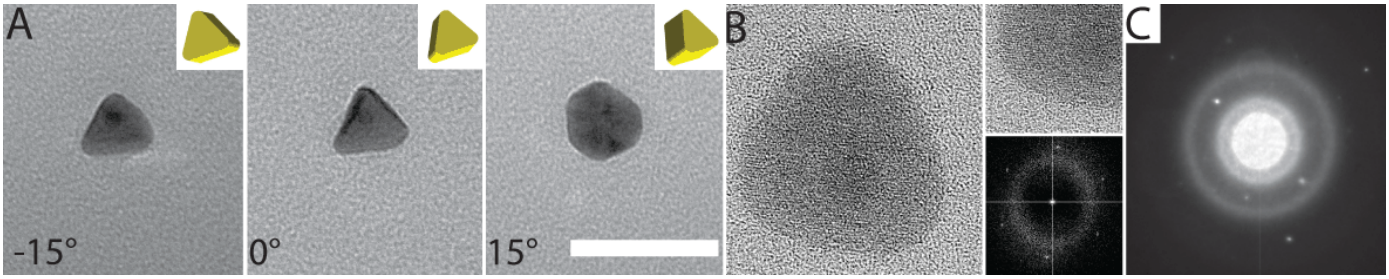

Fig. S57: **Structural characterization for Ag NP grown within the equilateral triangular shaped DNA barrel with 30 nm by 30 nm by 30 nm cavity**. (A) TEM imaging for tilted Ag NP growth within the equilateral triangular shaped DNA barrel with 30 nm by 30 nm by 30 nm cavity. Tilted angles of TEM grid were selected as: -15°, 0° and 15° along the x-direction. The insets show the schematics of the tilted orientations of Ag NP. The scale bar is 50 nm. (B) High-resolution TEM for the cast Ag NP. Left, zoom-out view of the whole NP. The dark circle represents a Au seed. Right top, zoom-in view of Ag NP. Right bottom, FFT analysis of the NP. Under 200 keV irradiation condition, the corners got even round, due to the instability of relative sharp corners. (C) Electron diffraction pattern for the cast Ag NP. The sample was not stained before imaging to prevent interference from staining agent to visualize the crystallographic facets.

S9.6 Ag NP growth within right triangular DNA barrel with 22 nm by 30 nm by 38 nm cavity

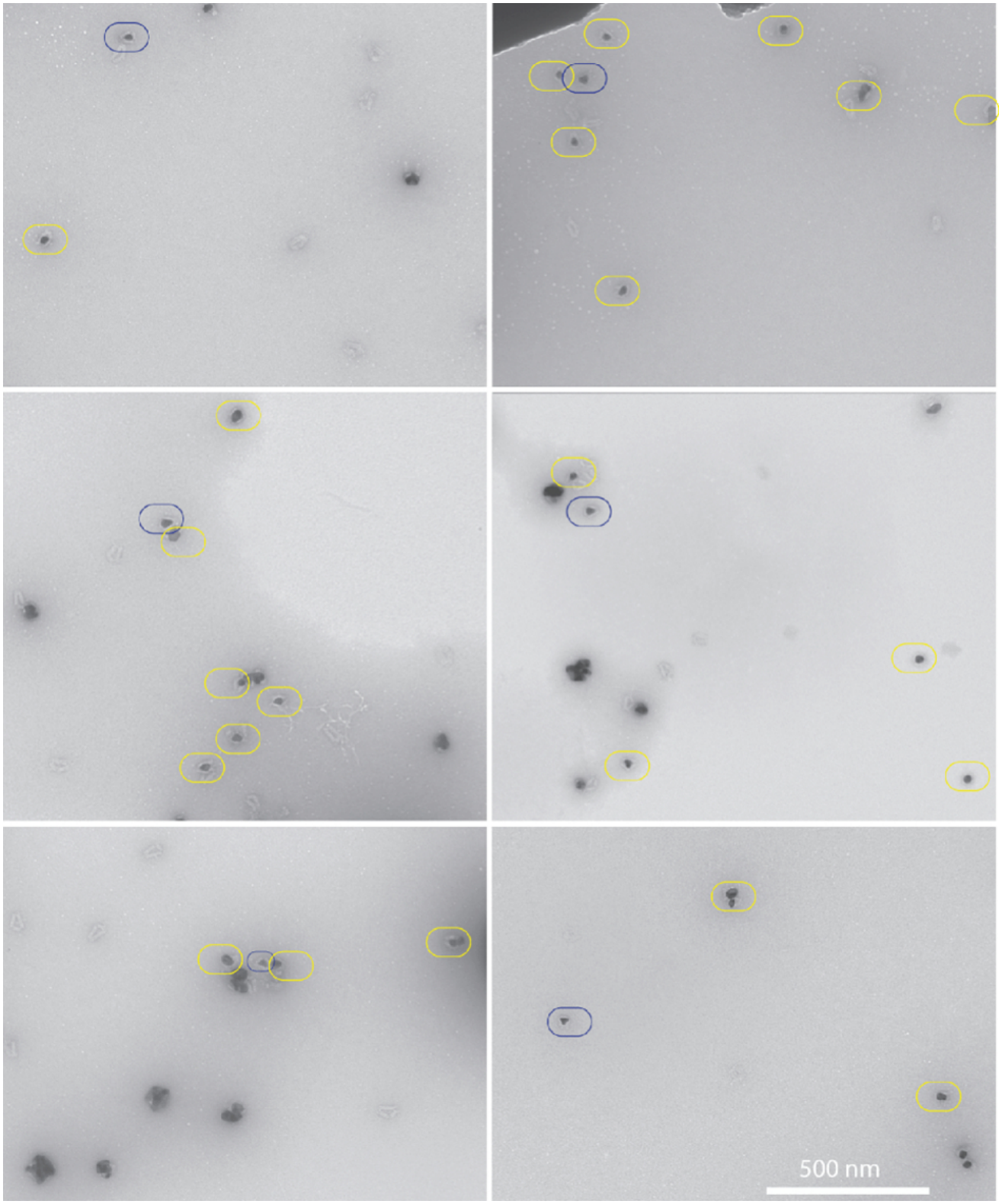

Fig. S58: **Ag NP growth within triangular DNA barrel with 22 nm by 30 nm by 38 nm cross-section**. Blue circle represents the well-formed Ag NPs. Yellow circle represents the defect structures that are counted in yield analysis. The unlabeled Ag NPs are uncounted in yield analysis.

S9.7 Ag NP growth within DNA ring with 25 nm inner diameter cavity

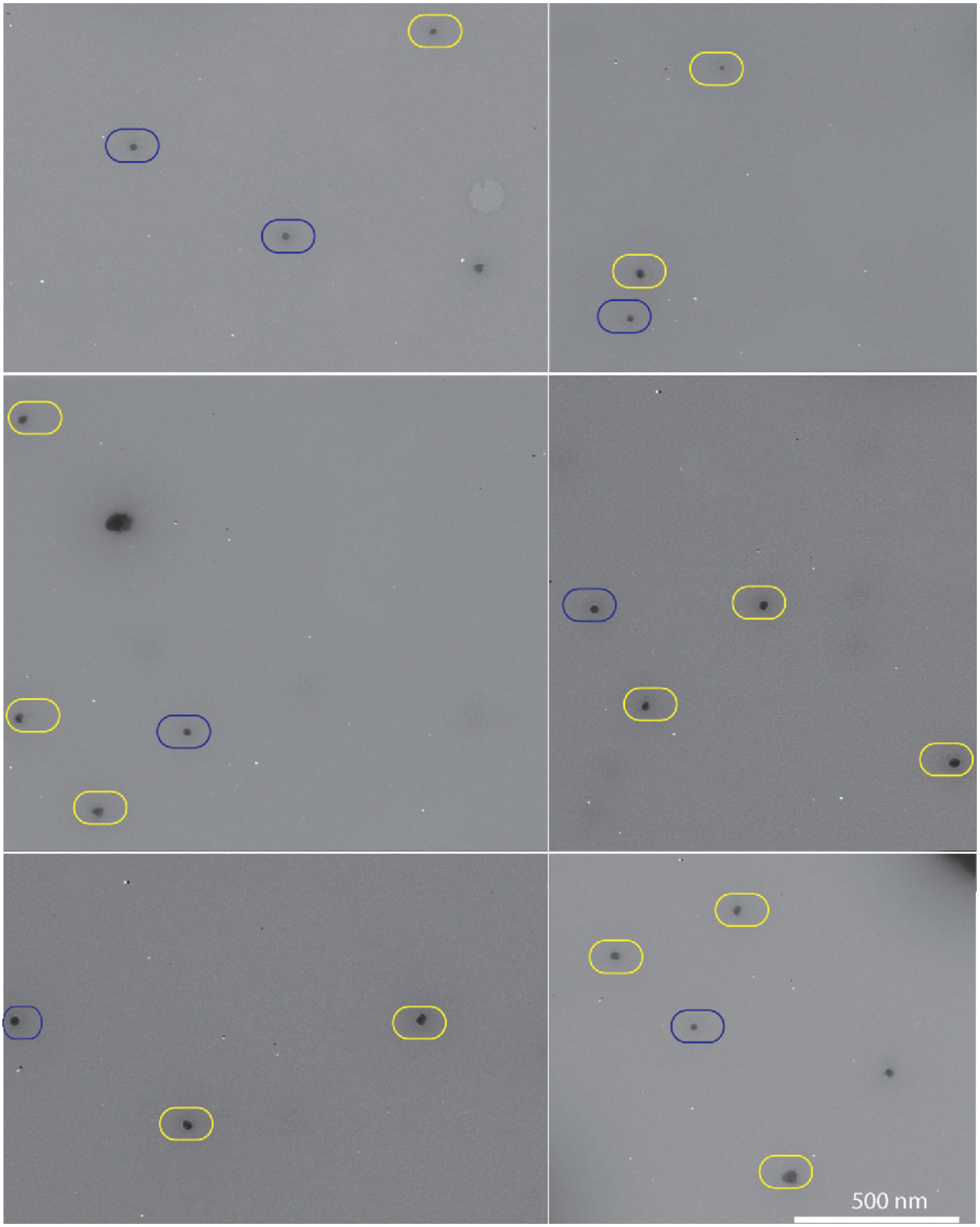

Fig. S59: **Ag NP growth within DNA ring with 25 nm inner diameter**. Blue circle represents the well-formed Ag NPs. Yellow circle represents the defect structures that are counted in yield analysis. The unlabeled Ag NPs are uncounted in yield analysis.

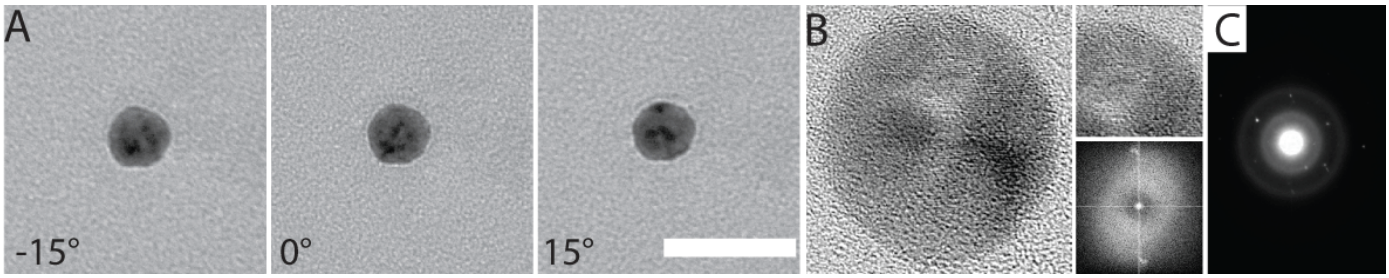

Fig. S60: **Structural characterization for Ag NP grown within DNA ring with 25 nm inner diameter cavity**. (A) TEM imaging for tilted Ag NP growth within DNA ring with 25 nm inner diameter. Tilted angles of the TEM grid were selected as: -15°, 0° and 15° along the x-direction. The scale bar is 50 nm. (B) High-resolution TEM for the cast Ag NP. Left, zoom-out view of the whole NP. Right top, zoom-in view of Ag NP. Right bottom, FFT analysis of the NP. (C) Electron diffraction pattern for the cast Ag NP. The sample was not stained before imaging to prevent interference from staining agent to visualize the crystallographic facets.

S9.8 Au NP growth within DNA barrel with 21 nm by 16 nm by 30 nm cuboid cavity

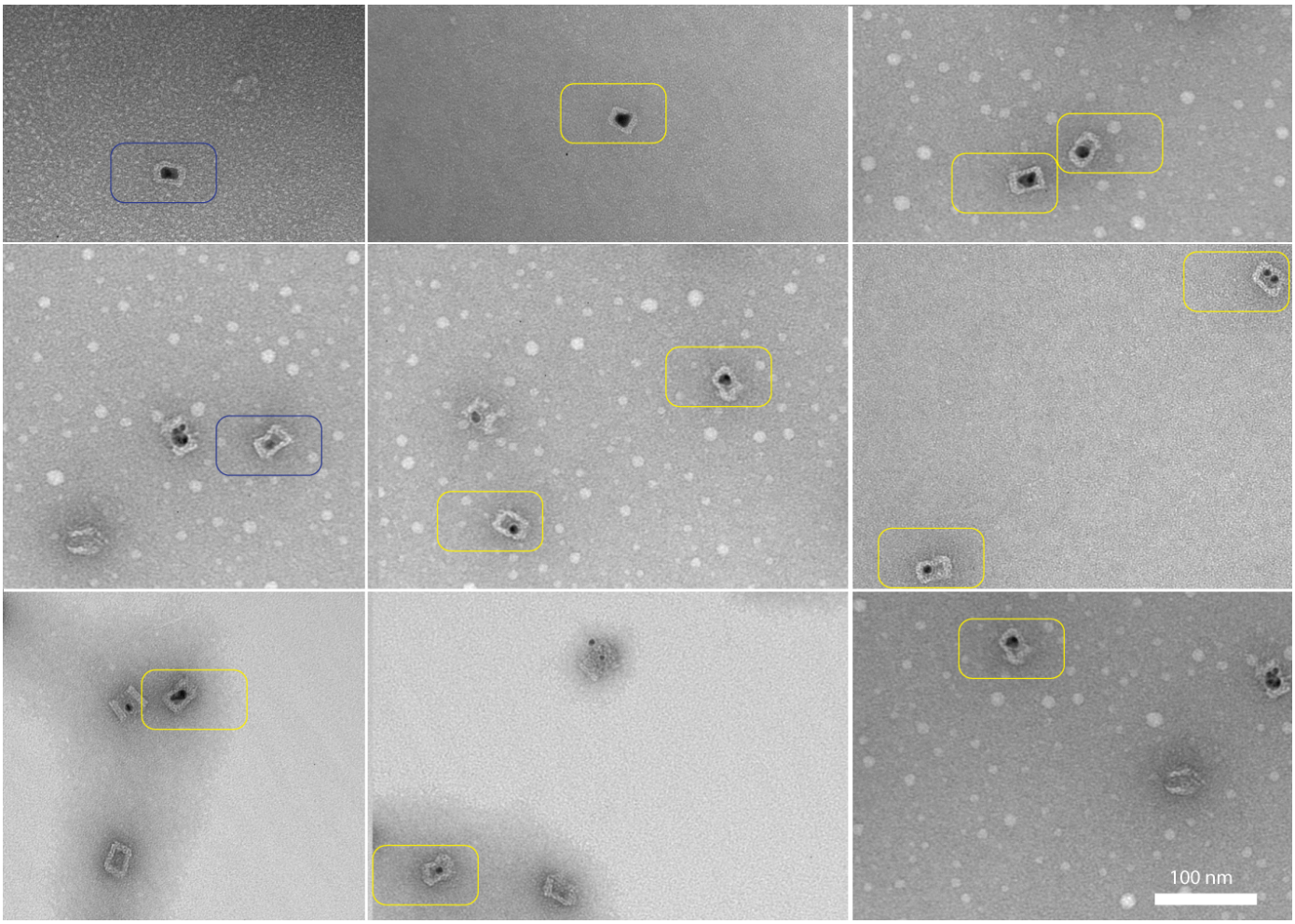

Fig. S61: **Typical TEM images for Au NP growth within DNA barrel with 21 nm by 16 nm by 30 nm cuboid cavity**. Blue circle represents the well-formed Au NPs. Yellow circle represents the defect structures that are counted in yield analysis. The unlabeled Au NPs are uncounted in yield analysis.

S9.9 Ag NP growth within Y-shaped DNA composite

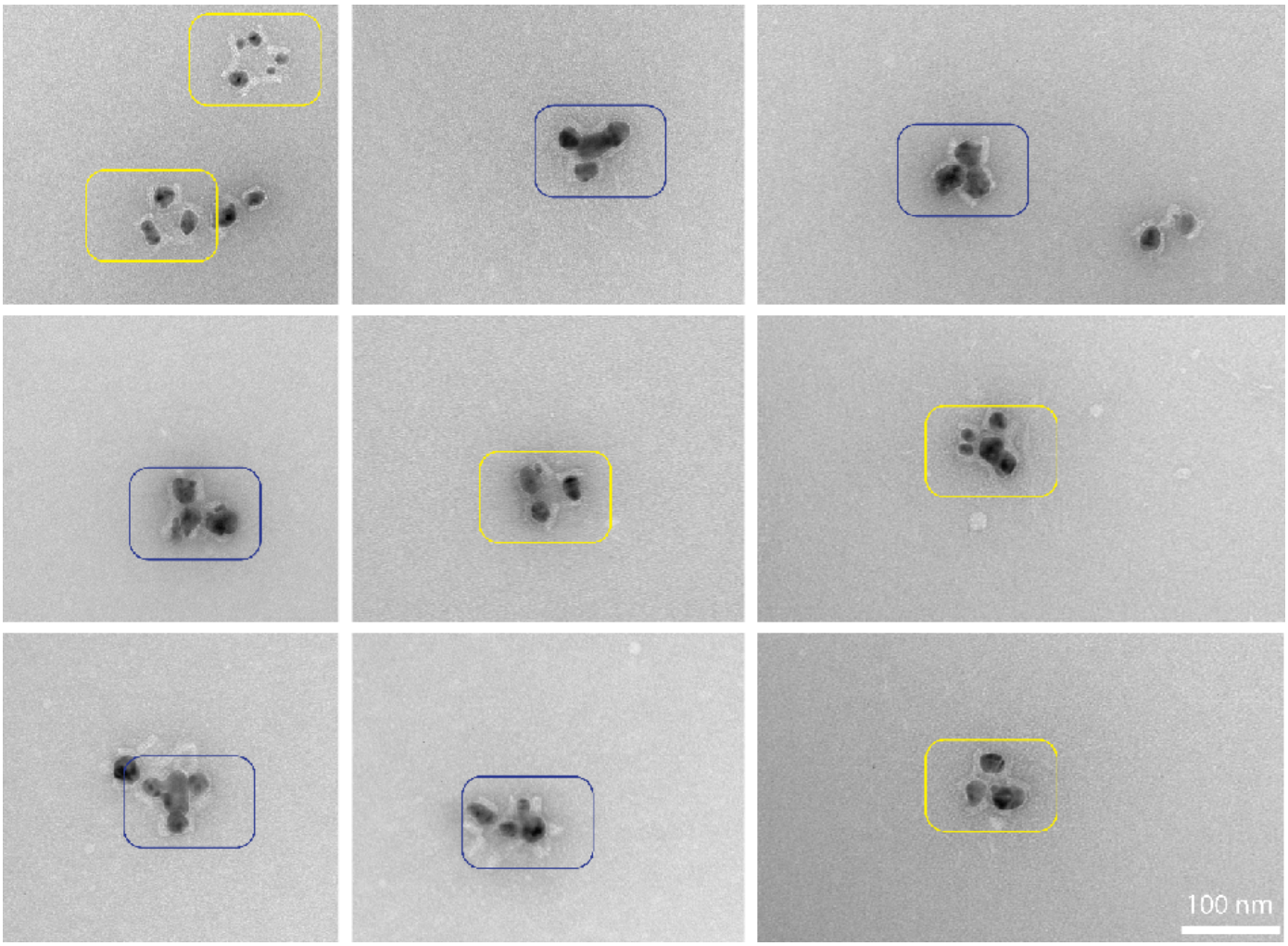

Fig. S62: **Typical TEM images for Ag NP growth within Y-shaped DNA composite**. Blue circle represents the well-formed Ag NPs. Yellow circle represents the defect structures that are counted in yield analysis. The unlabeled Ag NPs are uncounted in yield analysis.

S9.10 Ag NP growth within QD-DNA-QD composite

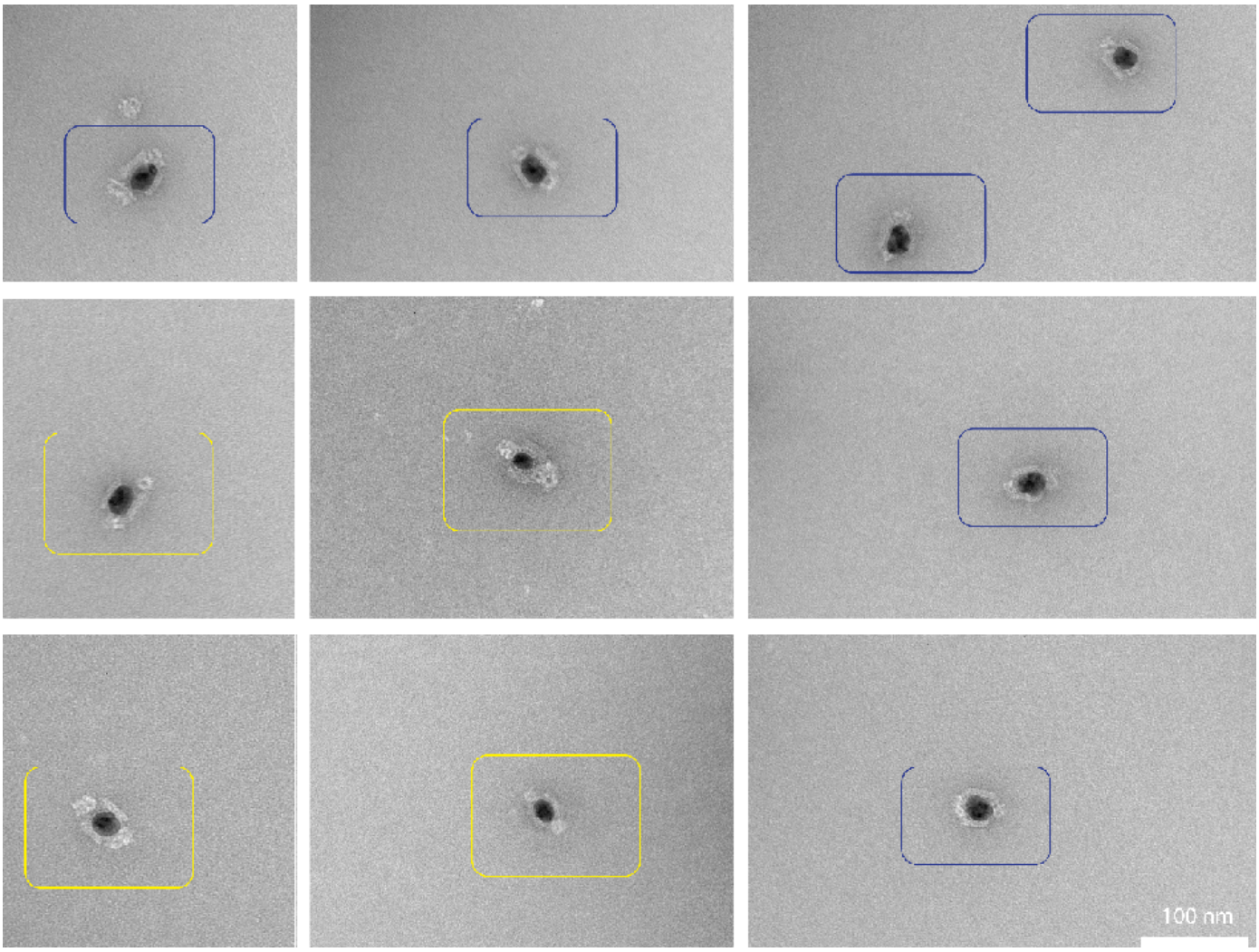

Fig. S63: **Typical TEM images for Ag NP growth within QD-DNA-QD composite**. Blue circle represents the well-formed Ag NPs. Yellow circle represents the defect structures that are counted in yield analysis.

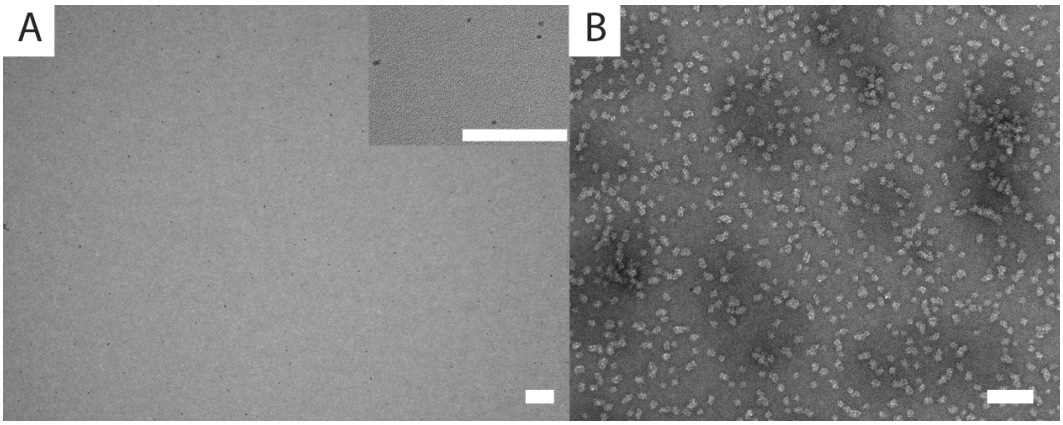

Fig. S64: **Typical TEM images for unstained (A) and stained (B) individual QDs**. In (A), the inset shows the zoom-in image of sub-5 nm CdSe@ZnS NP. In (B), the stained image shows the PEG and streptavidin coating layer around CdSe@ZnS. The scale bar is 100 nm.

S9.11 Parallel production of different shaped Ag NPs

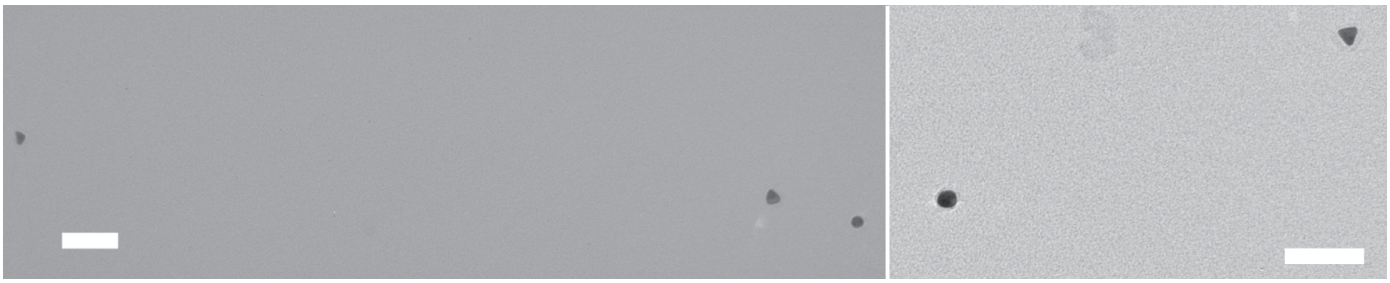

Fig. S65: **TEM images for the parallel production of different shaped Ag NPs within a single reaction solution**. Seed-decorated DNA molds from Fig. 4A-C were mixed within a single reaction solution, and produced three shaped Ag NPs simultaneously. Ag NPs were imaged without staining. The scale bars are 100 nm.

S10 Casting optimization

S10.1 Optimization process

Several key steps in the nanocasting process were optimized.

1. **Stiffness and integrity of DNA molds**

   Successful transfer of the cavity shape to the metal NP depends on the stiffness and integrity of DNA molds.

   (a) *Sidewall thickness*

   Single-layered DNA mold with fully enclosed cavities have been reported before. Our initial attempt with open ended DNA barrels revealed that the single-layered sidewall mold that we tested did not retain the designed cross-section shape in TEM images (see fig. S67 in Sect. S10.2.1). When the thickness of the sidewalls was increased to two or more layers, designed cross-sections, such as rectangle and square shapes, were well retained. Thus all the DNA molds reported in the main text were engineered with multi-layered sidewalls.

   (b) *Helix crossovers*

   During metal growth, the integrity of DNA molds appeared dependent on the number of crossovers between neighboring helices. DNA molds with 1 or 2 crossovers between neighboring helices exhibited much lower integrity than those with 4 to 5 crossovers.

   For example, a DNA barrel with triangular *x-z* cross-section cavity was designed such that mold contains several 10-nm DNA helices in one vertex of the triangular cavity (denoted by red arrow in fig. S68). Most of the 10 nm neighboring helices in this region were connected by only one crossover. After seed decoration, lid closure, and metal growth, the spacing between neighboring 10-nm helices was largely expanded, resulting in distorted DNA molds.

   Similarly, an equilateral triangular shaped DNA mold with 15 nm by 15nm by 15 nm cavity was observed to possess less structural integrity compared with the triangular mold with 30 nm by 30 nm by 30 nm cavity. The Ag NP grown within was mostly sphere like structures, with rare occasions for triangular shaped Ag NPs (1%, $N > 100$, Sect. S10.2.3).

   (c) *Helix packing geometry*

   Different helix packing geometry produced distinct structural integrity during metal NP growth. Honeycomb lattice packing geometry was used to build a hexagonal DNA mold (Sect. S10.2.4). Ag growth within the DNA molds produced distorted *x-y* cross section from the designed hexagonal shape. All the DNA molds reported in the main text were constructed with square lattice packing geometry.

   (d) *Ionic conditions*

   At 10 mM magnesium nitrate concentration, DNA mold remained intact for 1 day at 1-2 mM reactant (Ag nitrate and ascorbic acid) concentration. When Mg^{2+} concentration was decreased to 10 μM, DNA molds dissociated less than 1 minute in the presence of metal precursors (Ag nitrate). In addition, DNA molds turned less stable when Ag nitrate concentration was higher than 20 mM or ascorbic acid concentration was higher than 50 mM, even in the presence of 10 mM Mg^{2+}.

2. **Au seed decoration**

   (a) *Handle strands*.

   It has been reported surface binding groups, such as DNA or protein, may affect the seed-mediated growth kinetics and morphology of NPs (*82, 83*). To minimize the surface ligand effect on NP growth, the stoichiometry between anti-handle and Au seed was set to 1:1.

   (b) *Ionic conditions*.

   However, low surface coverage of DNA anti-handles on Au NP decreased the stability of Au NPs in the presence of 10 mM Mg^{2+} and produced the aggregation of Au seeds within 1 hour at 35 °C (data unshown). To prevent the aggregation, 50 mM Na^{+} was added to the solution, which increased the colloid stability of Au seeds to more than 19 hours at 35 °C.

   (c) *Mold geometry*.

   Seed decoration yield within DNA molds was affected by the size of the DNA barrel mold. For example, for a 10 nm diameter DNA tube, seed decoration was lower than 1% (Sect. S10.2.5); when the diameter of DNA barrel was increased to more than 15 nm, seed decoration was increased more than 70%.

3. **Box closure**

(a) *Connector/anti-connector design*

Box closure yield (Yield 3) was optimized by tuning the numbers of connectors on DNA barrels. The optimization was based on the rectangular barrel with 21 nm by 16 nm by 30 nm cavity. At a lid-to-barrel stoichiometry ratio of 3:1, 6 connectors on each end of the rectangular barrel produced less than 10% box formation yield; whereas increasing the connectors to at least 14 at each end promoted the box formation yield to 31%.

(b) *Lid-to-barrel stoichiometry*

Box closure yield (Yield 3) was also optimized by modulating stoichiometry between DNA barrels and lids. Raising the lid-to-barrel stoichiometry from 2:1 to 6:1 resulted in the slightly increase of box formation yield from 28% to 33%. However, at 6:1 stoichiometry ratio, each end of barrel was sometimes observed to connect to two lids, which prevented the correct lid closure. The yield of such defective structures with two lids at one end was also increased from 20% at 2:1 stoichiometry to 50% at 6:1 stoichiometry. The formation of such defective structures would prevent further increase of DNA box formation yield at even higher stoichiometry ratio.

(c) *Purification attempt*

Agarose gel electrophoresis was tested to purify the seed-decorated DNA box. However, after gel purification, both opened and closed seed-decorated DNA boxes were observed under TEM, which likely resulted from either small mobility difference between opened and closed isomers or from box reopening during purification or subsequent imaging process. As such, the structures reported in this paper were imaged as unpurified structures.

S10.2 Failed and sub-optimal DNA molds used in the optimization process

S10.2.1 DNA barrel with single-layered sidewall

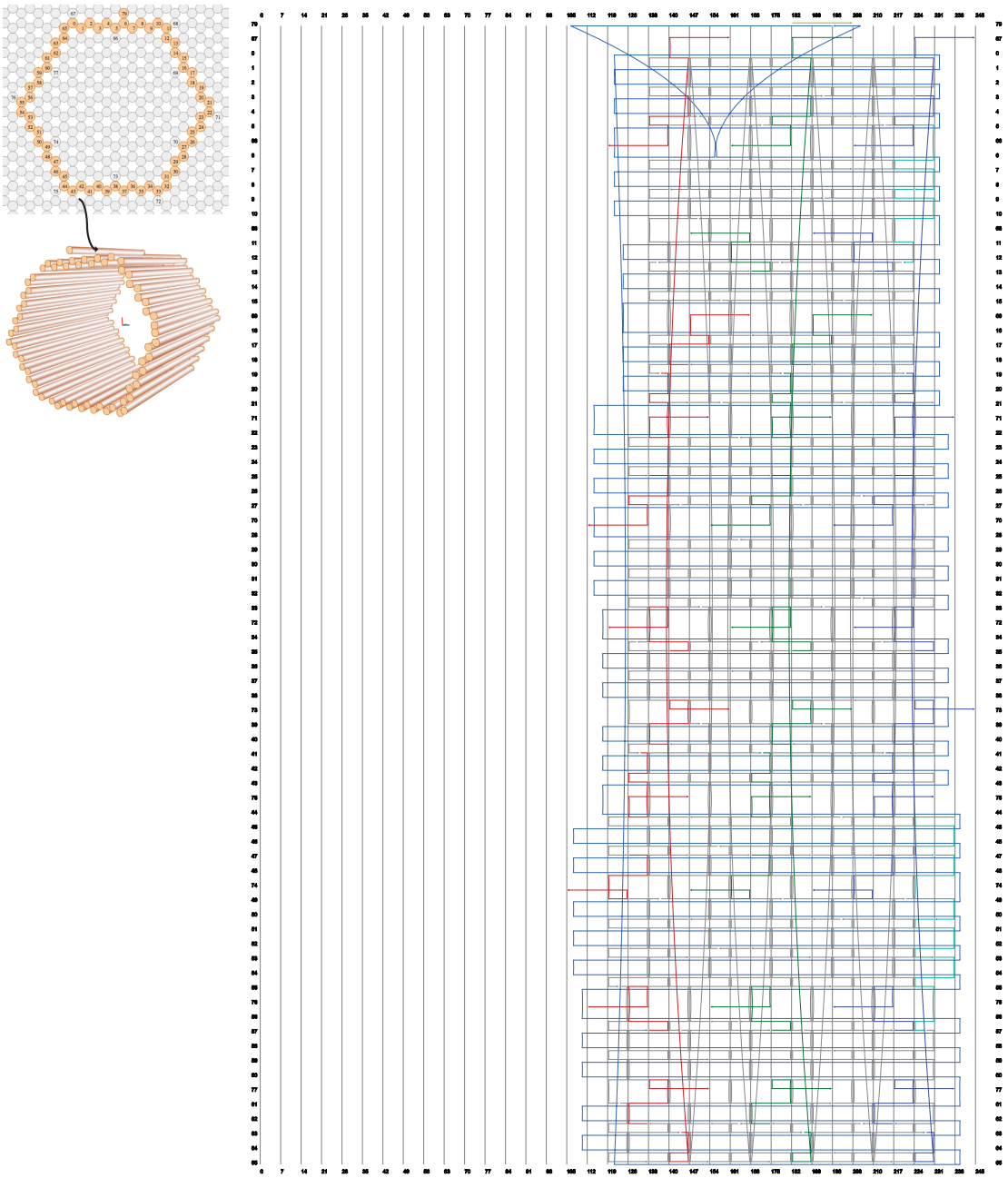

Fig. S66: **Strand diagram of DNA barrel with single-layered sidewall**. Left, cross-section view (top) and 3D view (bottom) in caDNAno format. Right, detailed diagram of all strands in caDNAno format. The numbers on the left and the right indicate the helices. The numbers on the top and the bottom indicate the position of the base pairs.

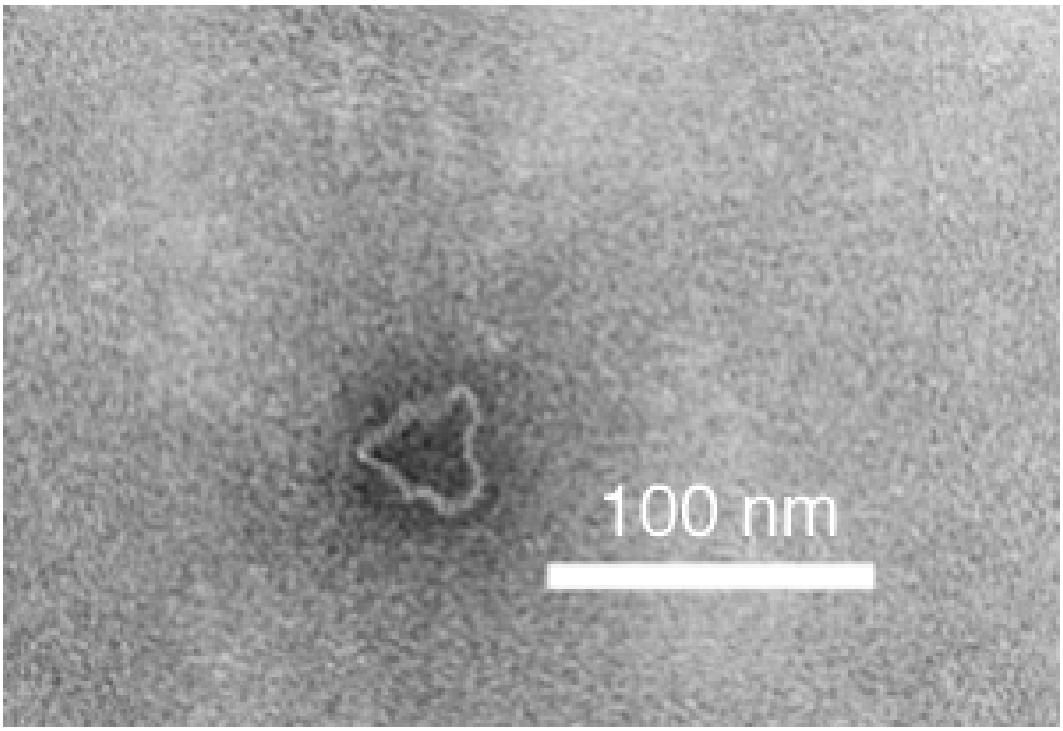

Fig. S67: **Top-view TEM image of DNA barrel with single-layered sidewall**.

S10.2.2 DNA box with triangular cavity

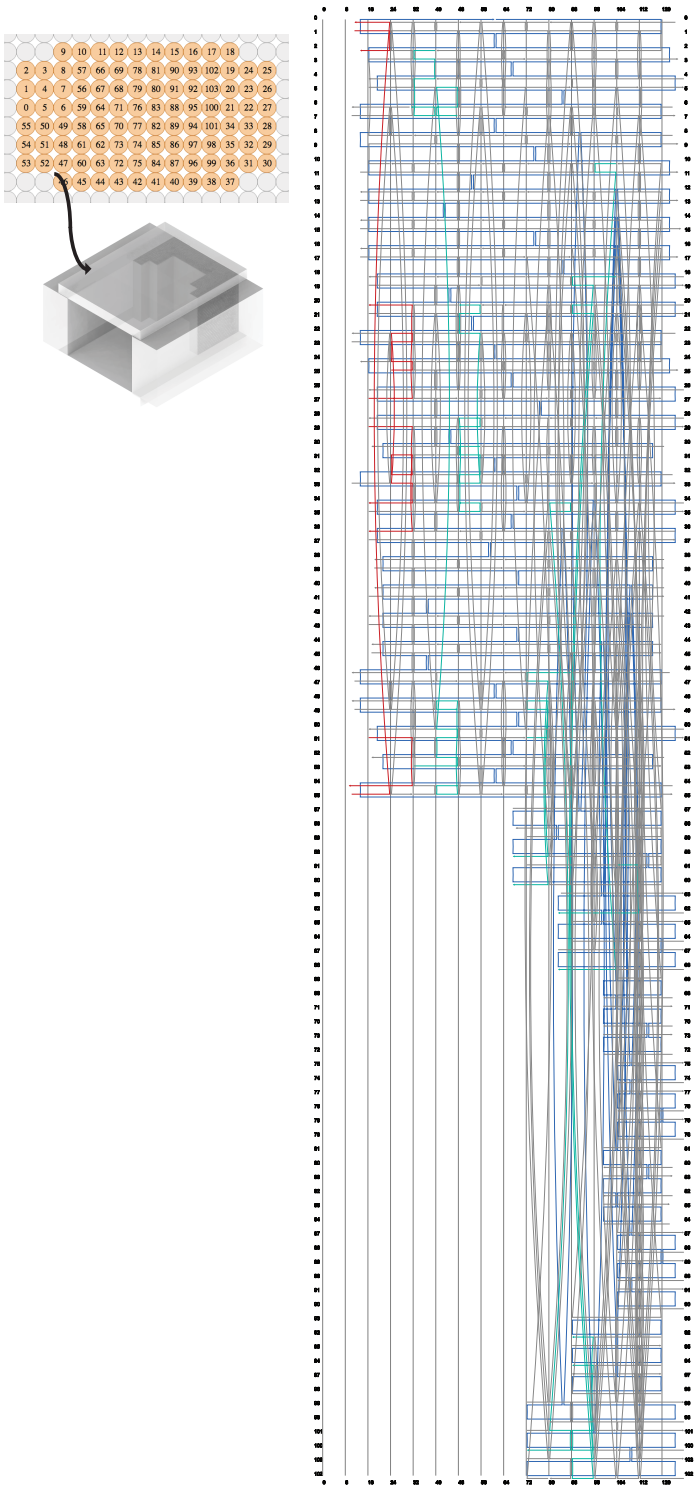

Fig. S68: **Strand diagram of DNA barrel with triangular cavity**. Left, cross-section view in caDNAno format (top) and corresponding 3D model (bottom). Right, detailed diagram of all strands in caDNAno format. The numbers on the left and the right indicate the helices. The numbers on the top and the bottom indicate the position of the base pairs.

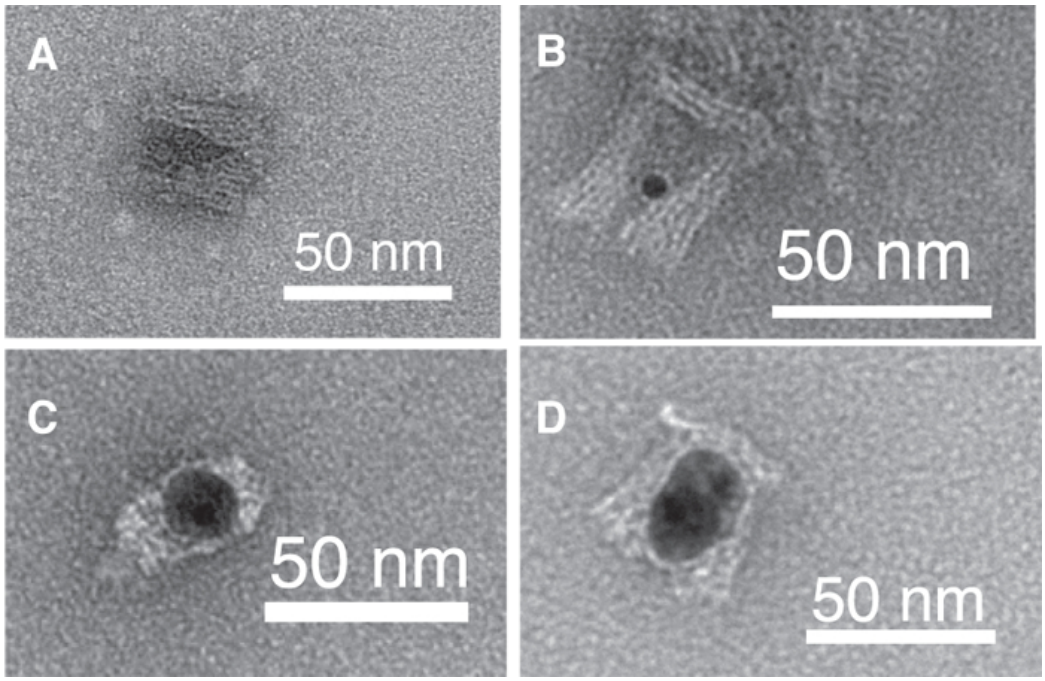

Fig. S69: **DNA box with triangular cavity for casting growth of Ag NPs**. (A) TEM image of triangular DNA barrel with triangular cavity. (B) TEM image of triangular DNA box after seed decoration. The black spot is 5 nm Au seed. (C) Top-view and (D) side-view of TEM image of Ag NP grown within triangular cavity. The reaction condition is shown in Sect. S2.5. Reaction time is 8 min.

S10.2.3 Triangular DNA barrel with 15 nm by 15 nm by 15 nm cavity

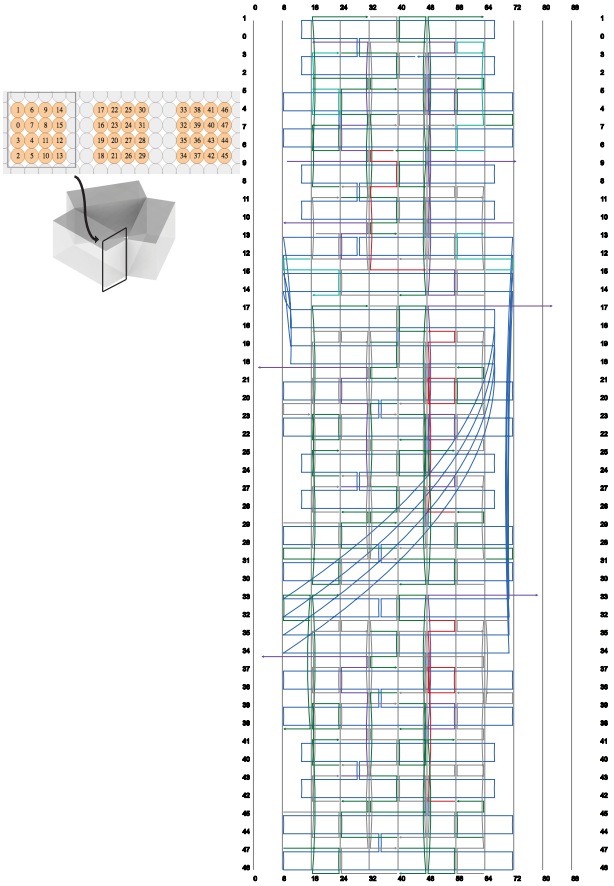

Fig. S70: **Strand diagram of triangular DNA barrel with 15 nm by 15 nm by 15 nm cavity**. Left, cross-section view in caDNAno format (top) and corresponding 3D model (bottom). Right, detailed diagram of all strands in caDNAno format. The numbers on the left and the right indicate the helices. The numbers on the top and the bottom indicate the position of the base pairs.

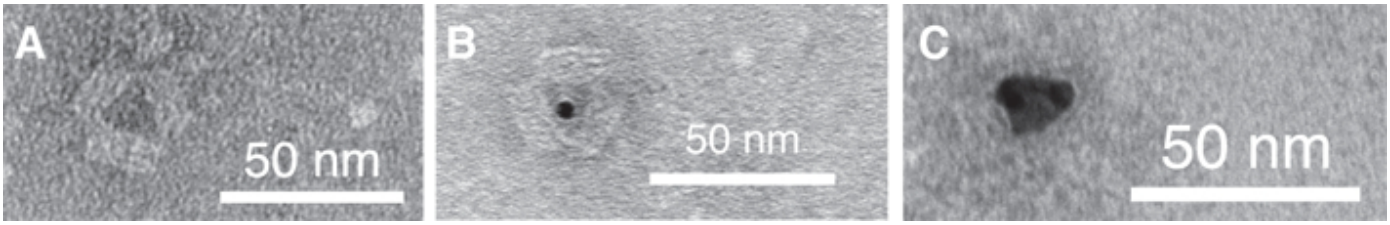

Fig. S71: **Triangular DNA barrel with 15 nm by 15 nm by 15 nm cavity for casting growth of Ag NPs**. (A) TEM image of triangular DNA barrel with 15 nm by 15 nm by 15 nm cavity. (B) TEM image of triangular DNA barrel with 15 nm by 15 nm by 15 nm cavity after seed decoration. The black spot is 5 nm Au seed. (C) Top-view TEM image of Ag NP grown within the 15 nm by 15 nm by 15 nm cavity. The reaction condition is shown in Sect. S2.5. Reaction time is 4 min.

S10.2.4 Hexagonal DNA barrel

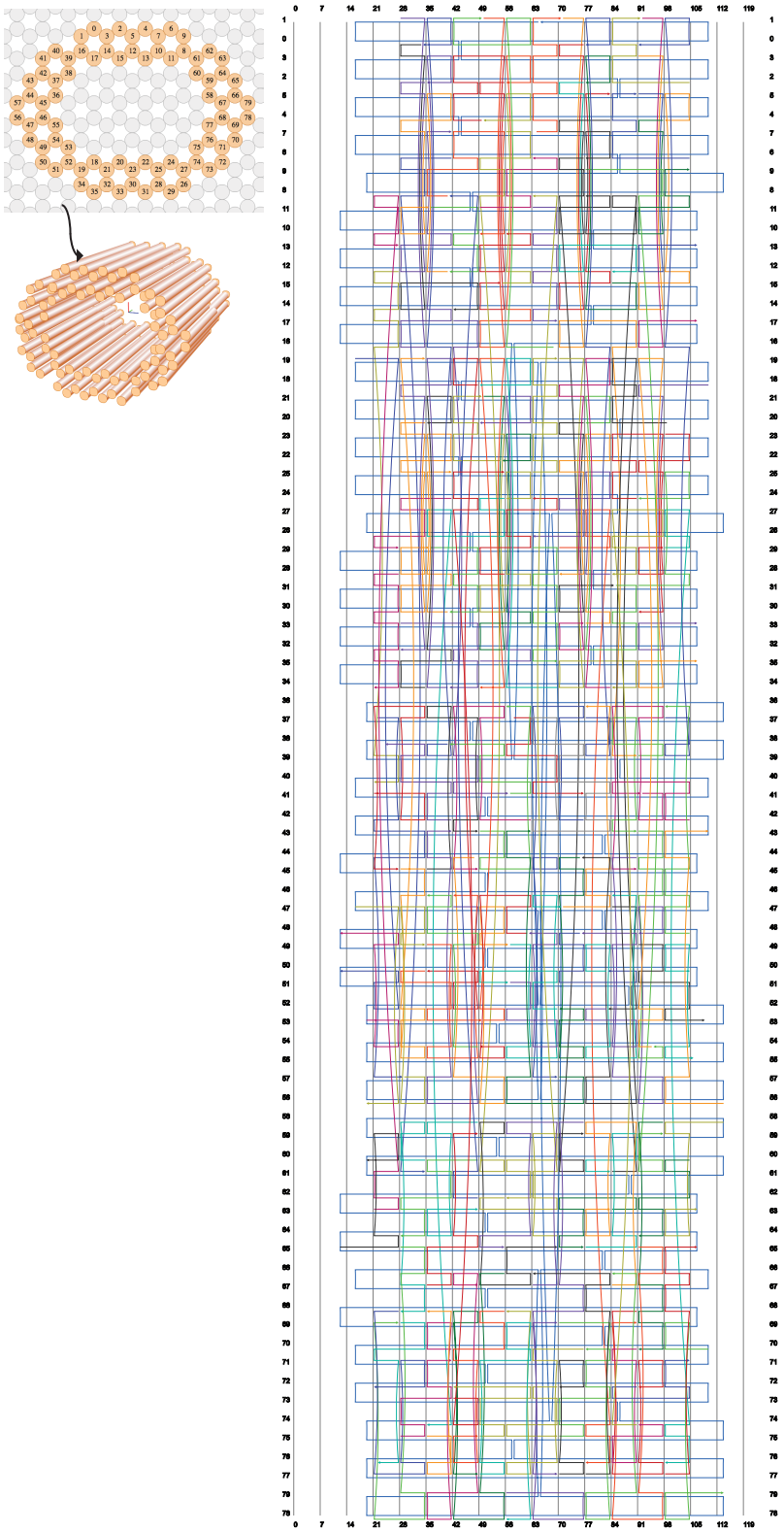

Fig. S72: **Strand diagram of hexagonal DNA barrel**. Left, cross-section view (top) and 3D view (bottom) in caDNAno format. Right, detailed diagram of all strands in caDNAno format. The numbers on the left and the right indicate the helices. The numbers on the top and the bottom indicate the position of the base pairs.

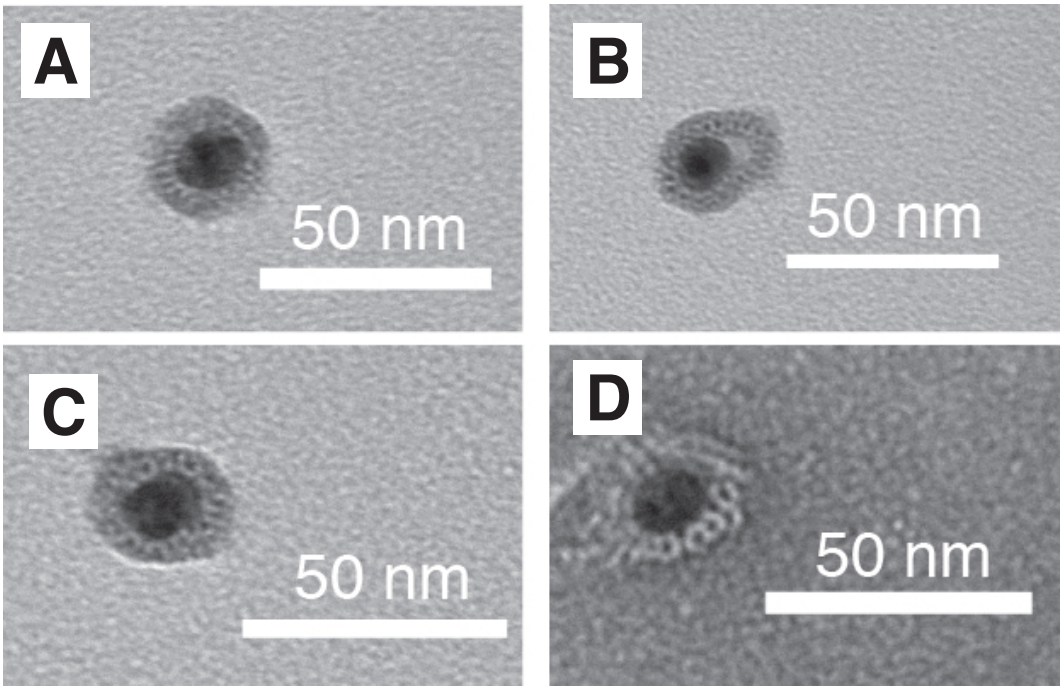

Fig. S73: **Ag NPs grown within open-ended hexagonal DNA barrels**. (A-D) The top view of different Ag NPs grown within open-ended hexagonal DNA barrels, assembled from honeycomb lattice packing geometry. The reaction condition is shown in Sect. S2.5. Reaction time for (A-D) is 4 min.

S10.2.5 DNA tube with 10 nm inner diameter

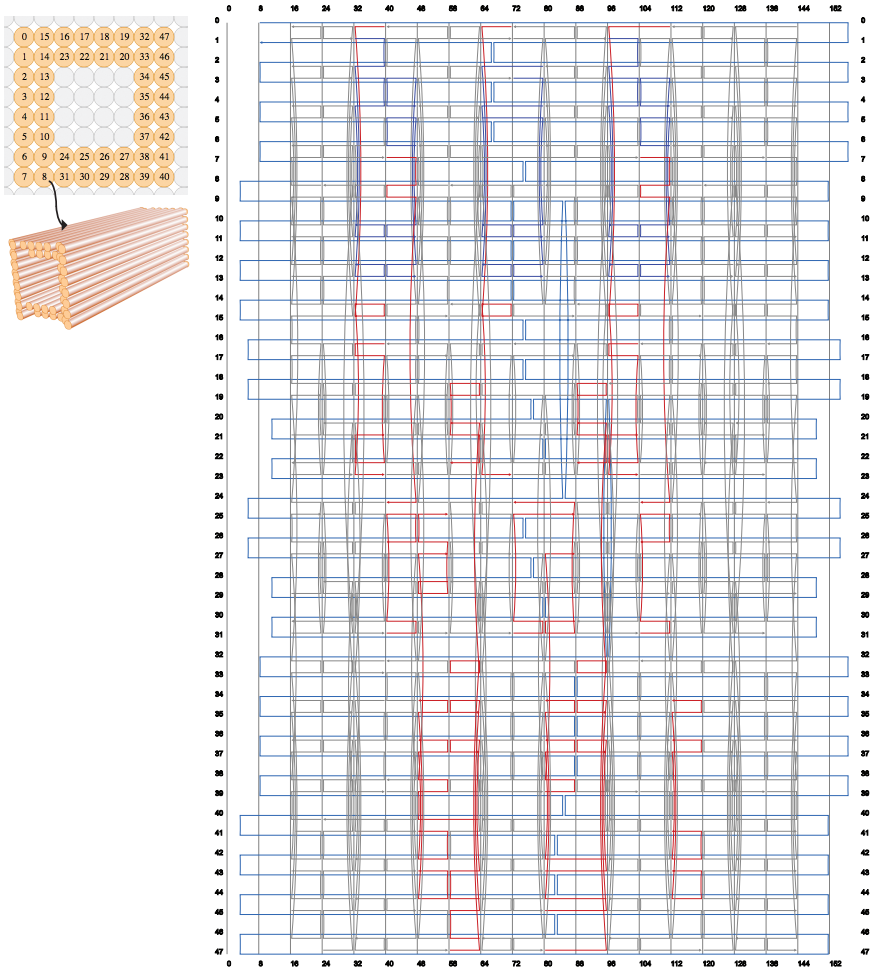

Fig. S74: **Strand diagram of DNA tube with 10 nm inner diameter**. Left, cross-section view (top) and 3D view (bottom) in caDNAno format. Right, detailed diagram of all strands in caDNAno format. The numbers on the left and the right indicate the helices. The numbers on the top and the bottom indicate the position of the base pairs.

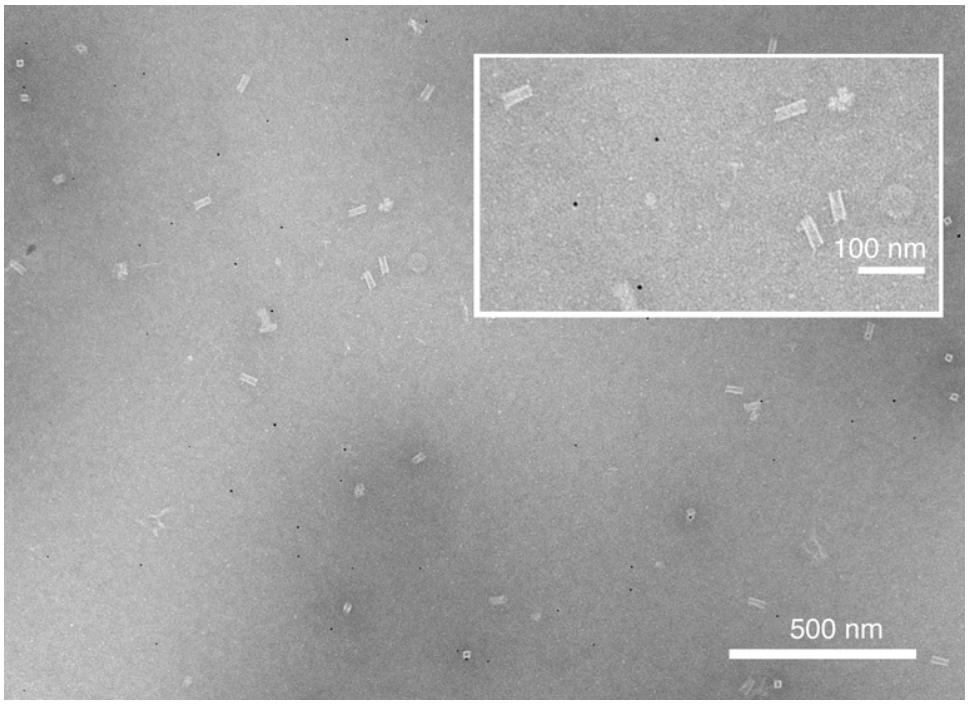

Fig. S75: **TEM image of DNA tube with 10 nm inner diameter after seed decoration**. Inset shows the zoomed-in view of the target structure. Black dots are 5 nm Au seeds.

S11 DNA-based nanocasting: Digital fabrication of inorganic materials

DNA nanocasting provides a simple and versatile strategy for *de novo* rational design and synthesis of 3D shape-specific inorganic structures with uniquely addressable coatings. *Simplicity*. DNA nanocasting reduces the challenging task of designing the shape of an inorganic NP to a much simpler task of designing the cavity of a DNA nanostructure, which can be readily achieved using computational design and simulation tools (*22, 26*). *Versatility*. Using DNA nanocasting, intrinsically sphere-shaped Ag NPs were fabricated into sub-25 nm 3D cuboids with tunable dimensions, and NPs with equilateral triangular, right triangular, and circular cross sections, demonstrating geometrical versatility. Both Au and Ag cuboids were casted, demonstrating material versatility. *Surface-addressability*. Each staple strand in the DNA mold may be uniquely modified with desired binding domains or functional molecules with 3 nm spatial resolution. The mold thus serves as a uniquely addressable coating for the NP to be casted and remains intact after casting, enabling the construction of higher order composite structures such as the branched Ag structures and the QD and Ag NP heterogeneous composites.

By encoding the 3D shape information of an inorganic NP into the linear sequence of the DNA molecules that constitute the mold, DNA nanocasting helps bridging the field of DNA self-assembly with the field of inorganic materials nanofabrication, with profound implications for both fields. DNA self-assembly has produced a wide variety of complex 3D nanostructures. DNA nanocasting provides a generalizable strategy to expand such sophisticated geometrical control from DNA to technologically relevant inorganic substrates (e.g. Au and Ag), and thus enables a new paradigm for shape-specific inorganic materials synthesis. This paradigm fundamentally differs from the widely used capping ligand strategy. In DNA nanocasting, arbitrarily prescribed metal shapes – both symmetric and asymmetric – can be rationally designed and produced by maximal filling of the mold cavities; whereas only symmetric shapes can be produced in a controlled fashion using the capping ligands method, which modulates the NP growth direction via dynamic tuning of the ligand-crystallographic-facets interactions. Additionally, in nanocasting, crystallographic facets with parallel orientation, which generally exhibit similar surface energy (and hence are hard to distinguish and differentially control using capping ligands), may now be independently modulated with distinct dimensions. In contrast to the complex and challenging process of ligand evolution, in DNA nanocasting, which uses computer-aided design software and one-pot annealing reactions, the templates for generating diverse shapes can be rationally designed and readily constructed.

It is striking that the linear, digital sequence of a genome (which is in essence just a large discrete number) is sufficient to encode and direct the formation of the sophisticated structure and function of a complex biological organism. Using DNA as an information dense media, researchers have also encoded the text and graphics of an entire book (*84*). The work here demonstrates a new framework to encode in DNA the instruction to manufacture the 3D shape of an inorganic NP as well as to retrieve and execute the instruction to physically produce this structure. We believe this is the starting point of a new kind of manufacturing scheme, a programmable digital fabrication scheme inspired by the most fundamental mystery of biology (i.e. DNA directed digital fabrication of the complex machine known as a biological organism containing an Avogadro number of molecular components). We have now computationally designed DNA "genomes" for producing 3D inorganic NPs – can we imagine a future of computationally designed DNA based materials genomes for manufacturing functional nanophotonics circuits, nanoelectronic computers, and sophisticated inorganic molecular robots? The work here lays the conceptual and methodological foundation for this seemingly distant but highly desirable and, we believe, foreseeable future.

Supplementary Material II

Casting Inorganic Structures with DNA Molds

Wei Sun[1,2] Etienne Boulais[3] Yera Hakobyan[3] Wei Li Wang[1,2] Amy Guan[1]
Mark Bathe[3]* Peng Yin[1,2]*

Wyss Institute for Biologically Inspired Engineering, Harvard University, Boston, MA[1]
Department of Systems Biology, Harvard Medical School, Boston, MA[2]
Department of Biological Engineering, Massachusetts Institute of Technology, Cambridge, MA[3]

E-mail address*: py@hms.harvard.edu; mark.bathe@mit.edu

Contents

Scaffold sequence (mutated P8064):

GAATTCGAGCTCGGTACCCGGGGATCCTCAACTGTGAGGAGGCTCACGGACGCG
AAGAACAGGCACGCGTGCTGGCAGAAACCCCCGGTATGACCGTGAAAACGGCCC
GCCGCATTCTGGCCGCAGCACCACAGAGTGCACAGGCGCGCAGTGACACTGCGC
TGGATCGTCTGATGCAGGGGGCACCGGCACCGCTGGCTGCAGGTAACCCGGCAT
CTGATGCCGTTAACGATTTGCTGAACACACCAGTGTAAGGGATGTTTATGACGAG
CAAAGAAACCTTTACCCATTACCAGCCGCAGGGCAACAGTGACCCGGCTCATACC
GCAACCGCGCCCGGCGGATTGAGTGCGAAAGCGCCTGCAATGACCCCGCTGATG
CTGGACACCTCCAGCCGTAAGCTGGTTGCGTGGGATGGCACCACCGACGGTGCTG
CCGTTGGCATTCTTGCGGTTGCTGCTGACCAGACCAGCACCACGCTGACGTTCTA
CAAGTCCGGCACGTTCCGTTATGAGGATGTGCTCTGGCCGGAGGCTGCCAGCGAC
GAGACGAAAAAACGGACCGCGTTTGCCGGAACGGCAATCAGCATCGTTTAACTT
TACCCTTCATCACTAAAGGCCGCCTGTGCGGCTTTTTTTACGGGATTTTTTTATGT
CGATGTACACAACCGCCCAACTGCTGGCGGCAAATGAGCAGAAATTTAAGTTTG
ATCCGCTGTTTCTGCGTCTCTTTTTCCGTGAGAGCTATCCCTTCACCACGGAGAAA
GTCTATCTCTCACAAATTCCGGGACTGGTAAACATGGCGCTGTACGTTTCGCCGA
TTGTTTCCGGTGAGGTTATCCGTTCCCGTGGCGGCTCCACCTCTGAAAGCTTGGCA
CTGGCCGTCGTTTTACAACGTCGTGACTGGGAAAACCCTGGCGTTACCCAACTTA
ATCGCCTTGCAGCACATCCCCCTTTCGCCAGCTGGCGTAATAGCGAAGAGGCCCG
CACCGATCGCCCTTCCCAACAGTTGCGCAGCCTGAATGGCGAATGGCGCTTTGCC
TGGTTTCCGGCACCAGAAGCGGTGCCGGAAAGCTGGCTGGAGTGCGATCTTCCTG
AGGCCGATACTGTCGTCGTCCCCTCAAACTGGCAGATGCACGGTTACGATGCGCC
CATCTACACCAACGTGACCTATCCCATTACGGTCAATCCGCCGTTTGTTCCCACGG
AGAATCCGACGGGTTGTTACTCGCTCACATTTAATGTTGATGAAAGCTGGCTACA
GGAAGGCCAGACGCGAATTATTTTTGATGGCGTTCCTATTGGTTAAAAAATGAGC
TGATTTAACAAAAATTTAATGCGAATTTTAACAAAATATTAACGTTTACAATTTA
AATATTTGCTTATACAATCTTCCTGTTTTTGGGGCTTTTCTGATTATCAACCGGGG
TACATATGATTGACATGCTAGTTTTACGATTACCGTTCATCGATTCTCTTGTTTGC
TCCAGACTCTCAGGCAATGACCTGATAGCCTTTGTAGATCTCTCAAAAATAGCTA
CCCTCTCCGGCATTAATTTATCAGCTAGAACGGTTGAATATCATATTGATGGTGAT
TTGACTGTCTCCGGCCTTTCTCACCCTTTTGAATCTTTACCTACACATTACTCAGG
CATTGCATTTAAAATATATGAGGGTTCTAAAAATTTTTATCCTTGCGTTGAAATAA
AGGCTTCTCCCGCAAAAGTATTACAGGGTCATAATGTTTTTGGTACAACCGATTT
AGCTTTATGCTCTGAGGCTTTATTGCTTAATTTTGCTAATTCTTTGCCTTGCCTGTA
TGATTTATTGGATGTTAATGCTACTACTATTAGTAGAATTGATGCCACCTTTTCAG
CTCGCGCCCCAAATGAAAATATAGCTAAACAGGTTATTGACCATTTGCGAAATGT
ATCTAATGGTCAAACTAAATCTACTCGTTCGCAGAATTGGGAATCAACTGTTATA
TGGAATGAAACTTCCAGACACCGTACTTTAGTTGCATATTTAAAACATGTTGAGC
TACAGCATTATATTCAGCAATTAAGCTCTAAGCCATCCGCAAAAATGACCTCTTA
TCAAAAGGAGCAATTAAAGGTACTCTCTAATCCTGACCTGTTGGAGTTTGCTTCC
GGTCTGGTTCGCTTTGAAGCTCGAATTAAAACGCGATATTTGAAGTCTTTCGGGC
TTCCTCTTAATCTTTTTGATGCAATCCGCTTTGCTTCTGACTATAATAGTCAGGGT
AAAGACCTGATTTTTGATTTATGGTCATTCTCGTTTTCTGAACTGTTTAAAGCATT
TGAGGGGGATTCAATGAATATTTATGACGATTCCGCAGTATTGGACGCTATCCAG
TCTAAACATTTTACTATTACCCCCTCTGGCAAAACTTCTTTTGCAAAAGCCTCTCG
CTATTTTGGTTTTTATCGTCGTCTGGTAAACGAGGGTTATGATAGTGTTGCTCTTA
CTATGCCTCGTAATTCCTTTTGGCGTTATGTATCTGCATTAGTTGAATGTGGTATT
CCTAAATCTCAACTGATGAATCTTTCTACCTGTAATAATGTTGTTCCGTTAGTTCG
TTTTATTAACGTAGATTTTTCTTCCCAACGTCCTGACTGGTATAATGAGCCAGTTC
TTAAAATCGCATAAGGTAATTCACAATGATTAAAGTTGAAATTAAACCATCTCAA
GCCCAATTTACTACTCGTTCTGGTGTTTCTCGTCAGGGCAAGCCTTATTCACTGAA
TGAGCAGCTTTGTTACGTTGATTTGGGTAATGAATATCCGGTTCTTGTCAAGATTA

CTCTTGATGAAGGTCAGCCAGCCTATGCGCCTGGTCTGTACACCGTTCATCTGTCC
TCTTTCAAAGTTGGTCAGTTCGGTTCCCTTATGATTGACCGTCTGCGCCTCGTTCC
GGCTAAGTAACATGGAGCAGGTCGCGGATTTCGACACAATTTATCAGGCGATGAT
ACAAATCTCCGTTGTACTTTGTTTCGCGCTTGGTATAATCGCTGGGGGTCAAAGAT
GAGTGTTTTAGTGTATTCTTTTGCCTCTTTCGTTTTAGGTTGGTGCCTTCGTAGTGG
CATTACGTATTTTACCCGTTTAATGGAAACTTCCTCATGAAAAAGTCTTTAGTCCT
CAAAGCCTCTGTAGCCGTTGCTACCCTCGTTCCGATGCTGTCTTTCGCTGCTGAGG
GTGACGATCCCGCAAAAGCGGCCTTTAACTCCCTGCAAGCCTCAGCGACCGAATA
TATCGGTTATGCGTGGGCGATGGTTGTTGTCATTGTCGGCGCAACTATCGGTATC
AAGCTGTTTAAGAAATTCACCTCGAAAGCAAGCTGATAAACCGATACAATTAAA
GGCTCCTTTTGGAGCCTTTTTTTTGGAGATTTTCAACGTGAAAAAATTATTATTCG
CAATTCCTTTAGTTGTTCCTTTCTATTCTCACTCCGCTGAAACTGTTGAAAGTTGTT
TAGCAAAATCCCATACAGAAAATTCATTTACTAACGTCTGGAAAGACGACAAAA
CTTTAGATCGTTACGCTAACTATGAGGGCTGTCTGTGGAATGCTACAGGCGTTGT
AGTTTGTACTGGTGACGAAACTCAGTGTTACGGTACATGGGTTCCTATTGGGCTT
GCTATCCCTGAAAATGAGGGTGGTGGCTCTGAGGGTGGCGGTTCTGAGGGTGGC
GGTTCTGAGGGTGGCGGTACTAAACCTCCTGAGTACGGTGATACACCTATTCCGG
GCTATACTTATATCAACCCTCTCGACGGCACTTATCCGCCTGGTACTGAGCAAAA
CCCCGCTAATCCTAATCCTTCTCTTGAGGAGTCTCAGCCTCTTAATACTTTCATGT
TTCAGAATAATAGGTTCCGAAATAGGCAGGGGGCATTAACTGTTTATACGGGCAC
TGTTACTCAAGGCACTGACCCCGTTAAAACTTATTACCAGTACACTCCTGTATCAT
CAAAAGCCATGTATGACGCTTACTGGAACGGTAAATTCAGAGACTGCGCTTTCCA
TTCTGGCTTTAATGAGGATTTATTTGTTTGTGAATATCAAGGCCAATCGTCTGACC
TGCCTCAACCTCCTGTCAATGCTGGCGGCGGCTCTGGTGGTGGTTCTGGTGGCGG
CTCTGAGGGTGGTGGCTCTGAGGGTGGCGGTTCTGAGGGTGGCGGCTCTGAGGG
AGGCGGTTCCGGTGGTGGCTCTGGTTCCGGTGATTTTGATTATGAAAAGATGGCA
AACGCTAATAAGGGGGCTATGACCGAAAATGCCGATGAAAACGCGCTACAGTCT
GACGCTAAAGGCAAACTTGATTCTGTCGCTACTGATTACGGTGCTGCTATCGATG
GTTTCATTGGTGACGTTTCCGGCCTTGCTAATGGTAATGGTGCTACTGGTGATTTT
GCTGGCTCTAATTCCCAAATGGCTCAAGTCGGTGACGGTGATAATTCACCTTTAA
TGAATAATTTCCGTCAATATTTACCTTCCCTCCCTCAATCGGTTGAATGTCGCCCT
TTTGTCTTTGGCGCTGGTAAACCATATGAATTTTCTATTGATTGTGACAAAATAAA
CTTATTCCGTGGTGTCTTTGCGTTTCTTTTATATGTTGCCACCTTTATGTATGTATT
TTCTACGTTTGCTAACATACTGCGTAATAAGGAGTCTTAATCATGCCAGTTCTTTT
GGGTATTCCGTTATTATTGCGTTTCCTCGGTTTCCTTCTGGTAACTTTGTTCGGCTA
TCTGCTTACTTTTCTTAAAAAGGGCTTCGGTAAGATAGCTATTGCTATTTCATTGT
TTCTTGCTCTTATTATTGGGCTTAACTCAATTCTTGTGGGTTATCTCTCTGATATTA
GCGCTCAATTACCCTCTGACTTTGTTCAGGGTGTTCAGTTAATTCTCCCGTCTAAT
GCGCTTCCCTGTTTTTATGTTATTCTCTCTGTAAAGGCTGCTATTTTCATTTTTGAC
GTTAAACAAAAAATCGTTTCTTATTTGGATTGGGATAAATAATATGGCTGTTTATT
TTGTAACTGGCAAATTAGGCTCTGGAAAGACGCTCGTTAGCGTTGGTAAGATTCA
GGATAAAATTGTAGCTGGGTGCAAAATAGCAACTAATCTTGATTTAAGGCTTCAA
AACCTCCCGCAAGTCGGGAGGTTCGCTAAAACGCCTCGCGTTCTTAGAATACCGG
ATAAGCCTTCTATATCTGATTTGCTTGCTATTGGGCGCGGTAATGATTCCTACGAT
GAAAATAAAAACGGCTTGCTTGTTCTCGATGAGTGCGGTACTTGGTTTAATACCC
GTTCTTGGAATGATAAGGAAAGACAGCCGATTATTGATTGGTTTCTACATGCTCG
TAAATTAGGATGGGATATTATTTTTCTTGTTCAGGACTTATCTATTGTTGATAAAC
AGGCGCGTTCTGCATTAGCTGAACATGTTGTTTATTGTCGTCGTCTGGACAGAATT
ACTTTACCTTTTGTCGGTACTTTATATTCTCTTATTACTGGCTCGAAAATGCCTCTG
CCTAAATTACATGTTGGCGTTGTTAAATATGGCGATTCTCAATTAAGCCCTACTGT
TGAGCGTTGGCTTTATACTGGTAAGAATTTGTATAACGCATATGATACTAAACAG
GCTTTTTCTAGTAATTATGATTCCGGTGTTTATTCTTATTTAACGCCTTATTTATCA
CACGGTCGGTATTTCAAACCATTAAATTTAGGTCAGAAGATGAAATTAACTAAAA
TATATTTGAAAAAGTTTTCTCGCGTTCTTTGTCTTGCGATTGGATTTGCATCAGCA
TTTACATATAGTTATATAACCCAACCTAAGCCGGAGGTTAAAAAGGTAGTCTCTC

AGACCTATGATTTTGATAAATTCACTATTGACTCTTCTCAGCGTCTTAATCTAAGC
TATCGCTATGTTTTCAAGGATTCTAAGGGAAAATTAATTAATAGCGACGATTTAC
AGAAGCAAGGTTATTCACTCACATATATTGATTTATGTACTGTTTCCATTAAAAA
AGGTAATTCAAATGAAATTGTTAAATGTAATTAATTTTGTTTTCTTGATGTTTGTT
TCATCATCTTCTTTTGCTCAGGTAATTGAAATGAATAATTCGCCTCTGCGCGATTT
TGTAACTTGGTATTCAAAGCAATCAGGCGAATCCGTTATTGTTTCTCCCGATGTAA
AAGGTACTGTTACTGTATATTCATCTGACGTTAAACCTGAAAATCTACGCAATTTC
TTTATTTCTGTTTTACGTGCAAATAATTTTGATATGGTAGGTTCTAACCCTTCCATT
ATTCAGAAGTATAATCCAAACAATCAGGATTATATTGATGAATTGCCATCATCTG
ATAATCAGGAATATGATGATAATTCCGCTCCTTCTGGTGGTTTCTTTGTTCCGCAA
AATGATAATGTTACTCAAACTTTTAAAATTAATAACGTTCGGGCAAAGGATTTAA
TACGAGTTGTCGAATTGTTTGTAAAGTCTAATACTTCTAAATCCTCAAATGTATTA
TCTATTGACGGCTCTAATCTATTAGTTGTTAGTGCTCCTAAAGATATTTTAGATAA
CCTTCCTCAATTCCTTTCAACTGTTGATTTGCCAACTGACCAGATATTGATTGAGG
GTTTGATATTTGAGGTTCAGCAAGGTGATGCTTTAGATTTTTCATTTGCTGCTGGC
TCTCAGCGTGGCACTGTTGCAGGCGGTGTTAATACTGACCGCCTCACCTCTGTTTT
ATCTTCTGCTGGTGGTTCGTTCGGTATTTTTAATGGCGATGTTTTAGGGCTATCAG
TTCGCGCATTAAAGACTAATAGCCATTCAAAAATATTGTCTGTGCCACGTATTCTT
ACGCTTTCAGGTCAGAAGGGTTCTATCTCTGTTGGCCAGAATGTCCCTTTTATTAC
TGGTCGTGTGACTGGTGAATCTGCCAATGTAAATAATCCATTTCAGACGATTGAG
CGTCAAAATGTAGGTATTTCCATGAGCGTTTTTCCTGTTGCAATGGCTGGCGGTA
ATATTGTTCTGGATATTACCAGCAAGGCCGATAGTTTGAGTTCTTCTACTCAGGCA
AGTGATGTTATTACTAATCAAAGAAGTATTGCTACAACGGTTAATTTGCGTGATG
GACAGACTCTTTTACTCGGTGGCCTCACTGATTATAAAAACACTTCTCAGGATTCT
GGCGTACCGTTCCTGTCTAAAATCCCTTTAATCGGCCTCCTGTTTAGCTCCCGCTC
TGATTCTAACGAGGAAAGCACGTTATACGTGCTCGTCAAAGCAACCATAGTACGC
GCCCTGTAGCGGCGCATTAAGCGCGGCGGGTGTGGTGGTTACGCGCAGCGTGAC
CGCTACACTTGCCAGCGCCCTAGCGCCCGCTCCTTTCGCTTTCTTCCCTTCCTTTCT
CGCCACGTTCGCCGGCTTTCCCCGTCAAGCTCTAAATCGGGGGCTCCCTTTAGGG
TTCCGATTTAGTGCTTTACGGCACCTCGACCCCAAAAAACTTGATTTGGGTGATG
GTTCACGTAGTGGGCCATCGCCCTGATAGACGGTTTTTCGCCCTTTGACGTTGGA
GTCCACGTTCTTTAATAGTGGACTCTTGTTCCAAACTGGAACAACACTCAACCCT
ATCTCGGGCTATTCTTTTGATTTATAAGGGATTTTGCCGATTTCGGAACCACCATC
AAACAGGATTTTCGCCTGCTGGGGCAAACCAGCGTGGACCGCTTGCTGCAACTCT
CTCAGGGCCAGGCGGTGAAGGGCAATCAGCTGTTGCCCGTCTCACTGGTGAAAA
GAAAAACCACCCTGGCGCCCAATACGCAAACCGCCTCTCCCCGCGCGTTGGCCGA
TTCATTAATGCAGCTGGCACGACAGGTTTCCCGACTGGAAAGCGGGCAGTGAGC
GCAACGCAATTAATGTGAGTTAGCTCACTCATTAGGCACCCCAGGCTTTACACTT
TATGCTTCCGGCTCGTATGTTGTGTGGAATTGTGAGCGGATAACAATTTCACACA
GGAAACAGCTATGACCATGATTAC

DNA barrel with 21nm by 16nm by 30 nm cuboid cavity:

ACGAGAAATGCAATGCTTTAGAACCCTCATAT
TAAAGATTAAAGCTGCGTAATCTTGACAAGAAAGAGGACAATGCCGGA
TACATAAATTCTGGCCTATTTTTGACGCTGCGAGGGCGCT
ATTTTAAACACCAGAATTTTGCGGATAAAGCT
CTGAGTAATCTTCGCGTCCTCACAGTTGAGGATCCCCGGGATTTCAAC
TTAATTACGAAACAAATATTAGTCTACCAG
CCCAAATCCTTATCGCCATTAAAAGTTAATAAAACGACAT
AACATAGCTGTGAGTGAATAACCT
GGAAACAGTGCTTCTGACGACCAGCAATCGTCTAAACAGGTACGCCAG
CCTTAGAAACGCTGAGCGCTCATGGTAATATCGTGAGGCCTAACCGTT
CATAAGGGTAAATTGTAAGAGAATCGATGGCCAGGTTTCTAGCCAGCG
CATCAAGATCATTCAGTGAATAAG
TCGCCTGAAACCGAACCATTAGCTATTTTTGATTACCTGCTTGCTCGT
CTACCTTTGATAGCTTAGATTAAG
ACTTTGAACCGGATATTGAAAGGCCGGAGACACGGCGGGCTGCATCAG
TATCAAAATCATAGGTGTTGGGTTGTAGAAGAAACGGCAGCACCGTCG
AGTACAACAGAGGCAACCAGCATCCAACCAGCTTACGGCT
CAGAGGCATTAATTGAGGAAAAAGCTGCTCAT
AAATGCTGTAGTTAATTTTTTCGTGCCGTTCC
AAAATACGTTGAGGACCCTTCCTGAGTAACAA
ATATATTTATGCAAATTCATAACGTGCTGGTCTGGTCAGC
ACAGACAAAACAGAGACTACAGGGAACGTGCTTTCCTCGT
CTCTGTGGTGCTGCGGGTGCCTGTTGTGTAGG
CAGCAGCGGAGGCTTGTAGGTCACTCTGCCAG
AAATAAGATAAATTTATGCTGATTCTCGTCGC
CGGTCGCTAAAGACAGTGTGAGCGTAGCCAGC
CATAATTAAGCCAACGTTAAATTTAGACGCAG
CGACAATGGCTTTCGACAGCTTTCAGCGCCAT
CAGTATAACTAGAAAATACATCGAGCGGCCTT
ATCAGCTTACAACAACACCGTGCAGTTGGTGT
AGTAGGGCTTTTCGAGGTGAGAGACCATGTTT
CAAAAAAACAACTAAATCTTCGCTCAAGGCGA
TGAGAAAGTACCGGGGTCGAATTCAAGAAAGC
GAAAGGAAAGGCTCCACCAGGCAACGGCACCG
GAGGGTGGGTGCCCCCCGTTTTCACGGGCTTA
GACGACGAATAAGAGAGAATAACAGCCACGGG
CATAGTTAGCGTAACGTTTTGCTAACCGGAACACGGCCAGTGCCAAGC
ATCTAAAGGCCACCCTCAGAGCCGCCATCGATAGTAGCAC
TTCAGCTATATCCCATCAAACCAACGCTAACGCTATCTTAGAGTTAAG
ACTACAACAATAGGAACAGGTCAGAAGCGCAGTCACCGTCGAGGGAAG
CAAAGGCTGGCGCAGAGTGTACAGACCAGGCG
TAATCGTACCCTGCGGGTCATTGCAGGCGCTT
AAAAATAAATGCAGAATTATTTATCCCAACCTCAAGAATTCCGAAGCC
GCAAGCCCGCCTGTAGACCACCACCAGAACCGTTGCCTTTAGCGTTTG
TTACGAGCATTAAACCACTTGCGGGAGGTTTTCAATAATATAAGCAGA
GAACCGCCGTACTCAGGTCATACACTTGAGTATATGGTTTGACACCAC
TCGCACTCGATAATCAATGTCAATACCAAGCGCCGCGACCTGCTCCAT
GTAGCAATACTTCTTTGATTAGGGCTGGTAATGGGGTTTT
GTATCACCACCCTCAGAGAATGGAACGATTGGAAATCACCAGCAGCAC
AAGCAAGCCATTCCAAGAACGGGTATGTAGAATATCCTGA

CGCACTCAATAAAAGTATTAAGAGCAGAAACGAGAATGAC
GAGAGGGTGTCAGTGCTGGCTTTTGATTGAGGACCGACTT
GTGCCGTCAGAAGGATCCCCTGCCCCCGAAAGACTTCAAA
GCGGTATGAGCCGGGTTCCCTTACAGAGTCTG
GTTAATGCTAGGATTAGCGAACCATTTGATAA
CGACTGGTAGAACTGGATAAAGGTGGCAACAT
CAGTAAGCGAGGTTTAGCGGATAA
TATAATCACAGAACAATTGCCTGAATATAACTCAGCGTGGGAACGTGC
ATCTTATAAAGAAAAGACGGAATACCCGCGAC
GGTTGAGGCCCATGTACACCCTCA
CATAAACACACTGTTGAAACTAGCGGAGGTGTAAGAATACAAACGTTA
ATAAGAAACTAATATCGAGAATTAACTGAACA
CTCAGAGCCTTTTGTCGCAGTACAA
TACAGAGAATATAAAGGTACAGCGTAGACTTT
AATCCTGAGAAGTTAAATTGCAACATTATTTATGATTAATTAATTTTC
CCATCTTTTCAGCGCATTAGACGGAGAGAGATAACGACAG
TCGTTAACGGCATCAGGCGCAGTGTCTAGCTGACCATCAA
TAGAACCGCAGATTCATTCTGACCTCATACCTTTTTTAAT
CCACACCCGCCGCTCACGTAAGAAATAGCCCTAAAACGAGTACCTTAT
TTCTGACCATAAACACCCGCACAGCATAAAAA
CCCAATAAATTGAGCGCGATTTTT
CAGAGGCTTAATGCCAATTTTTGTATATTTTG
AATCAAGTCCACCCTCTCAAAATCAACAACTTATGTGCTGATTACGCC
TAGTGATGTTAAACGAATGGTTTGTTTTTCAA
TATCGCGTGCTTCAAAGCGGGGTTCAAAGAAACCACCAGATTATCATT
TGCATCAAAAAGATTACAACAGGTGCTGAGACTCATATTC
TAGCCGAAAGCAATAGAGCGTCTTCAGCCATACGCGCCTGTCTGTCCA
ATTATAGTAAAAATCAATCATTAC
GCAAACTCAGAGGAAGTATTTCGGAACGCAAAACCAGCGC
GGAAACCGTATTACGCCGCGAGGCAAGGCTTATCGTAGGA
GCGGATTGACCGATTCTCCGGCGGGATCTTTTCATG
TCAGAGATTAGAGAGTTAGCTCAA
AGACTCCTAGGAAACGGAAGCCTTTACAATTTACCAATCATGAACAAG
CAAAGACAAAAGGAAAAATAAGTTATTCTGAAACATGGCAAAGCGGAT
GAGGTCATGGCTTAGATTGCG
TTAGCAAACGTAGAAAAGATATAGGTTTTAGC
TAATGCTGACCTTTAAAATTATCATCCTCAAG
GCAGAAGATAAAACAGCAAAATCGATTCAACTAATGCCAT
CGCCTGCAAAAATCTAATACAGGCTGGCATCA
TATTCATTTCACAAAAGAAAAGATT
AACCTCAAAGGTGAGGAAAACTAACGGAACAA
CAGCAGCAAATGAACAGTGCCCTCAGAGCGAGAAGCC
CCAAGTTAATATACAGTTTACCAGACGACTAG
GGTCAGTTGTTATCTAGTCAATAAGCGAACGA
TACATCGGGAGGGATTCGCGCATAG
ACTAACAAATATCAAATAGAGATACATAACGC
GGAATTGAGGAAGGGCAAATC
TCAGATGAACCATATCAAAATGTT
ATAATACACAATTCGAAGTACGGTGCTGAATA
ACGTAAAACAGATTGCGTAGGCAAAA
TAGACTTTACAAATTTGAGGA
TAGAACCTCAGATGATTAAACAGT
TTAATTTTATTAAATCCTTTGCCCCTAATAGACATGATAA

GAGTAACAAGGAGCGGTTGCTCCTGACCGGAA
ATCAATATAATCCTGATATACTTCATAAAT
CTGATTATGAACGTTACATTGGATAGCGTCCA
GGCGATCGGCAGGCTGCTCACGTTGTCTTAAAC
GTGGTGCCTAGAACGTATAAACCTAAAACGAAGGAGATTTCCAAACGG
GAAAAGCCTAAATTGTACTAAAACAAACGGGT
TTAAAATTATCCCACGAGCGTAATAACATCACTATTACCGGTAGAATT
TAAGCAAATATTCCAAAAAC
TTAAGTTGGTAAAACGCAGAGCCACCCTTATTAGCGTCAG
AACGGATAACCTCACCGGCGAAACTACCGACAAATTTAGG
TGGCAGCCGCACATCCCCAATCGCCGGCTTAG
TTTCAGAGAAAGGGGGTCAACAGTTTCAGGTACAATAAACCACTCCAA
CAAAAATAATTCTTAACCAATTTCCATTACTCATCT
ACGACGTTGGTAACGCAATTTTCTGAATAATA
CAGAGGGGAGGCTTTTATTTTCAGCCTTT
CATAAATCCAGAAGCAAGCAAATCATACATACCATGATTA
TCCCCCTCGAATCGTCTGAATAATTTGC
ATACTGCGAAATGCTTGGCAATTCCGCGCCCATCGAGAACGAACCTCC
GCTTAATTGTCTGGAAGTTTCATTGTTGATTCTTTAG
GCGATTTTAAGAACTGAAATCTACATACCGAACGAACGATATTTAACA
TTGCCGCCCGGTTGTGAGCCTGTTAAGGCGTT
ACTATCATATTACGAGCTGATTGCCGAAT
AAGATCGCGACGACGAATACCGATTAAAGGCC
AAACCAAAATAGCGAGGTAATAGTAAAATTATGGAAGGGT
TCGCCATTTGCGGGCCGGAATTGCGTATGGGA
CTCCGTGGGCTCTCACGAATCGCCATTCTTAC
CAAAAGGAAACCCTCGTAACAGTAGTTTAACG
TAACATCCTGTACCAACGGTCAGTAAATTGGGAACGTAACCAAAAGGG
ACCAGTCCGTGGAGCCTAAAAACAGGGAATAAAGAGCCACAACGCCCT
TGAAAAGGAAGGCAAAGAATTAGCAATAAAGCACGCTG
CATTATTAAATACCACCGCAGAGGTTTGAATA
CCAATTCTCCTGTTTAGCTATATTGCGCGAGCAACAG
TATGACCCTTGTGAATATGGTTTATACCGAGCGTTTCTGC
GATTTAGGCAGGTAGAGATCACCA
GGGAAGAAGCTCATTATTTAATGCCGGGCGCTCGTAACCA
TAAATCAGCTCATTTTGCGTCTGGTAAAGACTGTCACCCTTAACATTCCTAACTTC TCATA
CAGCACGCCCAGAATGGTCAAATCATAAATTAGATGAACGCGGTCAATTAACATT CCTAACTTCTCATA
CGGACTTGCGGTCCGTTTCGTAGCAACGGCTATAACATTCCTAACTTCTCATA
AAATCGGTAATAAATCAAGCATCACAATATCTTAACATTCCTAACTTCTCATA
AGCTGGCGGCCGGAAAAAAGGAGCCTTTAAACTAACATTCCTAACTTCTCATA
AAACAGCGCGGAATTTCCACGGAGTGAGAATATAACATTCCTAACTTCTCATA
CTTCTGGTGCATCGTACATCGCCCACGCAAATTAACATTCCTAACTTCTCATA
ATTCTACTCGCAAATGAAATATCTGTCAATAGTAACATTCCTAACTTCTCATA
CCCGTCGGTAATGGGACAGGGAGTAGTTGCGCTAACATTCCTAACTTCTCATA
TTTGAGGGACTCCAGCGGTGAATTAAAATCTCTAACATTCCTAACTTCTCATA
ATACATTTAATAGTAGCCCTCAATCCTTGCTGTAACATTCCTAACTTCTCATA
TTTAATCATGTAATACCGAGTAGTATTAACACTAACATTCCTAACTTCTCATA
GTAGATTTGCAACTAACAACTCGTAAAAGTTTTAACATTCCTAACTTCTCATA
TTTCATCACGCATTAACTACGAAGGCACCTGTTAACATTCCTAACTTCTCATA
GGCAAACGAAAAAAAGCGGTAACCGATATATTTAACATTCCTAACTTCTCATA
TAGACGTTTTAAATATAGTTTGACTTAGAGCCTTAGGAGCTAACATTCCTAACTTC

TCATA
ATGCGCCGTAGAACCCCCAGTCACTAAATCGTCGCTACCATAACATTCCTAACTT CTCATA
ATAAAAGAAACCTATTTTAACGGGTGATATAAGTATATACTAACATTCCTAACTT CTCATA
AATCCCGTGATCAAACCTCATTGTATCGGTTTTAACATTCCTAACTTCTCATA
GTGTCAGAGCGGGAGCTGAAATGGAGGAAAAAAAGAGTCAATAGTTCATAACAT TCCTAACTTCTCATA
ACGATCCAATGCCGGGGAGATCTAGAGCAAACGTCGAAATCGAAACAATAACAT TCCTAACTTCTCATA
ATTCAACCGATGATACTTAAAGCCAGCCACCACCCTCAATTAACATTCCTAACTT CTCATA
GAGCCATTTGGGATTTAATCCTCAAGGAGTGTAAGGCCCGGAATAGGTTAACATT CCTAACTTCTCATA
GAAAGGAGGCGAACTGTACGTGGCATTTCATTTGAATTTATAACATTCCTAACTT CTCATA
CTTATTAGAGCCAGCACCTTGATACCACCAGACATTCCACAGACAATGTAACATT CCTAACTTCTCATA
CGTAATCAGTAGCCCACAGAGCCGTTCACAAACCTATTTTCAGGGATATAACATT CCTAACTTCTCATA
AGATGGGCACATTAAACATCGGAACGAGGATCTAACATTCCTAACTTCTCATA
AGAGGGTATAAGAGCAAGACGTACCTGGAGTTCAT
AACGTCACGCGTTTTCATCCGTACCTGGAGTTCAT
AATGAAATCAAAGTTACCACGTACCTGGAGTTCAT
ATCAATAGTGACGGAAATTCGTACCTGGAGTTCAT
AGTACCAGGTACCGCCACCCGTACCTGGAGTTCAT
ACTGTAGCCAATGAAACCGCCAGCATTGACGTACCTGGAGTTCAT
CATTACCAGTGAATTATCTCTGAATTTACCGTACCTGGAGTTCAT
GTAAATATAAAATTCAACAGTGCCCGTATCGTACCTGGAGTTCAT
CATTAAAGTTAGCAAGGCCCGTACCTGGAGTTCAT
TTTCGGTCATAGCCCCACCGGAACCGCCGTACCTGGAGTTCAT
AGAACCGCCCGTAACACTGCGTACCTGGAGTTCAT
CCCTGAACGCAGCCTTTGTTTAACGTCAAAAACGTACCTGGAGTTCAT
AAAATAAATCCAGAGCCTAATTTGCGTACCTGGAGTTCAT
CACCCAGCAAATCAAGATTAGTTGCGTACCTGGAGTTCAT
ATAAGTCCATAATCGGCTGCGTACCTGGAGTTCAT
AAAGTAATTTTATCAACAACGTACCTGGAGTTCAT
TTCCTTATCGTTTTTATTTCGTACCTGGAGTTCAT
TTCGTCACTCTTTCCAGACCGTACCTGGAGTTCAT
ACGCAAATACCGAGTAAAAGAGTCTTTTTTTTTTTTTTTT
AGGAACGGAGGCCGATTAAAGGGATTTTTTTTTTTTTTTT
ATTGCCTGACTGGTGTGTTCATTTTTTTTTTTTTTTT
CCCCGGTTAATCCGCCGGGCGTTTTTTTTTTTTTTTT
GCACGTATCGCGTACTATGGTTGCTTTTTTTTTTTTTTT
TCAACCGTTCACTGCGCGCCTTTTTTTTTTTTTTTT
AGAATGCCACTCAAACTATTTTTTTTTTTTTTTT
GCGATTATCATATGTATTTTTTTTTTTTTTT
GCTGACCTTTATGATATTTTTTTTTTTTTTT
TCCTTGAATTGACGCTTAATAAAAGGGTTTTTTTTTTTTTTT
CTGAGAGACCTTGCTGGAAATACCTACTTTTTTTTTTTTTTT
CGGAACGAATCAGGTCTTTTTTTTTTTTTTT

Blue color indicates the ssDNA handle for 5 nm gold seeds; green and cyan colors indicate the ssDNA connectors.

DNA barrel with 21 nm by 16 nm by 20 nm cuboid cavity:

AACAAAGTTACCAGAAGGAAACCTACGATCCA
GTGCCCCCCATTTTTTTTTTTCAGATCCTCAT
TAAGAGCAAAATAGCATGGAAAGCTTGGCCTTACCA
GCTCGAGTTTTTCACGCTGTTCTTCGCTTACA
GTTGAGGACTGCCAGCGTATTTTTTTTTTAAGCGCAACCACAACCGCA
AAAATAGCAGCCTGTCGTATTAAGCAGAGGCTTTGAGTGCAGCGAAAG
GTGGTGCTTTATTTTTTTTTTCACGTCAGCAGAACGGAAC
TTTCGCACGCTTACGGCTGGAGGTCCATCCCAGTTTCTTT
CGTTGGGACCTGCCTAAGAGAAGGTTTAACGTATCCAAAT
AGTCAGGAAACTAACGCCCGTATAGTACTGGTCGCTAATACCCAATAA
CGGTGGTGGTCCAGCAATGCGGCT
TAGGAATACTACGTTAATAAAACG
CTGAACAATAATTGAGAATAAGTTCAGTAAGCTAACGCCAAAAGGTCA
TTCATCAGCAGATACAGTCATACAAGCCAGAAATAGCTATGATAGCCG
AGAATGCCCTGGTCTGTGGTGTGTTCAGCATTTGTCACTGAATGCGGC
GCGTGGTGAACGGCAGGTCTCATA
TCATAACCCCACATTCAACTAATG
GGGTCATTGGTGACTAAAGACTTTTGATATAAGTATAGCC
ACTCCTCATTTCGGAAAACATAAATGAACACC
CCCTGAAACGTGAGCCTCGAATTCTAAACAGC
TTTCTCGTTTACAGAGGGGGTATTT
TTTTAATCATTGTGAATTAGGTTTAATATTAGCGGAGTACCAGTTT
CGAGGCATAGTAAGAGCGATAAAAGATATTCAGAGGCAGGTCAGACGA
TTTATAGTAAAATGCCCCTCAAATGTTT
GGATAGCGGCAAAAGAACCCTCAGCCACCAGAGCCGCCGCCAGCATTT
CGTTCCGGCCGTTTTTACGCAGTACTGGCATG
ATCGTCATACCATAAAGCATTTTCTCAGACTG
TTTCTTTAAACAGTTAGTCAGAAGCTTT
CGAGAATGAAATATTCTCATAATCCGCCTCCCTCAGAGCCGCCACTTT
CCGCACAGGTGATGAAACATAAAGTGTTAGCA
ATCAGGTCAGGAAGCCCGATAGCACGGAAACG
TTTAAAGCGGATTGGAGCTTCAAAGTTT
AGATTAAGTTTACCCTCTTTAGCGGGTCATAGCCCCCTTATTAGCTTT
CCAGCAGTTGTACATCAAGACACCGTGGCAAC
ACTTCAAAAGGTCAGGGGAATTAGACCGTCAC
ACTCCAACTATCGCGTAGCAAGGCGCACCGTAATCAGTAGCGACATTT
AAAAAGAGAGCGGATCATCAATAGACGGAATA
TTCTCAAAGACAAAAATTCA
GGCTTAGAGAGTACCTTAATGCCGGGGAGGGA
ATTTGTGAGAGTTTTTTTTTTATAGATCGCACTTTTTTTTAAAGGGCG
TATAATGCTTCCATATTGGAAAAATTTTTAGAACAGGAAGATGTCAAT
TTTGCCAGCGCCATTCCAGCCA
AAGTTTCATGTAGCTCTTCAAAAGGGTGAGGTAAACTAGCATTGTATA
TGATTCCCCAATAACCGGATAAATCGGTTGTAAATCAGCTTTGTAAAC
TTTCCTCCTCTTCGTCGCCATT
GGGCGCGAACATTTCGCAAATGGTAATTCTGCTCAACGCA
GCTATATTATTTAAAACGACGGCCCGGCGGAGTGAGAATA
TTTTTCGTTGGGTACTATTACG
AAAGCTGTTAGGAACGAATGTGAGCGAGTAAC
GTGCCGGACAGAGCACATGCCGGGCAAAAGAATTT

AGGATGAATATTTAAACATTTTTTAACACGGC
AAATCAGAACCAAGCCACCA
GCCGGAGAGAATCGATTACAAAGGCTATCAGG
TGATAAATTTAATTGCGAATTATCAGCCAGCAAAATCACCAGTAGTTT
AGGCTTTTTCCAATACACCGGAACAAAATCAC
ACGACAGTATCTTTTTGAGAGATCGAACGGTA
CATATTATAACGGCTAAGGCTGAGGATTTTAAGAACTGCG
TTTGAGTCTGGAGCCCCCGGTTAATGTGTA
CATATGTAAAACAAGACAGTCAAA
GTAACCGAGTTTGAGGCTTTCCGCTCAGGAAGACT
TTTAATCAGAAAAGTTTGTTAAGGGAGAAG
CGGAACCATTTCATCGTCACCCGTAAAAAAAG
GTTAATATCCCCAAAAACCCTCATGGTAAAGAAACATGTTTTGCGGAT
ATTTTTTCCAACTAAATACTAATAAAATCCGCGACCTGCTCCATGTTT
TTTTCGCATTAAATGCGTCTGGTTAAGCAAAGGCAAGGATCAATTC
TTTCCTTTAGGAGTTTACGCCAGG
GAAAGGAAACGTTGAAATCCAATACAACATTACCATCAAA
TCCGTGGGAACAACAAGCTGCAAGAGTCACGACGTTGAACAATCTCCA
TTTTCCTGTAGCCAGCTTTCATAATCATACTAAAGCCT
AACCCGTCGTTTTCCCGCGATTAAAGAGGTGGAGCCGTTA
TTTAGTAAATTGGGCTGAGGTTTATTT
TTAAACGGGTAAAATAAATAAGGCCCCTCAGAACCGCATT
ACCTAAAACGTAATGCAAGGCCCGGAATAGGT
TTTTTACCCAAATCAAGGGATAGCTTT
CGTAACAAACGAGAAACACCAGAACGAGTTTT
ATTCAGTGTTCATCAAGTAACACTGAGTTGAC
AAACACTCCGAAAGAGTATCACCCTCAGAGCC
TTTGAACGGTGTACAGAGCATTCCTTT
ACCAGGCGTTGACAAGAACCGGATATTCATTT
GGCTGACCAGGGAACCAACGATCT
TTTTTACTTAGCCGGAAATTTTCTTTT
ACGAGGCGCAACTTTGAAAGAGGACAGATTTT
CAATCATACTGATAAATCAACAGT
TACAACGGGATTATACCAAGCGCGATCTTTGAAATTCGTC
ATCATCGCAAACAAAGTTATTTGTCGTCTTTC
AGGTAAATATTGACGGAAATTTTT
ATAATAACGCCGCCACAGCGGCAGCCTCCGGCCTTGTAGATGAAAATC
ATTAAGACGGAATACCTTACCGAGGAAACGCAGCAGTCTCACGAATTA
TTTCCTCAGAACCGCCAGTTTTGCCCAGACGA
CCCTCAGAGAGCCACCTGCCGATGCTGATTGC
AACGTAGATCCTTATTTCGTCTCGTCGCTGAG
TTTGTTTGCCATCTTTATTGAATCTTTAGACT
TTCAGTTTATCAGCTTTGAATTTC
GTGCCGTCGGTTGCTCGGTTTAGCTTATCCCACAAAAATG
TTTGAATCAAGTTTGCGACTATTATCAGAAAA
TAGCGCGTGAAACCATCGATGCTCATTTGCCG
GCTTTTGCCCCTCAGCGGTATGAGTACCGAGCTCCTCACA
TTTCACCATTACCATTTTTAATTCCATCAAAA
TCACCAATGCCATTTGATTATAGCTCTCACGG
TTTGTACCGCCACCCTCAGGTACTCAGTGATTCCA
TTTATTCATTAAAGGTTCCTTTTGGGAAGCAA
CGACTTGACCGATTGAGAGAGGGTAGCTAGGCGCACCGCTGCTCCGGA
CGGTCGCTGGGAGTTACACTACGACCGGGCGCGCAGGCGCCACTGTTG

ACATTCAAACCAGCGCCCGTGGTGAAGGGAGAGCTTAATTTCTGAAAG
ACAGCATCGGAACGAGGAGAGGGTTTCATGAGGAAGTGATCCTTATGC
TTTCGTCAGGGATTTTTCAATCCG
TTTAAGCCCAATAGGAACCCATTTTCA
AACAACCAATAACCGAGCAAAAGAAGGCACCA
CAGACGTTAACAACTTTTGTGTCGGTAGTAGCTTCATTTGCAGAGCAT
AAAGTAACAGCTTGATGCGCCGACCCCCCAGCATACACTA
TTTGTATGGGATTTTGCTAAGTAAATG
TTTACAGACAGCCCTCATAACGCCTGT
TATGGTTTTTGTCACAAAACTTAAATTTCAAGTAACATTCCTAACTTCTCATA
ACCACCCTCATGTACCGAGTAATCCATAGGCTTAACATTCCTAACTTCTCATA
ACCAGTACAAACTACAGTTAGCGTGAACTGACCAGACGGTTAACATTCCTAACTT CTCATA
GGGGAGGGAGTCACCGGCCTTGAGTCTGAAACTCAGGCTCATTATACCTAACATT CCTAACTTCTCATA
AATAATTCTTTTGTTACCAAAAACCCTTTATTGAACGAGTGTGTCTGGTAACATTC CTAACTTCTCATA
GTATCACCAACCGCCATTGCCCTGAGCTGCTCTAACATTCCTAACTTCTCATA
AGTTTATTGAAACGCAGACATAAAAAAATAAATAACATTCCTAACTTCTCATA
GGATTGACCCAGCTGGGGTGCGGGCACCGGAAACAATAGTTAACATTCCTAACTT CTCATA
GATAGGGTAGATGGCAGGCTGCCCAGGCAAATGTTTACCAGTCGAATAACATTCC TAACTTCTCATA
GCGCAATGAGAAACAGTACCGTTCTTAACGGGCACACAGGTAGAAAGATAACAT TCCTAACTTCTCATA
ATATAAAAAAATACATGGGTAAAGTTAAAGGATAACATTCCTAACTTCTCATA
GAGAGAATCCTATTATTAACAGTGGAACAACATTATTCGTTAACATTCCTAACTT CTCATA
ATATTTTAAAAGTACGAGATTTAGTTTCGTACCTGGAGTTCAT
ATTATGACCATTAGATGCTGAAAAGGTCGTACCTGGAGTTCAT
TCATTGCCGTTCTAGCTCACCATCGGTCATTTTTAAATATGCACGTACCTGGAGTT CAT
AAAAAAAGGCTCCAAAAATTGTATAGTGCCAAGCTCGTACCTGGAGTTCAT
ATCCTGCCTGCATGTAGCCGGAAAGCAACTGTAACCGGCGAAACGTACAGCCGT ACCTGGAGTTCAT
AGCTTGGTTCACGAAAGGGCGATCCGAAAGGGTGTCCACGGGAACGGATAACGT ACCTGGAGTTCAT
GGTAATGGACGCGTGCGTCATACCGGGGGTTTTTTTTTTTTTTTTTTT
GTTAACGGTGCATCAGGCAGCCAGCGGTGCCGTTTTTTTTTTTTTTT
AACATCCCGCGGCCAGCGCGCCTGTGCACTCTTTTTTTTTTTTTTTT
TTGACAGGAGGTTCAAACAAAAGTAAGCACTTACCGAAGCCCTTTTTTTTTTTTT TTTTT
CAACACTACTCATTAATGGCTTTTGAGTTAAGTCAGAGAGATAACCCATTTTTTTT TTTTTTT
TTGAGATTACAGGAGTAACAGTTAGAATTAACAACAGGGAAGCGCATTTTTTTT TTTTTTTTT

Blue color indicates the ssDNA handle for 5 nm gold seeds; green and cyan colors indicate the ssDNA connectors.

Square DNA barrel with 16 nm by 16 nm by 20 nm cavity:

ACAACGCCTGTAGCATAGCAAGCCAATTACCT
CAGAACGAGTAGTTTCACTGAGTAGAGATGGT
AGTGTACTAAGGCACCGGTAAAATACGTAATG
TAAGCGTCAATACACTCGGAGATT
CTTCGTAAATCAATCCATTTTAAGAGGTTTAGCAGTAGGGATTTTCGA
ACGGGTTTATTAAACGAACCTAAA
CAAGAGTACTGACGAG
CGACGATAGCAAAGCGAGTTCAGA
TTACCCAACAAAGCTGTCATTGTGCAATAGGACCGTGTGA
TATTACAGTAATTGCTAATTCGAG
CTCAGAGCTCTAAAGTCAGCCCTC
CAACAGTTAAAAAAGGAGAGGGTTTTAGGAATGTCTCCAACAAACCAG
ATCTCCAATCAGCGGATACTCAGGAACTGGCTAATATGCAGGTGTCTG
GAGCAACATAACCCGAGGAAGTAT
ATGACCATAGTAAAATAATAGCGAATCGCCTGGGATCGTC
CTTTAAACGATTGCATCCACCACC
TTACCCTGAGGTTGAGGCAGGTCAGCCTTAAAACGCTAACCAAATAAG
GCGCCCAAATCAGATAATAT
TCAATAATTATTAAACAAGGTCAG
AATTTACGATTTCGGACTGAAACACGATATATTCATAAGG
CCCATCCTAGTCAGAAAAAACCAAGTTTAGACAAGTACAAAAAACACT
GGCTTGCCATCTTGACACGTTGGGTACGTTAAACAATGGCTGCGGACG
GTGCAACTCTGACAATTTCAACTATTAAGAGGATCAACAAGAAACCAA
TCCTGAACCGAACCAGACATAACGATTCATCAGGACAGATCGTTGAAA
ACGACGACGCCTGTTTCTGAGACTATAAACAGGACAGCATTGAGGACT
CTTCAAAGAAGAAAAACTATTATTACCTATCACTTTTGCGATAAATTG
CGCGTTTTCCTTTTGA
GAACCGAATTGAAAGAGTTGA
GATTAGAGTAATTTAGTATAGCCCTATCACCGGTGAGAATGATATTCA
GATTAAGAAAGACTTC
CCAACATGAGTACCTTGTAGAAAGCCAAAAGGACGGTCAATCGGTCGC
GTCATTTTTTAGAGCT
TAAAGCCAGCGTTATAACCCTCAGAACCGGCGAGACGTTAACAACTTT
ATCGCCCACAGCGAAATTAATGCCTGCAAAAGCAAGGTCTAATCAGTA
CATATTTATAAAGGTGGGAATAACTTTTTTCAGAACGGTG
TATCATATACGCTCAATACCGCCATGCCGTCGCTCCAAAACTTTCGAG
ACCCTCAGCGCATAACTGAAA
TGTCGAAAGCGAAACATGGATAGCGCGGAATCTTCATTGAATCCCCCT
CCATATTAATTTCCAGTCAGGAAGAACCGAGAAAGGA
TAACAGTTAATGCTGTGGCAAGGCAAAGAATT
TAAATAAGCAAATATAGTACCAAAATTTTCATTTAAATGCAATGCGGT
CGAACGAGTAGTTTAACTAAAATTATAAAGCCCAT
TATTCTAAATTTTCATATCGAGAAAAGTTTTA
AAAGACTTAAGTTTCCTGCCAGAGCTTTTGATTCATTACC
TGGCCTTGTAGAAGGCCACCGGAA
TCAGGGATTCCACAGATTTGTCGT
ACCGTAACGTCACCAGGTGAATAA
AGAGCCGCCCAGCCGCTCAGAGCTTTCATCGGCATAGCCCGAGCCAGC
CAGAACGCAATAAACATTAGGATTAGCGGACATTCTTAAACAACAACC
CGCGAGAAAACTTTTTGCGTTAAAAAAAGCCTTATCCACC

CTTCTGACTGGTTTGAATT
CAAAAACCTTCCAGAGGAGGCGTT
CCGCCTCCCATCTTTTAAACGATTCCAATGAAGCAGCACCTTACCAGA
CACCACCCCACCAGAATAGCGTCA
GTTTTGAAGACGAACCTCCCGACTAGAACGGGCGGC
TTTTGCACCGCCAGCAAAATCCTCAAACGAGATTCAAATAGTCATCAG
TATATAACAAGCCTTTGACCCTGTTTACTAGATAAGAATACCTCATTT
CATATATTTTGGGGCGGTGAATTTGAAAACATAGGGTAGC
CAAACCCTTTAGATAATAAAGCTAGAAGTTTCAATACCGAACCCATGT
GATGCTATAACATTATATTTCAAC
CAATTTAGTAGCAAAGGCCGGAGACAGTC
GACCATTAAAGATTCAATGATACGCTGGAGCATCGATGAAGTACCCCG
CATAATCAATCAGAGAGATAACCCAGTTAAGCTTTTTAAGTACATACA
GCGTTTGCCTCAGAGCATCCTGAAAAACAAATTTGACAGGACTATTAT
AACGTGTTACAATTTTCGCCACCCCTCTGAATTTAAGCAATAGCACCG
TTACAGAGCGGCGATAACCATGAGCGAAGCCCCCAATAATTCACAATC
GACTGTAGGAATCAAGCCATTAGCATTAAAGGCCGTCACCAGCGCCAA
AGGTAAAGCCTTTTTTGCTATCAGATATTTAA
AAGGTAAATAAGAGAACGGATAAGCCCTCAGATTTGCTAAGTAAATGA
ACGAAAGAGGCAAAAGATACATGGGGGGTAATAAATCAAA
CTTAGATTGATACATTAAAGGTGGTCAGAGCAATCATACAAGCTCAAC
AATTAACTGCGCTAATAAATCACCGGATAAAC
CACCATTATTTGCCTTTAAATATT
GCATTAGAAGAATAACTCCCAATCGAGCGTCTAGAGCCACTTATCCGG
TAGCGACACGCCAAAAATGAAAATAGTTGCTA
AAATCAATGGCTTAGGTGAGAGACTAAATGCT
GTAAAACTATTCAAAAAGTCAATACGAGCTGATCGCAAATAATTTCAT
AGAATCGCATGTTTTACATTATACAACTTTAACTCATTCATACAAACT
TATTTTTGGCAAAACGTTAATATTGTCACGTTGGTGTAGA
CTAGCTGATAAATTTTAAAACAGGAAAAATAAGCCTTCCTAGCCAGCT
GAAACAATGTAATTGAGAACACCCATTATTTAATAAAAAC
CCAAATTGACAAGTTTAAACGTCATTTTGTTT
AGGAAACCGAACTGGCTAAAGGTGACAACTCGAGATACATTTGAGGAT
GACGGAAAGTAGAGGGCGATTTGT
TTGAATTAAACATTAACCGTAATGGAGAAACAGCATCTGCCTTACGGC
TGTCATAAGCAAGTCATTGCTGCCGGAGAGCGATAG
ATTGTAAACGGATTGAATGTGAGCTAACGTCATTCGCCATCTGCCTCA
ATTCGCATTAAATTAACTGAGAGTCTGAGAAGGGGTGAGATTAACATC
AATAGAAATTTGTGAGTATTAAAT
CTGAATATGATTCCCAATTAAGCA
CATTCAACAGGGAAGG
ATGATTAAAAAGTTTGCAGTGCCACGACATAA
ATTACGCATTATAGCCGCAGATTCAAGGCCGGGGGAATTACCTTATTA
ACCCGTCGATTAATTATGAAACAAGAGTGAAT
CCGTGGGAGCGCAGAGCATTTCAATTACCTGAAGATGCTTCTGTAAATC
TTAGCGATCCGCACTCCGTAGGAAGATACAGG
TGGGCATCACAAACGGGAAGATGACATTTAACCAGTACAT
ATCAGCTCCGACAGTAGAAGATCGTGGCGCAA
TTAGAAGTGAATAAGTTAAAAGAAGCAATAGCGCAATAAT
TCCCGGAAATTCATATGTAGA
CAATCGGCGCGCCATGCTCTCACGGAAAAAGA
TGCGGAACAACGGAATACCCAAAAGAGGAAACTATCTTAC
TATCATTTACAATTCGGCAACATATTATTTTGAAGAGCAA

ACCACCAGATTATCAT
ACGACGGCAGTAACATTATCAAACGGTTATCTGGGCGCTGAATTCGGC
GCCGCCACAACCTCACGCAAAACT
TTCCCAGTCATCAATACACCAGCACGAACTGACAGGAACGCAGCAAAT
CCTGATTATACCATAT
TGGCAATTCACGACGTCTGTCCCGTAAAAAAAGTGCACTCAGCTAAAC
TGTTGAGGTTTCAATCGAGGC
CTGAATAATGTTGGGAGGCCAGAGCACATAAAGGTGTGTTGTACGCCA
TATTTGCAAAATAAAG
TGCGCAACTGGAAGGGTTAATGCGGAAGATAAAGAGCGGGTGTGGTGC
ATTAAAGCAGCGCAGTTCAGAACCGCCACCCT
AAGCGCCAGATGAATATCACCAGTATTTTGACCCTGAGTAATTGCAGG
AATCGGTTTTTTAGTTGGTCAATAACCTGTTTGAATCCTT
CAGTATCCGTAGCCAGCTTTCATCAGCA
GTAACCGTATAACGGAATACCTACCACACGACCCGTTGTAACATCCCT
ACTTTCTCCGAGCTCGGCAAGTGTAGCGGTCAAACCACCAAATAT
TTGAGGAACCTCAATCCACCCGCCGGCGGGCC
GGATCAATTCGCGTCCTCACAGTTGAGGATCC
AATTAATTTTCCCTTAAGCAAATCCAATCGCA
CTGGTGTACATAGCTTTCACCAGGGTT
GTCAGTTGCGGGTTATCGAACAAATAGCAAACGGTTTACCGACTTGAG
AAAAAAGACAGAATGCGCGCTTAA
TGCGCCGCGGGCGCTAAAAATATCCGTCAATAGATAATAG
ATATCCAGAACCATCAGCGGGGTCGAAGAACT
TACCGGCGGCCTGGGTAACGGAGGTGGA
CGCTTTCGCACTCAATCATC
CGGATAACTAGTAGTCATTTACATACTTGTAGTGCCGGAACGGTGCGG
CAAACTATCAAATTAACAGTAATACTTCTGACTCAAACAGCGTAAGGC
CCATCACGCGGCCTTGAAAAACGCATTACCGCCAAGTTACAAAGCATC
TAAAGGTTGCATCAGAGTCG
ATAGAACCAAAGGGACCGTAGATTATTGCTTT
TAACGGAACGTCATAAGCAATACTTCTTTGATATCACTTGGCTCAATC
GCAACATTACTGTTGCGTAATGGG
GGTCAGCAGAATGCCA
TGGAGGTGTCCAGAATTCATGGAATTCGCCTGTTCAGGTTGAGTAACA
GCAACCAGCAGTTTGAGGGGACGAATTTTTTAACCAATAGTTGTTAAA
CCACGTCTGAAACACCCTTTTACATCGGGGATAGGA
GCACCGTCGGTGGTGCCCGCCGGGGTATGAGC
GAGAAAGGAAGGGAAGATTAGAGCTTTAGGAGCTTTACAA
CCAGCGCAGTGTCACTGGTCATACGGGCGGTT
TACACCGAAGGCCACTGCGTAAGAATTAGTCTTTAGAACCTCAGATGA
TGCACGAGCTTTGGGCGCCAGCAGACCTCAAA
CGCGTGCCTGTCGCGTCGCTGTCTCAACAGTTAGGGATAGTTTACCAG
CGTTAACGTCTTTGCTCGTGCCGGTGGCAGATTACAGTAA
GTTTTCACGCGCGCCTGCCGCACAGAACGAACTAATCCTGATTGTAGG
CAGCGGTGCCGAAGGGGATTAGTGAAAA
AGGAGGCCATTTTAGATAGCCCTACAGC
CCGGGTACCGTGGTGAGAAAGGAACCTTTGCCTAATTTTAGACTCCTT
GAATCCTGTTAGAATCAACAGAGGGTGCCACGTGTGCGGAAAGGAAAA
TCACTCTTACCATCAAGATTAGCAGCCTTAACATTCCTAACTTCTCATA
GATGATATAAGGCAGAGGCCTTAATTGTAACATTCCTAACTTCTCATA
TTTCCCTGCCTAGCATGTATAGATAAGTAACATTCCTAACTTCTCATA
GTAATGCAGATACCGGAAGCAGGTCAGTAACATTCCTAACTTCTCATA

CTGGAAACATCGGAATTGGATTATACTTTAACATTCCTAACTTCTCATA
CTCCAGGGCGATACCAGGCATAACATTCCTAACTTCTCATA
ATCAAAATCTACAAAGAATGGAAAAATTTCATTAACATTCCTAACTTCTCATA
AACCTGATCATAGGTCTTGCTGAGTAATGTGTTAACATTCCTAACTTCTCATA
GTTAGTACACTAATAGGCAAGGATTAACATTCCTAACTTCTCATA
AAAAAAAGTAAGAACAAAGGTAATCAGTAACATTCCTAACTTCTCATA
ACGCCATCAAGATTGTAATCATATCGGTAATCTAACATTCCTAACTTCTCATA
TCCGTTTTCGTGGTGCTGGCGTACCTGGAGTTCAT
GCTTCTGGAACGTCAGTTCGTCTCTGCCGGGTTACCTCGTACCTGGAGTTCAT
AATCAGTGGTAAAAGAGTCCGTACCTGGAGTTCAT
GGGATGTGATTAAGTTTTAGTGATCAGCAGTTCGGGGGTTTCTGCCGTACCTGGAGTTCAT
AAAGGAGCTACAGGGCCTTGCTGACAAATGAAAAATCTAACGTACCTGGAGTTCAT
TTTGCCGCGAAGGGTAAAGCGTACCTGGAGTTCAT
GAATGGCTATACGTGGCACAGACCGTACCTGGAGTTCAT
TTTCCTCGAGAAGTGTTTTCGTACCTGGAGTTCAT
CTGCAACATGAGGCGGTCAGTATTCGTACCTGGAGTTCAT
GCCTCTTCCAGCTGGCCCAGCCGTTGATTTTACCCCCTGCATCAGCGTACCTGGAGTTCAT
AACGATGCTCCGGCAAACGCGTACCTGGAGTTCAT
GAAACAGCTAAATTTCTGCCGTACCTGGAGTTCAT
TATGGTTGCACGTATAACGCGTACCTGGAGTTCAT
TGAGGCTTAAAGGCCGTAACCCTCGTTTATTTTTTTTTTTTTTTT
TACAGACCAGGCGCAGAATTACGAGGCATTTTTTTTTTTTTTTTT
TCAGCTTGGGAGCCTTTAATTGTATTTTTTTTTTTTTTTT
GCTTTGCGAGGAAGACCTTTTTTTTTTTTTTTT
GACAATGACAGCTTGATACCGATATTTTTTTTTTTTTTTT
ACAACTAAAATAATAAGAACTAACGGAACTTTTTTTTTTTTTTTT
CATGAGTTGCAGGGTTACTTTTTTTTTTTTTTTT
CCGGAACGAGGCGCATAGGTTTTTTTTTTTTTTTT
TACCAAGCTCCGCGACCTGTTTTTTTTTTTTTTTT
TGTCGTGCCCGTCCTCAAGAGAATTTTTTTTTTTTTTTT
GCCAGTAAGTAATTCTACCGGTTTTGCTCAGTACCTTTTTTTTTTTTTTTT
TGCCTTGAAGAGGCTTCGGAACGAGGGTAGCATTTTTTTTTTTTTTTT

Blue color indicates the ssDNA handle for 5 nm gold seeds; green and cyan colors indicate the ssDNA connectors.

Equilateral triangle DNA barrel with 30 nm by 30 nm by 30 nm cavity:

CAAGAGAATCAGACTGTAGCGCGTAAATATTGTGGGTAAC
CTAAAGTTGATAGCAACATCAAGA
TTGTCGTCCAACTTTAAAAATGTTATTTTTGAGTCAAATCCGGCGAAC
AACAAAGTAGCTATCTATTCTGTCGACCTGCTCAATTCTA
CCACCAGACAAATAAATTCAGCTA
CAGTGCCTTTATTCTGTTTAGGAA
GTAGTTTTAATAATAGCCCGGAATAATGAAAAAGCCTTAA
GAGAGGGTAGACTCCTTTATTACA
AGTACCAGCCAAGTACAACGCGAGCAGTTGGGCATCGACATTTTTCGT
TGTACCGTAGCCCTCATTTTAAGA
TAAACAACGGAACAACTAAAGGAAGAGCCTTTATAACCGA
GATTTTGCTCATTACCTAAGGGAATATAAGCATTGTAAACCTACCATA
ATAGCAATTCAGAGCCAGTACCGA
GGCAGGTCAGCAATAGAT
TTGATGATCATAAAAAGGGTAAAA
TTTTCAGGTTTCGAGGGCGCCGAC
TTAAAGCCTAATTGAGACAGCATC
AGAATAAACAGGAGTCGAAAGAGAGAAACCATTAGAATCTTTATCAA
TTTGTTTAACGTCAAAAGGTGTATCCCGACTT
CAGTTACCCACCCTCGGCCCGCGCATTAGCACGGCGGATTCTGCCAG
CGGTTTATCAGCTTGCGGAGTGAGTGAAAGAG
ATAACCCAGTTAAGCCAAATCCGCCAGACGACAAAATTAA
GAACAAAGTCAGAGGGAGAATGGAAGATTTGT
GAATTAACTGGAGGCTTT
TACGTAATTTAATTACTATATGTGCTGCGGCTACGCGTGC
GAAGGTGATAGCAGCCTTTACAGAG
ATCAAGATAAAAAGCCAAATTTCTGCGGTTGC
CTAATTTGTTTTTTAATCATCAACAACGGCAGATCAATAT
CGATAGTTTGAATTTCTTAAACAGC
AATGACAAAATTCGCAAAAGCCCCCAATATAATCCTGATT
GATCGTCACAATAACCCTAATAGTATTAATTTTTACAAAC
AGCGAAAGCGCTAATATCAGAGAG
GGAACGAGAGTTTGACAGTACGGTGCGGTGCC
TTCCTGTACAAGCAAAAGCGTCTTCAGCCATATTATTTAT
GGTGGCATCCATGTTAAAGGCCGCTCTCCAAAAAAAAGGC
ATCTTTGAAAATAATATCCCATCCTAGGGCTTGCCCCCTGTTTCATAA
GCGGGAGGTCTGTAAAGCACAGGCTGCTGATTGCCGTTCC
AGAAGGCTAAGCAAGCCGTTTTTAAGTCAGGACAACGCCTCAGTAGCG
GACAGATGTAACAACCTTAAATTTATTATACT
GAACGAGGAGCTGCTCATTCAGTGGCCCTGACAGTAAGCAAGGAAACG
ATCATCGCAATAAATCCATTAGATGAAACAAT
TACAACGGAAGCGCAGCCTTGATATTCACAAAACCACCAC
AAACAAAGCGGCTACAAACACCCT
AAGCGCGCCATATAACAGTT
CCAATAGGCAGCGTGGTGCTGGTC
TCCCGTAATAGTTGCTGCGAACCTCACCGTACGTGCCGTC
GTATTAAAGCGGATAATCAGGAGGTTTAGTACAAATAAGACCCAGCTA
TTTTCATCGTTTCGTCGCCACCCTCAGAACCGAAAATAAATCCAGAGC
GTAATCTTTAATCAGAGCAAACAAAATATTTTACCCGCCG
AATAAGTATACCGAAGTTTCACGTTGAATTGACAAGAAAATTTTGCGG

ATGCAGAAGCAACTAAATTTTTGCATTTTGACGCCAGAAT
TCAGCTCACTTGATACACAGACCAAGAGCCACGGAACCCA
TTTGTTAACAACCATCACCAACTTAATAGAAATTTCAACAGTTTCAGC
TACCAACGATAGTGAACTTGAAAACTGCCAGCGGTAATGG
CGTTGGGAGACGATAA
ACTGGCTCACCGTGCATGACCGTAAACCCTCACACCGTCG
TTATGCGATAGTTAGCACCAATGAAACCATCGAATTAGAGGTTGGGAA
GAGAAACAATTCATTG
CAAAAGGTATTATGACGCAATAAAATTAGACTTAAAAGTT
GAATATAAACCACCCTCTCAGAAC
GGCATTTTACCGGAATACCAGACCTCAAAAAGGGGCGAAA
ATGTAATTTTTATCAAACGATTGGTCTCTGAATTTACCGTTC
CGCCAACAATTGCTGAATAT
AGCAAAAGAAGATGATTTCTTTGCTAATGGAATAGCTTAG
CATCAAGAAAACAAAAGGGTAAAGCTGTTGCCAGTGAATA
AACTAATGAGGTCTGAGCTGATGCTCGGCAAA
AAAGGAATGGTAGAAAGAATTTGTTCGTCGCTTGAGCCTC
TACGAGGCAAACAATCGTAAAACGGGCGAAAATCCTGTTT
GCAAAAGAGGGACGACTGGTGCCGGCGAAAGGAGCGGGCG
GTTCAGAAATTAGAGAGACTATTAACTACGTGAACCATCA
TGGTCAGCAGAATGCCATTAAATGGGAACAAATAGGCTGG
CGGACTTGATCCCACGGTCTGGCCGGTCACGT
AAACTTTTATGTAAATGAGACTACAGTAATAACTGAGTAGAAGAACTC
GACAAAGATCAACCGATTGAGGGAGGGAAGGTTTTCATCG
AGGGTTGAGTGTTGTTCCAGTTTGGAAAAGAGTCTG
GGATGTGCTTTCAGAGCACGGGAACATTAATGGTATTAAC
GGGCGATCACCGCTTCGACAGTATCGCTGGCAAGTGTAGC
AGGTGCCGTAAAGCACTATAACGTGCTTTCCTAGGGACAT
AGGGTGAGAGACTCCTTATTACGCAGTATGTT
TAGGTAAATCAACCGTAAATTAATACAGGGCGAGCGTAAGAATACGTG
TACTTTTAAAAATCCTCCTGTAATACAGGAGGCCGATTAA
CCTGAGAGAGTTGCAGGCCAACGCGCGGGGAGAAAACAGA
CGACCGTGTATTTTGTCACAATCAATAGAAAA
AATGGTTAAAGACTTCAAAT
AAATTATTTGCACGTAAAACAGAAAAGGAGCG
CATCCTCAGCTGGAGGTGTCCAGCCAAATGAAAAATCTAAACCACCAG
ATAACTATTCAAATATGTATAAAGTGCCATCTCCTATTTC
TCGCAGTCACGACGTTGGCGAAACCTTTCCAGTAATGAGT
TGCCAAGCTGCAAGGCAGCAACACCTTTAGCGGGATTAGGATTAGCGG
TTTCCGGCGGTGCGGGATAGCGAGACCGTAATGTAGCATT
CATTACAGAGATCTAACCACCACTGAATGGC
AGAGGCTGTGATATAACTTTCCTTATCATTCCTCAAACTT
CCACAGACAACACTGAGTAGGAATCCCAATAGGCCAGCTT
GATTGCAGGAAGCAAAACGGTACGCTCAATC
GAAGCCCGTGAAATACCTAGAAAACAGAGCCACCGCCAGCATTGACAG
CCTCCGGCTCTTACCAATTTTAGTGTTTACCA
CTTTTTAAAAGAGTCACTCAACAGTAATTTACAGTGCCCGCATGGCTT
CTCACCGGATAGTAAGGATTAAGTACGGAAATTATTCATTAAAGGTGA
ATCAGGAGAGTTTTGCGCGCAACTCCAGCAAAATCACCAG
AGGTCAGGAACGAGAATCAAAAATAAAAGAAACGCAAAGA
ATCGCGTTTTAATATAATCAGAAAAACGC
GAGAGATAATTCTGCCTCGGGAAACCTGTCGTCCCCAGCAACGGCCAG
AGATGGGCGGAAGATCAAACCAAACCTCTTCGCGTCACCG

TGCCTGAGGAATTACCCTGACCTTGCCCAATACACCCTCA
CGGTTGTAGGGAGAAGAATCCCCCATATATTTTAGAAAAT
GTACCTTTTTACATTGGCAGATTC
CTTTTGATTAATAAGAACAACATGTCCAAGAAAGAGCTCA
ATTTTCCCATCAATAAAGTTGAGAAAACATGAGGTCATAG
AAAAAGAGTGCAACAGGCTTTCGCACTCAATCCGGTCCGTTAAAAAAA
CGTCGGATTCAACAGTTGAAAGGA
CCGGTTGAGACAAGAATTTAATTTTTTCCAGAAACTGGCA
GTCAATCATAAAATATGATTATCAGATGATGGGTTAGAACGTTAATAT
ATACAGGCTTACCCCTGCATCAGA
TTAAATATCGCGCCTGTAGGCAGACAGAGCCGCCACCGGA
AATGCTGTAGCTCCACTGCGC
GCCGCCAGGCGTTTTAATTTTGCAAACGATTT
AACATCCCTTAGCGGCGGGCCG
TGTTCAGCAGGCGAATTATTCATTTCAATTACCTG
TGAATTACGAAGTTTCAAACACTCGCGTCATATATAAACA
GTGATGAAGCCACTACACCTAAAAGTACTGGTAACGGGGT
GGACTCCAGTGTTTTTTCGAGCTTTAGAGCTT
CAAAAATACGCTAACGTCAGATATTCAGAACCACCAGTAC
CTGTTCTTTCACATTAAATTTTACCAGTCCCGGATTCATCTCGGCTGT
GGGGGTTTCATAGCGAACAGTACAATACACTACATTAAACCAGGGAAG
GATGGTGGACTGCCCGGTACAGCGCCATGCATCAGATACA
CATTTGGGGGGAGTTACTTAGCCGAATAATTTCCCTTTTT
TGTTTAGCAATATACAGTAACAGT
CAAATGGTCCCTCAGCTTGTGTCGCAATAATAACAATGAA
GATTCCCAATTCTATACCAAG
CTGGTCAGTTTAATGCTTTGTCAT
ATTGAGGAGCACAGACGAGAATCGGGGTAGCTTAGACTGG
GGCAAACGCGCCGGGCGCTCATTTACAGCGGAAAGAACGGGAACAACA
CCCAAATCGGAGCTAAACTTTTGCCCAAAAACAAAGGCTT
AACCGTCTATCAGGGCTAGACAGGACTCCAAC
TCTGAATAATGGAAGGCAATTCATAAAAACAG
TCAGGTTTAACATTATCATGCTGAAAAGCATAAAG
ACCTTTTACGAACGTTAGTAGCATGAATTAGCGACAATAA
AACGGATTCGCCTGATTGCAGCCAGTCTGGAA
GTGGCGAGAAAGGAAGTGCGCGTACAAAGGCT
AGCTTGACGGCGCCGCTGCCGGAGAATGAACGGTGAGATGGCCGGATAT
TTACAAAATCGCGCAGAAATCGTTAACGGCAT
TCGTCATATTTTCACGGTCATACCAAACTATCACGCTGAG
GTAAAGGTGAAACAAAATTTCATT
GGTATGAGCCGGGTCATTAAACGAGGCCTTTA
CAACCAGCCACCTTGCTGAACCTCGCCATTAA
GTGGTGCCTAGAACGTAACGCCAT
GTTCCGCAAGCAATGGTTGTTAAA
TTTGCGGATAATACATTTGAGGATCACGACCA
TGAGTAACGTCAGATGTATATTTT
GGTGCAATCCTTTGCCCATCGGGAACATTTCG
GGGTTACCTGCTTTGAGCGAACGAGTAGATTTGGTAGCAA
GGTCATTGCGCTGGCAGCCTCCGGCCAGAGCA
GAATTATCCTAACAACTAATAGATACAGAGATAGAACCCTTGCTTTGA
GGTCCACGCTGGTTTGGCCAGCTGCGGATAACCCGTGGTGAACTAACG
CTACCAGTTTTCAGGGCGGCCTCAGCATCGTAATTATACC
ATCCCTTATAAATCAACTTTGATT

GTAATAAACGTTAGAATCAGAGCGAAGTTTTTTTTCAACG
CTCACAGTTGAGGATCGAGCTCGAGACTTTCT
ACCAGTCATTAGAAGTGCCTCAGA
TGAGGCCACCGAGTAACAAGAGTCCACTATTA
AGGTTATCTATGTACCGAAGATTGCCGAACTGGCCCACGCAATTGTAT
AATTCGACTGGATTATAATTGCTC
CGATCCAGATACCTACGGATGGCTCAAAGCGACATAATTA
CTTTAGGAGCAATCATATTCCT
CCTGTGCACTCTGTGCAGCCATTGCAACAGG
GGCCTTGCCGTTGTAGCAATACTTAAGAATAGTGGGTTAT
ATTCTTGCCATCAGCGTTGCGCTCTTCCGAAAAAATCCAA
GAGCTAACCGCGTCCGATTAATTAACCTTGCTTTTCACCA
ACCGTACCCCCGGGCCACGCAGAA
AAATACCGCCAGGGTGGTTTTTCTGAGACGGGCAGCCAGC
GCGAACTGATAGCCCTAAAACATCAAATATCAATGGGATA
TATTAGTCTTGGCAAATCTCCGTGTGAGCGAGAACGGTGT
CGAGCACGTAAATCGGAACCCTAAAGGGAGCCCCC
TCCATCAAGAACAATATTACCGCGTGCTGCGGCCAGAATCACTGGTG
GTCTGAAAAACTCGTAAAGGCAAATAACATCCCTGATAAA
TCATGGAACGCAGTGTAACATGTTGTTTCATT
GGTGAGGCCGCTGAGAGCCAGCAGATCAGCGG
CAGAAGATAGGCGGTTTGCGTATTCCCTTCACCGCCTGGC
TCTGGCCATAGAGCCGTCAATAGAACAAAGAAACCACCAGATAAAGAA
GGTAATATCCCGCAAATTAAC
GGTCACGCGGAAGAAAGAAACCAGGCAAAGCGC
CGCTTAATGGGAAAGCACCATCAA
AGGGATTTGATGGCCCTAGTCAGAAGCAAAGCG
CCTGAGAAACGTCAAAATTAAGAG
CGTACTATGGTTCTGACCTGAA
ACCGCCTCAATAAGTTTGATAAAT
GGAACCTATGAGTAACGAGCATGTGCAAAAGATAAATCAAATTTAACA
TCACCGGAACAGCCTGTT
TGAATTAGTTACCTTAAAAGGCCG
CGCCACCCCAACATATCAGGTCTT
ACGGAATACAATACTGATTGGGCTTAATCGTA
CACCACGGCCTCAGAGGAATAAACCGAGCCAGAAGAGGTC
AAGTTTGCTATCATAAATAAAACGAAGGGATA
CCCCCTTAGGCGACATACGCGAGA
ACTTGAGCCATTTGGGATAGCAGCAGGCTTTT
ACATACATAAAGGTGGTACCAGAATTTAAACA
TAGCACCACAAGGCCGGTAATAGTATCATTGTAGTCTGGA
TATGATATGATTCAAAATAGCGTCCCCAAAAGCGTTAGTAAATGAATT
CAAGGATAGAACCCTCTCAAATGCGGAAACCGGATAGCCG
GCGCCAAAGACAAAAGTTAGCGTTCCACATTC
CGGAATCGAGTAGTAA
TATGCGTTATCGCCATATTTAACAAAGTCCTG
ATTCTAAGCGCACTCATCGAGAACAGAAAAAT
TCTTCTGACCTAAATTTAGTATCA
CAATTTTATCCTGAATTATCCGGT
ATGCCTGAGTAATGTG
CGCAGACGCGTAACAA
CAAATCAAGTCAATCA
TATATTCGGTCGCTGA

CCAGAACGTCATAAAT
AACAAGAACCCCCAGCGATTATACGAGGACTAAAGACTTT
CTACGTTACCCTCGTTTACCAGACCCAGCTGGCGAAAGGG
GAGCGCCATTCAGGCTCAGAGGGGGAAACGTCGTAACGATTAACATTCCTAACTTCTCATA
AAGGCGTTAAAATAAATGACCTAACCGCCACCCAGAGCCGTAACATTCCTAACTTCTCATA
GCCAGGGTTTTCCCAATAACGCCAGCATTTTCAAGTATTATAACATTCCTAACTTCTCATA

Blue color indicates the ssDNA handle for 5 nm gold seeds.

Right triangle DNA barrel with 22 nm by 30 nm by 38 nm cavity:

AGACGTTATGCTGATTGCCGTTCCGGCATTACTGTGAAAA
AGATTTAGTAACCCTCGGTCAGTACTTCTGGTGCCAACGC
TAATGCAGCGGAATTTGTACAGCGCGGGGTCAGCGGTTGC
GAGAAACATACGCCAGTGACGAGCGGTCTGGTAGCAAATC
GTGAGTGAATAACGTCTACCTTTTTGGCAAATCACTAAAT
AGGAACGGATAACGGAAAGAAGATACTAATAGCACGGTCA
GAATACCAAGGCCGATGAATCAGAGTGCCGGAGCAAATCA
GGCAGATTGGTGAGGCGTTTACCAAAAACGAC
CGCTCAATCAGTGCCAGGCATAGT
TATCGGCCTGGTCAGTTTAATGGAGACGGGGACGATAGCTATTTATCA
ACATCACTTGAGGAATACATTTAGAAGGGAACAAGTGTAAATAATCG
AGAAATTGGATAATACTATTCATTACTGCGCG
TACCGATAAGGTGAATCTCCAAAAATTATCATCCGTCGAG
GAATTATCATCATATTACCACCAGCGTTGAAA
TGACCTGAAAGCGTAACTATTAGTAACTAAAG
GTTGCGCCCGATATATCCTCCGGCCTAAGAACGCGAGGCGCAAAATAA
ATTTTCTGGTCTTTCCATAGGAACCGCGGTCCGACTTGCG
CAACAGTTTCATAGTTGTCACCAGTGGTTTAAGATTAGTTGCTATTTT
TCTGTAACCTTGAAAACCAGCTTCTGCGGCT
TGGCAATTCATCAATATGAGTAACGGAGCCTTTCACCGTA
ACCGCAAGTCATTTGCGAAGTGTT
GTCTCGTCTTAAACGACAGCTTGA
TTAATCATCTTATGCGGATCTAAAGTTTTGTCTATGGGAT
ACCCGCCGATTTGAATCATCACGCGTAGAAGAACTCAAAC
CGCTTAATCCACCGAGAGCGGATCAAACTTAA
ACGTATAAATGCCGGGCATCAGACAGTTTGGATTCCGAAATAGAACCC
CGCATAACGACAATGAGGCCTTTA
TGAGGTAGAAAAAAGGTTCTTAAATCAGATGA
CCATGTACCAGAGCCACGCCACCCCGGAACCTTACAGGAGGCATTAAC
CGTAACACAATAATAATTTGCTAAGGCACAGA
AATCCTGACGCCAGCAGTTGGGCGGTTGTGTAGTGGTGCT
GATGAAACGCCCCCTGTTACCTGCAACGGGTAATAGCAGCGAAACAAA
CTGAGCAATTCGCCTGTTCAGGTTTAACGTCAGATGAATACACTAACA
TCAATTACCCTCGTTATAAAGGGATAAAAAAA
TTTTTTCAAAGGAGCGAAAGCGCAGTCTCTGATTTGATGA
AATAGAAAGGAACCTTTAATGAAACAAATAAATCCTCTTTAACGG
CAGAAGATAAAACAGACACCAGTCCCAAAATAGCGAGTTG
CCTGCAACGTCTGAACATTCAAC
TCAATATCTTGCTGGTCAATATAT
GAAAGGAATTGCCTGAAAATTAAC
TTTAGGAGTACAGTAATACATCGG
TAAAAGTTTAATCCTGTATCAGCTTGCTTTCG
ACAAAGAACCTGATTAGTAAATGA
TTGAATGGGAATACGTACAACTTT
TTTATAATCAATACTTAAATTAATGGTTATCTGTGCCTGTTCTTCGCG
GCTTTCGCACTAACGGAACAAAGAGATAGACT
GGTGCCATGCAGAAACTAAAAGAGTCTCTTGCT
AGAAAACACTTCCTTTCAGTATGATTAGTAATA
GTGAATAACAAGAGTATGACCGTATCTCCGTG
GGTAATGGAATTAACTAAAACGAG

AACATCCCACATAAAAGCTGTCTTTTACCTGATAAGTCTA
GTTAACGGAAATGAAATTAAACCAGCGTTAAAGCGTTATA
AATAGCAACTTGTAGAACGTCAGCCATCGACATTTTAGAC
GGAGGTTTGAGCGTCTAGAACCGC
CACGGGAACGGCGGATATCTTGACGCTGGCTG
TCAGAGGTAAACAATCCACTATCAGAATACCAATGGATTATTTACATT
TAACCTAGAAGCCGGCTATCAGGGCCGTAAAGCTTAATTG
TCATCGTAAGAACAAGAAACGATTCCTGATAA
AAAGGCCGAGCCACCAACAGCCATTCCATGTT
ATTTTAAGAACTGGCTCATTATACGCTTGAGATACAAACTCGCCAGCA
ATCGTCGCGATAGCTCTCACGGAAAAAGAGACCCCACGCAACAACCAC
CGACGACACGTGCATCTGGTGTAGGCGCTAATGCCCAATA
GATCCAGCGCCGTTTTATTAGAGCCGTCAATACGTAGATTATTGCTTT
CTCAGAACCCACCCTCCCACCCTCTTCCAGAGGGTCAATC
GACGATTGTTGACAGGACCCTCAGATCCTGAATTGAAAGA
GCCTTGATCCGTATAAGGTCAGTGAAAAGGTG
ACTCCAGCTTCAGGCTTGGGAAGG
CGGAACCCTCGAGGTGCGATGGCCGTTCAGCT
TACCGGGGGATGGTGGACAAGAGTTATCATATTAAGAATA
GGCCAGAATAAATCAACGAGATAGTAAAGCCA
TTACAGGTAGAAAGATTCATCAGACGGATAACCTGACGAGCTCATTCA
GATATTCACAACGTAAAAATGTTT
GAACACCCGCAATAGCTATCTTACGCATGATTTAACTATA
GACGGGAGGTAAAGGTGCTGCGCG
ACAGGGAAAAAAGTAAGCAGATAGACGCAATACGCAAGAC
ATTTCTGCAATGCCAAACAGGGCGGGCGCTGGGAAAGCGA
GTGATGAAGGGTAAAGGCTGGCAGTCGGTCGC
TAAAACGAGGCTTGCCCTCACCGGGGAGCCGCGGCCAGTGTCTTCGCT
ACAATTTTAGCCGCCATTGACGGAGGCCGGAATGAAACCATTGTAAAC
AATAGTGATAGATTAACTGTTGCCACGGCTGG
CATGTAGAAAACCGTCGAACGTGGCCTCCTCACAACAGTT
CAGCGAAACTTTTGCGCCGGTATTCAGAGCAC
CCGGAACCAAATCACCGCGTTTGCCTGTAGCGTGTACCCC
GCCTCCCTAAAGTATTGTTTAGTATTCCAGTATTTGCGGA
AGCTGGCGTAGCGTCCTAATAGTACAAAGCTGAAACACCA
GCGATCGGGGTCACGTTGCCAGTTCGCCGGGCTTGCAGGC
TGGACTCCGCTCGAATGAGTAATGTGTAGGTAGTCAAATCAGAATATA
GAAACATGCAGAGCCGATTTTCAGAACCTCCCGTTTTTTC
ATTATTCTGAGCCAGCCCGACTTGGGAAGTTTGGTAAAAT
ACAGTTAAATTAGCAAAATTATTCGGGCGACAACAATCAA
TGCAAGGCGATTAAGTCAGGGTTTTCCCA
TGGGTGGAATTACGCCATTAAATGGGAACAAAATCCCCCTTAAAAGAA
AACCAGGCTAGTTTGACCATTAGAATCAAAAACTGGCCTT
ATTCGCCACAGCTTTCTGAGGGGAAAGAGCAAGGCGAAACGTGCATTA
TTTTGGGGTAAAGGGATAGAGCTTAACAGTACCTTAGAAT
GATCCCCGTCCGTGAGCGAGAAAGACAATTTC
GGTACCGAAACGTCAAACAATAGAACAAGAAAAATCCAATATAACGGA
TCCTGTTTGTTTCTGCGTGCCGGTAAACATCAGGTTGCTT
ATCCCTTATGCGGCGGGCAGTGTC
TGCTCAGTTATAAGTATAGGTGTATAATTGTA
ACATGGCTATTTACCGCCGCCACCATCTCCAACAAGCCCA
TAATAAGTATTAAAGCGCAGGTCAGAATTGCGTGAGTTTCAGCGTAAC
ACCTTCATGCAACATACAAATGCT

ATAAGAGCTAGCAAACGACCATAA
GTACAACGCGATTATAAATATATT
ACTTAGCCAAGGCACCTGAGGACT
ATAAGGGATTTAAACGCCATTACC
GGACAGATATTTTGTCTTCAACCGATTGAGGG
CGTCGGATATGGGATATGCGGGCCCCAAGCTTCGGCACCGTTAACACCG
TAGGTCTGGGGTTATAAAGACTCC
AATTTTCAAATGCAGATAAAGTAAGCTTAGAG
AATCATAATCCTTATCAAAGAACGAAGGAGCGCAGCACGCAAAATATC
AATACCGATCTGACCTAAAACACTCATCTTTG
CACCGTCAAAAATCACGCGACAGAAAACAGGA
TGAATTATCACCCTCAGCCTATTTTCAGAACCCAGAATGGCAATATTT
GGTAAATACCAGAACCAACAGTGC
TGAGCGAGATACGCGTTAATTTCGCGTTTTAA
AGTCAGAATCAGGTCTACGAGAATGTAGAAAA
GTTTATCAAGGGCGAAAACCAATCGCGGTCACTTCTTTGCCCGTCGGT
CTGTTTAGCCACTATTATTCCAAGAGCCAGCGGTGTGTTCCAGCAGCA
TACCAGTAGGTTGAGTACTCATCGGGAATCATTACCGCAGCGTGCTTT
CCTTATTAGGAACCAGAGAGGCTTAACCTAAAACGAAAGA
CCATTACCTGCCCCCTGAGCCACCAGGTTGAGTAAATCAATTTCAACT
AGTTGATTCCCAATTCTCAAAGCGAAGAGGAAGCCCGAAA
CTGAATATTGCGGATGTTCTGTCC
TCATATATTCTAGCTGTTAGGCAGA
TTTCAACGCTATTTTTAATCGCCATATTTAAC
TAGCAAAACAATCATACGTTTTCA
ATCCAATAAGCCCCAAATCAAGTT
GCATCAATTATTTAAATCGATAGC
AGGGAGTTCTCAGGAGAAGAGGCTGATAAGTGCAAAGAAT
GACGTTGTGACGACGAAGAGGGGGGGCTTTTGGAAAAATCTACGTTAA
AGGGTTGAACCAGGCGGAGACTCC
ACGCAAAGACACCACGCAGACCAGGGAATCGTAGACTGGAAAAGGGGG
TACATACATAAAGGTGACAAGAAT
ATACCCAAAAGAACTGCGAAGCCCCCCATCCT
ACCCCCAGGAGATTTGTAAATAAGAGTACCGCGTTGTTCC
ACGTAATGCCACTACGGGAACGAGCATAATCA
TAGAAAATTCATATGGACCGAACT
TTAAACAGGACTTCAATAACAACCAGTAGATTAAAGCGCC
TTCAGAAATTACCCTGTGAGTTAAATCAGAGAGATAACCCACTCAATC
TGTAAATGACAAAAGGACGCGCCTAAAGGGTGCAGTTGAG
AAAGAACGTCGAGCCAGAAAAAGCCAATGCCTTCCGAAAA
CTTTTTCACCAAGCGCGAAGGAAACCGAGGAACCGAACAA
TTAGTTAAAACGCCAACAAATTCTAAAATTTTTCGGCAAA
TTTCATCTCCGTGTGATATCATCGTTTTGTTTAACGTCAACATCGCCC
AAAGACTTGCGTCAGACATCTTTTAGGCAAGGAGCGTCAT
AGCGCCAAAATCAGTACAGTAGCATAGTAGTATGTACTGG
CCTGTAGCTTCATTGAAATACTGCGCGCATAGAAGAACCG
AGACGACGCTTAGGTTAGAGACTAATGAAATATGAACAAA
AAGTACCGCTGATGCAAATAATATTTTTTAAGGCGCATTA
GTAATAAGACCATCAATATGATATTCAACCGTTTTAAATG
GCCAGTTATTTTAGCGGGACTTGC
CATGTAATATAAATTAATGCCGGAGAGGGTAGCAAGGATA
TCGGCATTACGGCTACGACAGCATCGACCTGCATTATTTA
TGCCTTTATTTCATGAAGCCATTTGCGCAGACCCTAATTT

AGCACCGTAGACAAAAATTAAAGGGACCAACTTCTTACCA
AACCAATAGGAACGCCTACATTTCTCATCAAC
TTCGAGCTTGCGAACGACTATTAT
GTCATTTTAATGCTGTAACAACATCACTACGT
AGAAAGGCCGGAGACAAAGATTCA
TAGCATGTTTAAGCAACATAGCCCTCAAGAGA
GGTTGATAATCAGAAAAATCATACGGGAATTA
AGATTGTATAAGCAAATCTACTAA
AGAGAATATTACACTGGGCGCTAGCGTACTAT
ACGCTAACTGAAGCCTGCCACCCT
TACAAAGGCTATCAGGTCATTGCCATTATGACCCTGTAATACTTTTGC
CGGAAGCAAACTCCAACAGGTCAGACGGTGTCTGGAAGTTTCATTCCA
CGGTTGTACCAAAAACTGAGAGTCTGGAGCAA
ATGTTTTAAATATGCAACTAAAGTGATTAGAGAGTACCTTTAATTGCT
TCAATAACCTGTTTAGCTATATTTTTAAATTTTTGTTAAATCAGCTCAT
TATTAAATCCTTTGCCTTATACTTCTGAATAA
ATTTAGAAGTATTAGACTTTACAATACCATATCAAAATTATTTGCACG
GATAGCCCTAAAACATAACAGAGATAGAACCC
AGTAATAAAAGGGACATTCTGGCCCGCCATTAAAAATACCGAACGAACC
TGGAAGGGTTAGAACCACAATTCGACAACTCG
GCCAGCAGCAAATGAAAAATCTAACAACAGGAAAAACGCTCATGGAAA
TTGTTAAAATTCGCATCATTTGGGGCGCGAG
GAACAATATTACCGCCAGCCATTGAGCATCACCTTGCTGAACCTCAAA
ACAAGAGAATCGATGAGAGCATAAAGCTAAAT
GGCATTTCGAGAAAAAACACCGGAGTTACCACTTTACAGTAACATTCCTAACTTC TCATA
GTTGTAGCAGTGAGGGCGCCGCTCGGCAGCATCGTCATATAACATTCCTAACTTC TCATA

Blue color indicates the ssDNA handle for 5 nm gold seeds.

DNA ring with 25 nm inner diameter:

ACCGCCAACGTATGTGAGAGATAGACTTTGCCGTTCGACGATTGG
GGAATAACCCAACTTTTTAA
GAGAGGGGACTCCTTGAAATAGCAATAGCAATTTTATCGCCACCCTC
GGAAATCAAACGTTAAGCCCAATAATGTCTTTCCACAGAGCCAC
AGTCACGACGTTAGAAAATTCAT
GCCACAAAGGGGGTAACCTGGATAGCT
GCGCAACATAGTTGTACTGGACATGGCTTGTTGGGCGG
GCGATCCGGAAAGCTTGAGATGGTTTACCCAAATCTAAATGAA
GCCTCTGCGATTAAGTTGGGAGGTGGAACAGCGG
GACAAAAAGACATGAACAAAGTCAGAGAACGATTTT
ACCACCGCCTCACTGGCTCATTATACCACAGACCA
TGAGGGGGTGGCATATCAGAGAGATAAAACAGCCAT
TTACGCAGCTTTATTGTGAATTACCTTAAGAGTAAACTTTCAA
ACCCCGGGCGCATCAACGGAACAACATTATCAGAAGCGGAGCCTT
CCAAAAGATAGGTTCATCAGTTGAGATATCAAAAATTCGAGGT
AAATATACAAACTCAACTA
TTTATTTATGGTTTGATAGCAGCAATGC
AACGCAAGGGCGAGGCCGGTTCAAAAATGACCCTG
TGTCACCATTAGACGGGAGAACAGCCTTTAAAGTTTGCC
CCATTCGCCATTAAAATA
CTGGTGCGGTGCGGCAACGCCT
AAAACTGTTTGAAAGAAAAATCTACGTTGACCAAC
GTATCGCTCATTTTCAGGCTCAGA
CTGCCAAGCATGTGGAGCAAGAGACTCCCCAGAGCCGGCAGCCT
AGATGGTTGATAAAAGGCTAGCGGGGTTAGCCACCAACGTGCCG
TCAATCACTCAGGAGGTTCGAGGAACAAAGTT
CGAGTATTAAAAGAGACAGTCAGTAGCATTATTAGC
AGCTTTAAATCAGGTAAAGAAAACGTCA
GCAGTATGTTAGTATTCACTTGAGCTTCTAGC
ATCAAACAAAAAATCCGAATTTACCACTGGTGTGTACTACGAAGG
ACGCAGAAGCCGCCACGGGAACGGAATGTGCTAAACAG
CTCACGGTTTAGTGATCCTCATTAAGGGTTACCTGTGAGGAAGTT
GGTGAAGCACCGGAAACAAT
CGGAATTCAGCGCCATGTTTGGAAACTAGTACAGAGGCT
ACCAGAACTCGTCGCTGCCGCCAGCTGTGGTGCTGCACCCTCAGC
GAAAAGTCATAACGGACCCTCAGAGTCATACCGGAGGCTTGCA
CGAAGCCAAGAACTGGCAT
AATTGAGTAGAAAATACATA
AGCGAATCAATGTAAAACGACGTTTGCCGCCACAGGGA
ATTTTGACAACCGGAATTA
AACGCAATAATAACGGAATGGTGTATAGGATTA
GAAGGGTAATTGCAGGCGCTTTCGCACTCAATCCGCCGATCAGATGCC
GATGCTGATTCTCCGTTATTTCGGAGAACC
CGGCGAACCCTCAACCTATCCAATAG
ACCAATAGTCTGGCAAAAACC
TTTGTTCATCAAATCATAA
ATTCGCGGAACGTTTTAAAT
ACAAAATACCCACAAGAGCCAGCA
ATTATTTACAAATCAGATATAGAAGGCTTATCCGGTATTAATGCAGAA

ATAACATAAAAAGCATTGATGATGTAGCGACAG
GGGTAAAGGAGAACGGGTATTAAA
GTTGCCCTGCCATCCCTTACGTTCCAGTGTCTTTCCTCCACAGA
GGCTGGAGGTGTCCAGCATCCCCCTGCATCCCTTGATA
ATGCCAACGGCAGCACCGTCGGTGGTGCCTGTGCACTC
TGCTGGTCTGGTCAGCAGCGTTTTCACGGCCGCCACCA
AAATCAAGATTAGTTGCTATGCCTGTTCTTAGAACCGC
TCCCGACTTGATCCCCGGGTCACCGGAAAAACAGCTTGATAAAT
TAGGAATCATTACCGCGCCTGAACAAGATTTCGGTC
AGAACAAGCATGTAGAAACCTTTAGCGTCAAGCCTTTACTGAGTA
TCGTCATAAAGGCTGGTAATTTGTGTACA
AGACGATCCACAACGGCTACAGAGGCTTTGAATCCGCGACGCTGGCTG
ACTGCGCGCCATCCCACGCAGCGGTCCGT
GCGGCGGGCCAACCGCAAGACCGGCCAGA
CAGCACGCGTTTTGTAGAACGTCAGCGTGG
CGCGTCCGTGACAACCATCGCCCACGCATACGAACCAGACTACCCTGA
ACCGAGCTCGACAGGCAAGGTGATACCGATGAGAGTACCTAACGAGAA
ATGTTCAGCTCTAAGAACTTGCCAGTT
AGATAAGTCCCAATAGCAAGTCCCAATCCAAATAAGAGGTAATTG
TTTACGAGCAAGCCGTTTTTCGTCAAAAATGAAAATAGTTAACTG
AATCAATAATAGATACATTTCGCAAATGGTCTGGAAGTCAGAGGGGG
TTCCTTATCATTCCATTTCTTTGC
AGCCAGAATGGGATTTCACCAGTACTTTAATCCCGGCACCGCTT
ATTGACAGTGCGAATAAATCGATGACGTTGGGGGGGACGACGAC
CCTCCCTATCACCGAAACAATATTAC
CTTTTCATAGCCTCAGCCATCAATCGCCAAAACGTCGGATTCTC
GTTTGCCATCGCGCCTGTTTTCTACTAAT
CATCGGCATAAAATAATATTATTTTCATT
CGCGTTTTTTGTTTAAATTTTCATCG
AATCCAGAGAGACCAAGTACCGCACTCATCG
TGCCTTGACAGTCTCTCGTAAAAACGGTATGAGCCGGGTCACT
CATTTGGCACCGGAACGAGCCTAATGCGAGGCGTTTTAGCGAACC
AAATCACCAAATCAAGCATAAAGAAATATTCAGCTTAGAGCT
CCATTACAGCGCTAAACATATAAAAGA
AGTAGTAGCATTTGCGGATGTTGAATCC
ACAATGACAAGCCTCCTCACAGTTGAGGCGGGAGGTTTTACCAACGC
GCACCGTAATCAACAGGAGTAGCCCCTCATATACCATCACAGGCT
GTTTCGTTGCTAAACATCTTGACAATTGTATCATCGCCTGATAAA
TAGCAAGCTATTCTGAGCAGGTCACGGCAAACACCAGCTTAC
ACAAGAGATAATTTTTTTTGAAAGACAATCATAAGGGAACCGAAC
TCAGGTCGCTCCAAAAAAAGCGGATAATATCGCGTTTTAATTCG
GGAGAGGGGTGCCGTCTCAGAGCCCTGAATCTTGAAGCCTT
AGTTTTGTCAAGCGTCATTAATAAGCTGCTCAGCCAGTGCCAAG
AGACGTTAGAACGTAACAAGCGATTATACCAAGCGCG
CGGAGTGAGAACCCATTTTAAGAAGGAAGATCGCACT
GAATAGAAAGGCGCATAGCTGCTCCATG
GGAACAACACGAGGGTAGGCGCAGTGTC
TAAAGGAATGAGGTTGAGAACATGA
TCACGTTGGCGGGATCGTCGGCCAGAAT
TCCGAACCACCATCAAGAGTAGCCGA
AAAAAAAAGATTGCCTACGAACTGTAACCGTGCAT
CGGTTTATTTTTGAGATAGAAAGATCACGTTGGTGT
CAAAGAATTAGTTCAGAATTAATTGCTCCTTTTGATAA

AAAACATTGGGTGAGAGCAACACTCATTAAATGTGAG
TTGCGGGAGAGACTGTAGCCAATGAAACACCCCCACGGAATAAG
TTTCAACGCAAGTTTTGCTTCATTCCATATAAC
AAATTTTTAGAAGTATGCCCTGAGGCTTTTGCA
CACCAACCTATTTGACCCCCAAGCTGCTCATTCAGTG
CGTAATGCCTCAGCAAATCGTTAACGGCGGCGCGGTTGAAGCCGCAC
TCCATTAAACCAACGGAGATGAACCGGA
GACTTTTTCACAGCCAGCGGTGCCGGTGCAGCGGGGTCAAGTTAAAC
AGCGAAAGAGCAGACGGTGGACAGATGAACGGTGTAGTCAGGAACGGGA
GGGAGTTAAAAAAGACTTCATGCATCAAA
TCGGTCGCTGGGGTTTCTGC
CGACGATCTTCCTGTAGCC
AAAATAGCGAGACGAGAAAC
TGGGGCGCGGTAGCTCAAGCGTCCAA
AAACAAAGTAGGGTAAAATATTTTCTGTATGGAAAGCGGTAACAG
TTGTGTCGAAGGACTAAACAGTTTCAGTTCACAAACCCCTGCC
TTACTTAGCCGGAACGAGGCCAGCATCGGA
AGGAAGCCCGGGCCGCTTTTAAAATC
AGCTTCAAAGACCGATATATTAATTGTATCACCCTCAGTTGCTCA
GTCAGGATTAAGTTGCGCCGGAATTTCTTCCG
GAGGTCATTTTAACATCCAAGCAATAAAATCAAAATGAATTAG
TAATTGCTGAATATAATGCTAGCTGAAAAGGTTGTACCAATAGCCCCC
AGTTGATTCCCAATTCTGCATACACTAAAACACTCATCAAACGAAAGA
TATTCATTAATTTCAACAAACTA
TAATAGTAATACCAGAATGTGTAGCTCATGCCAAA
AAGATTAAGTAATAAAGAGAGTC
CTATTATAGTTACAGGGATCTACATCAGATAGCCC
TCAGGTCTTCGGAAGCAAACTCCAACAG
TGACCATAATTAGGAATAATGCCGATTGTGTGAAT
CCCTCAAATTACATAAATGATATTGTAAACTATTGAC
TACTGCGGAAGTAAGAAAGGCCGTTCGCAACCGAT
GACTGGATACATGTTTTAAATATGCAACTAAAGTACGGTGTCAATAACC
TAAATTGGCCAGGCAAAGCG
AAAGAAGGATAAGTTTGACCATTCGGCTGTCT
ACCAGAAAATAAGGCTACGATCTAAGGCAAAAGAGAACGAGTAGATTTA
CGAGTAGCAGCCCTCTGTTGTTTTCCC
ATGCAGAGCTTTAAACAGCAAAATTAATAAATCATAATTCACAAC
TACCACATGGCGGATTGACCGTAATGGACAGGAA
CGAGGCATATCGTCATCTAAATCGGTGGCATCAATATCAACAAT
CCCTCGTTAATGTTTATAATACTTTGTTTAGCTACCCATCCTAA
CATTAGCAACATTCATTAAATT
GACTTGCACCCAGCTACTATCTTACGTACCAGGTAAGTAAAAGCC
GCACATCCTAAGCAGAAAGGATTCACCGTATATGT
AACCATCACCAGCTTTTTA
AGGCGGCCAAAAAGAGTGCCCGTATGCAAGTCGCTA
CATAAAAGGGAAGGTAAAGTTAAT
ACCTTCATCATGCGATGTACCGTGCGCCTCAGAGCC
TCGACATATTAAATTTTTTTAACGCCAGGGGGAAGGTAACATTCCTAACTTCTCATA
TTTTTCGTACCAGTCCAAGTATTACGCCACCTAATCGTTAACATTCCTAACTTCTCATA
TAACGAGCAAGAGCAAGTCACCGATTAAAGATAAGCTAACATTCCTAACTTCTCATA

Blue color indicates the ssDNA handle for 5 nm gold seeds.

DNA lid

AGGTGCCGAGGAGCGGAGAACAAGCTTATCATGAGCGCTAAGAAAAGT
TGCGGCCACCGGGTACACATAACGATTCATCATTACCTTATGCGATTT
GAGGATCCGAATGCGGAAGTTTTGTCGTCATAAGGCGCATACTTAGCC
AGGGAGCCAACGTGGCGGAATCATTGTAGAAAATTGAGTTTAGCAATA
TGTTCTTCGGGGTTTCAAAACCAATGCTTTAATTGAAAGAATAAGGGA
TCCACTATTAAAGAACTAAAACGACACTATCACCCTGACGTGCTCATT
CCACTACGTGAACCATAAGCCTTAGAACGCGAAATCCAAAAACTGAAC
AAAACCGTACCCAGCTATCAGATATCAAAAATAAAAACAG
TCATACCGGCGTCCGTAAGAGCAAACTAACGGATACCAGTCAGGACGT
AGCCGGCGCCCGATTTGCAAGCAAACAATTTTATCCTATC
AAAGCGAATAAAGCACTATTCTAAAATCAAGATAATTTGCCAGTTACA
GGCGCGGTGGCGCTTTAGAGTACCTTTCATTCTTTGAGGAGAGGGTAG
CCTGAGAAAAGAGTCTGCATTTTCAGTATCATTAGAAAATGCGACATT
ATCCAGCGCTTACACTATAGTCAGATCGCGTTTGTATCATAAACGAAA
GCCAGCGGGCATCAGAAAATCAAAAGACCGGATACCAAGCCTCATCTT
TCATTGCATGCGGTATAGCGAACCAATCAGGTGGTCAATCGGACAGAT
CCGAGTAAGTGTTTTTAGAATATAATCCCATCCAATGAAAAAGCCCAA
GCTTAATGGACGAGCAAAAATAATAAGTACCGATACCCAACAGTATGT
GTCACGCTAATCAGAGGTTTATCAAGACGACGGAAGGAAATAAAGGTG
GTGCTGGTCCGGACTTCGAACGAGAACATCCAGACAACAAGATACCGA
TGCTGGTAAACAGGAAGGAATCATCGAGAAAATAGAGCCAAAGGCCGG
AAACATCCCAGTGTCACTGCGGAACCAGAGGGAAGAACCGGAGATGGT
CGTTAACGTGCCGGTGCCCTCAAAAATAGCGAAACAAAGCAGAAACAC
GGAACGTGCTGGTCAGTCTGGAAGTTTAATTGCTAAAACAGCGAAACA
GCCATTGCATATCCAGGCCTGTTTGAGCCAGTTTATTACGAAGAACTG
GTTGCTTTCGCCGCTATACGAGCATACCGCGCAATAACATGAAAATAG
CTCGTTAGGCGCGTAATGTCTTTCCAAGCCGTGGAGAATTTAAGAAAC
AGTGATGAAAAAAAGCTTAGCAAACCCTCATAATTGCGAAGAATAGAA
TAAAAGGGACCTGAAAGATGCAAAGATTAAGACATCGGCACATCTTTT
AATCAATATAATCCTGTATACAGTTTTGATGATTCCAGTA
ACCGAACTAGCGATTAAGCAAACTCCAACAAGATAATCAGGTACTATG
ATCCCGTAAGGGTAAAGTAGCATTTAGATTTAATCGGAACCTAAAGAC
CCCTTCTGACATTCTGAAAGAACGAATTACTAACAAAAGGTCATATGG
AAGTACAAGCGCAGACCTTTACCCTTGAATCCCCCCCTGCTTTCACGG
GCTATCTTATAACGGAACAAAAGGAGGCAGAGGTCCATCAATCGGCCT
AGGGATAGAGAGATAGGTGTAGGTAGGCTATCCAGCCCTCACAACGCC
TACCGAACGCGGTCAGTAGAATCCTTTAACAACCTCAGAGAGCATTGA
GCATGATTGCAAGAAACTACGAGAATGACCATTGCCGGGTATCCGCCG
CTATTTCGTAATAAGTTTTTCAGGAACGGATTGAGGATTTTTATCTAA
AATTTGTGCTCTCACGTTTTAGAAATTAAGCAAACAGCTTCCATCGCC
GAGGTGAGGAACCACCATAGCTTATCCAATCGCCATTAGCGCAAAATC
ACGCAATAACCGAAGCTAAGTCCTTAATCGGCCCACCACAAAGGGAAG
GATTAGGATGTATCACACCAATAGAAATTGTACAACTGTTAGTTGGGT
AAACGACGGGTTTTCCAACAAGAGTATTTTGTGAACCGCCGGAGGTTT
CCTCAATCAAGGAATTACAAACATCATCGGGAATTTACCGTACAGGAG
AGTTACCAACAATAAATCGCCATACTTCTTTG
AGTACCGCGAGGCTGATTGACCGT
AACGCCAGGCCAGTGCATCTACAAAAAGATTCCGGAGTGATAATAATT
ACAGTTGAAATATCTGTAATTACATTGAAAACGCGTTTGCTTTTCGGT
CGAAGGCAGCTTAGAGCCGAAAGATGGGTAAA
CGATCGGTCTCCAGCCTCAAAAATGTAACAACGTTTTGCTCAGTACCA

CGCCATTCCCGGAAACATCAGCTCACGGCGGAGACTCCTCAAGAGAAG
TAGACTTTTGCCCGAACAGATGAAATTGTTTGTATTCTGAAACATGAA
AATAGATATAACATTAAAAGAAATGGTTAGAAAGTTAATGCCCCCTGC
AGATCGCAGCGGGCCTGGAAGATTTCAATCATCCATGTACCTTTCCAG
TTCTGGTGAGGCTGCGAACGTTAAAATCGATGTACAAACTATAGTTAG
AAATCCTTACAAACAAACCTTTTACAAGAAAACCGCCGCCCCGCCACC
AGTTTGAGATACATTTCGCCTGATACCTGAGCGTCAGACGAACCGCCA
ATCTGCCAGTTTGAGGGTGAGCGAAATTCGCGGATATAAGCCTCATTT
CGTTGGTGTAGATGGGGGGAACAAATTTTTTACGTACTCAACCCTCAG
TATCAGATGATGGCAATTCATGGGCTCGTATT
AGAAGGAGCGGAATTAAATGGAAGTGCGTAGATTTAACGGCAGAATGG
GGGTTGAGTGTTGTTCGTAGAAAGCCAAAAGGTTGGGCTTGATATTCA
TGAGTAATACTTTCTCACGTTGTA
TACGTTAAGTGGACTCCGCGTGCC
AAGAACTGTAGTAAAAATTACGATGCAAAAGCGGGCCGTATCAGACG
TGGGAAGAAAGGCTTGTAACCCTCGTTTAATAAGAGCTTGCAACGTCA
GCGTCTTTGTTTAACGTAGAAGGCTCATCGTAGAGAAAGGCCCGCCGC
CAGAACGAGGCTCATTAACAACATTATTACAGCAGTTTGGTCACAGTT
CAGCCTTTAAAGAATCTTACCAACGCTAACGA
GATTTTTTCCAGAGCCTTAGTTGCTATTTTGCCTATCAGGAACCCTAA
TTTATCCCGGCGTTTTACTCATCGGCGCTAGG
ATCTTGACGGTAATAGATGCAGATCGAGCTCGCCGAGATA
TTACCCAATACAGACCAATATTCATGACTATTGGTGTGTTTCACTGTT
CAGTGAATGACCAACTACAGTTCAGAAAAATTCAGGGCGCACGGGGAA
GGAAGCGCCCACAAGACCAATCAAGAACAAGACGTATAACGCCAGAAT
GAACGGTGATCAACGTGAGGCTTTGGCATAGTGAGCCTCCAACAAGAG
TAATAAGAACAGAGAGCCACCAGACGACGATATGCCAGCATACCTGCA
GAGATAACATTAGACGTTTTATTTTTATCCGGTAAATCGGGCGATGGC
GGGTAATTTCCAAGAAACGCGCCTCGGGAGCT
CGACCTGCCGGATTGCGTCCAATACTGCGCGC
GGAACGAGCGGAGATTTTAATTCGGATAAGAGTCCAGCATGCAAGAAT
TGTATCGGGTACCAAAGGCGCGAGGCGGTCCG
AGTATTAAACATGGCTAACAAATTTTTGTTAACAGGCAAAATAGGTCA
TGTACTGGGAACCTATGATTATACTTCTGAATTCATCATAATTTTAAA
GGAATAGGTTAGCGGGCCGTCGGATTCTCCGTCGCATCGTGGCACCGC
AAATCCTCATACCAAGACAGAAATTCATTTTG
AGAGGGTTTCTGGCCTCAAAAACACTTCGCTA
AAACGTCACGCGTTTTCGCTGAGATTTTCCCTTATTAACATATCAAAC
GAGGCAAAGAGGAAGTCAACTAAAATTAGATAAGCACATCATGCTGAT
TGACCCCCACAGAGGCCATATAACAGTTGAAAAACAATATTGAGGCCA
TAGCAAACACAATCAAATGCGTTATAAACACCAAACGCTCACCAGTAA
TTTTTCATAGAATACACTCCTTTTAGCTTCAAGAGCCGGGCAGCAAAT
TTTACCAGAAGACTCCAATAGGTCAGGATTAGCGCACTCATCAGCGTG
ATTTTGTCGTAGAAAATGTAATTTTAAAGTAAAACGGTACGTGCTTTC
GCAAAGACCAACGCTCGACCGTGTTCAATCGT
CGCTTTTGAATAACCTGTAGCTCATCGGTGGT
AGCAGCGAACCGATATAATTCTACTCAGAGCAACATCGACGACGCAGA
CAACGGCTCCGACAATATAAATCATACAGGACGCCAACAGTACCGCCA
CAACCGATTTGGGAATCTTTTTCATAAATGCTGCGTAAGAATTAAAAA
CACGCATAAAGACAGCGTTTGACCGTACGGTGCAGCAACCCAGCGGGG
ACCAGTAGCGCCAAAGGAAATTCCCAATTCTGGTAGAACGCGGCCTTT
TGAGCCATTGAGGGAGAATAAGAATACAAATTCTCAAACTCGCAAATT
GGTGAATTTCTGACCTCTCCGGCTGAATGGCT

CATAATCAGCCACCACTTTCATTTATGATGAAGAGGAAGGAGAAGTAT
CGAGGTGATTGAAAATACGCAAGGGAGAAAGGTGTTTACCCAGAGGTG
TAGTTGCGCTAAAGGATATTTTAAATGCAGCGAGCAGAAGAGATAGAA
AGAACCACCCTTATTAATAATGCC
TTTTCACGATTTCTTAATAAAGCCTAATAGTAGTTAAACGCTCATAAC
CATAGCCCCACCATTACAAGCAAGGCAAAGAACGCACAGGCGTGGTGA
GACTGTAGCCAATGAAACTATATGAATATATTGTCACACGATGGAAAT
GAATCAAGATCATAGGCCTTGCTTGAGCCAGC
TCTGTATGCACCATCATTTGCGGGTAAATTTC
CTTTCAACTCTAAAGTTAGCTATTTCGTAAAAGGCGATTAGGGAAGGG
AGGAACAATCCACAGAAGGTCATTGCCTGAATGTCAGTTGATAAAACA
TGAGTTTCCCCTCAGAAAATATTTGAACGCCAAGCTTTCCAACCGTGC
CGTAACGAAGTTTCAGAAAAGGGTATAAAAATGAAAAAGAATAAAAAA
TGTAGCATCACCCTCATAAAATTCGCATTAGTTTCGACAAGCAAATCA
CCCTCAGAAAATCACCTTAATTAAAGAGTCAAACATCGCCATACGTGG
GAGCCGCCGTACATAAATTATTCACTAACAAC
ATAGGAACATGTACCCCTGATAAAGGATAACC
AACCGCCAGTCACCAGAACGGTAATTTGAGAGCAAGCTTTAGTCCCGG
AGCGTCATCACCAGAGCAAAGAGTCTGGAGCACAGTCACGGCGCCATT
CAGGAGGTGTCTCTGAGAAACAATTTTAACGTCGTTATTATTCCTGAT
AAAGCGCATGAGGCAGAAAAGAAGGAATTACCACCTCAAACCGCCTGC
ATGAACTCCAGGTACGATTGGCAGATATTTTTTAGGTTGGTTATCAAATTTGCCTTAGCC
ATGAACTCCAGGTACGCACAGACAATTCACCATTAGTTAAAGGCGTTAGGAAGGTAATAA
ATGAACTCCAGGTACGAATATCTTCTTGCTGATTTTTTAACGTCGCTAGGAACCAGTAGC
ATGAACTCCAGGTACGAACTGATACACGCTGACTGTAAATTGGAAACAACCCTCAGATTG
ATGAACTCCAGGTACGTGCCTGAGTTTGACGCGATAAATATTTCATCTATCACCGTTAGC
ATGAACTCCAGGTACGACCTACATTAGAAGAACTTACCAGCGCCAACATACATACACCGA
ATGAACTCCAGGTACGAACCGTTGTAGACAGGTTCTGTCCACAATAGACCTTTTTAATAT
ATGAACTCCAGGTACGAGCATCACTAGGAGCATTTCAATTTGCTTTGAATTAAAGCGGTC
ATGAACTCCAGGTACGAACAGTGCGCCCTAAATAGTGAATGTTATATAACCATCGACACC
ATGAACTCCAGGTACGAGGGATTTTAGCAATATTTAACAATATAAAGCACCACGGAAATA
AAAAAAAAAAAAAAAAGCCCTGCGTGGAGGTGGTCATTTTTAAATATGTTCCATTATCAC
AAAAAAAAAAAAAAAAAGTTGGGCCGGCAAACCTGAAAAGAAATGGTCCGGGATCGAACG
AAAAAAAAAAAAAAAAGGGGGATGACGGGAACTTAATGCCAGTCAAATGGATTTTGAAAA
AAAAAAAAAAAAAAAACTTACGGCGCTGGTAACTTCAAATAAGCAAAGTCCATGTTAGGC
AAAAAAAAAAAAAAAAGAGCCGCCTGCTGCAACTAGCATGGTATAAGCGCCACCACTATA
AAAAAAAAAAAAAAAAGCCAACGGCCGGCCAGCATTTCGCGTGGCATCATTCGGTCCTT

AAAAAAAAAAAAAAAAGAAACGTAATCAAACTAGAAGCCTAATCGGTTTTTATCAGGCTG
AAAAAAAAAAAAAAAAGGCAGCCTCAGCACCGACATGTTTTGCGGATGCCAACCTACGCC
AAAAAAAAAAAAAAAAAACAGCGGCAGCGCCACCGGAGACGGAGAGGGTTTGTCGTCGTA
AAAAAAAAAAAAAAAAATGCCGTTCGGTTGTGTTAAAGCTATTATTTCACTCCAAAACTAA

Green and cyan colors indicate the ssDNA anti-connectors.

DNA barrel with 21 nm by 16 nm by 30 nm cuboid cavity for quantum dots decoration

ACGAGAAATGCAATGCTTTAGAACCCTCATAT
TAAAGATTAAAGCTGCGTAATCTTGACAAGAAAGAGGACAATGCCGGA
TACATAAATTCTGGCCTATTTTTGACGCTGCGAGGGCGCT
ATTTTAAACACCAGAATTTTGCGGATAAAGCT
CTGAGTAATCTTCGCGTCCTCACAGTTGAGGATCCCCGGGATTTCAAC
TTAATTACGAAACAAATATTAGTCTACCAG
CCCAAATCCTTATCGCCATTAAAAGTTAATAAAACGACAT
GGAAACAGTGCTTCTGACGACCAGCAATCGTCTAAACAGGTACGCCAG
CCTTAGAAACGCTGAGCGCTCATGGTAATATCGTGAGGCCTAACCGTT
CATAAGGGTAAATTGTAAGAGAATCGATGGCCAGGTTTCTAGCCAGCG
CATCAAGATCATTCAGTGAATAAG
TCGCCTGAAACCGAACCATTAGCTATTTTTGATTACCTGCTTGCTCGT
ACTTTGAACCGGATATTGAAAGGCCGGAGACACGGCGGGCTGCATCAG
TATCAAAATCATAGGTGTTGGGTTGTAGAAGAAACGGCAGCACCGTCG
AGTACAACAGAGGCAACCAGCATCCAACCAGCTTACGGCT
CAGAGGCATTAATTGAGGAAAAAGCTGCTCAT
AAATGCTGTAGTTAATTTTTTCGTGCCGTTCC
AAAATACGTTGAGGACCCTTCCTGAGTAACAA
ATATATTTATGCAAATTCATAACGTGCTGGTCTGGTCAGC
ACAGACAAAACAGAGACTACAGGGAACGTGCTTTCCTCGT
CTCTGTGGTGCTGCGGGTGCCTGTTGTGTAGG
CAGCAGCGGAGGCTTGTAGGTCACTCTGCCAG
AAATAAGATAAATTTATGCTGATTCTCGTCGC
CGGTCGCTAAAGACAGTGTGAGCGTAGCCAGC
CATAATTAAGCCAACGTTAAATTTAGACGCAG
CGACAATGGCTTTCGACAGCTTTCAGCGCCAT
CAGTATAACTAGAAAATACATCGAGCGGCCTT
ATCAGCTTACAACAACACCGTGCAGTTGGTGT
AGTAGGGCTTTTCGAGGTGAGAGACCATGTTT
CAAAAAAACAACTAAATCTTCGCTCAAGGCGA
TGAGAAAGTACCGGGGTCGAATTCAAGAAAGC
GAAAGGAAAGGCTCCACCAGGCAACGGCACCG
GAGGGTGGGTGCCCCCCGTTTTCACGGGCTTA
GACGACGAATAAGAGAGAATAACAGCCACGGG
CATAGTTAGCGTAACGTTTTGCTAACCGGAACACGGCCAGTGCCAAGC
ATCTAAAGGCCACCCTCAGAGCCGCCATCGATAGTAGCAC
TTCAGCTATATCCCATCAAACCAACGCTAACGCTATCTTAGAGTTAAG
ACTACAACAATAGGAACAGGTCAGAAGCGCAGTCACCGTCGAGGGAAG
CAAAGGCTGGCGCAGAGTGTACAGACCAGGCG
TAATCGTACCCTGCGGGTCATTGCAGGCGCTT
AAAAATAAATGCAGAATTATTTATCCCAACCTCAAGAATTCCGAAGCC
GCAAGCCCGCCTGTAGACCACCACCAGAACCGTTGCCTTTAGCGTTTG
TTACGAGCATTAAACCACTTGCGGGAGGTTTTCAATAATATAAGCAGA
GAACCGCCGTACTCAGGTCATACACTTGAGTATATGGTTTGACACCAC
TCGCACTCGATAATCAATGTCAATACCAAGCGCCGCGACCTGCTCCAT
GTAGCAATACTTCTTTGATTAGGGCTGGTAATGGGGTTTT
GTATCACCACCCTCAGAGAATGGAACGATTGGAAATCACCAGCAGCAC
AAGCAAGCCATTCCAAGAACGGGTATGTAGAATATCCTGA
CGCACTCAATAAAAGTATTAAGAGCAGAAACGAGAATGAC

GAGAGGGTGTCAGTGCTGGCTTTTGATTGAGGACCGACTT
GTGCCGTCAGAAGGATCCCCTGCCCCCGAAAGACTTCAAA
GCGGTATGAGCCGGGTTCCCTTACAGAGTCTG
GTTAATGCTAGGATTAGCGAACCATTTGATAA
CGACTGGTAGAACTGGATAAAGGTGGCAACAT
CAGTAAGCGAGGTTTAGCGGATAA
TATAATCACAGAACAATTGCCTGAATATAACTCAGCGTGGGAACGTGC
ATCTTATAAAGAAAAGACGGAATACCCGCGAC
GGTTGAGGCCCATGTACACCCTCA
CATAAACACACTGTTGAAACTAGCGGAGGTGTAAGAATACAAACGTTA
ATAAGAAACTAATATCGAGAATTAACTGAACA
CTCAGAGCCTTTTGTCGCAGTACAA
TACAGAGAATATAAAGGTACAGCGTAGACTTT
AATCCTGAGAAGTTAAATTGCAACATTATTTATGATTAATTAATTTTC
CCATCTTTTCAGCGCATTAGACGGAGAGAGATAACGACAG
TCGTTAACGGCATCAGGCGCAGTGTCTAGCTGACCATCAA
TAGAACCGCAGATTCATTCTGACCTCATACCTTTTTTAAT
CCACACCCGCCGCTCACGTAAGAAATAGCCCTAAAACGAGTACCTTAT
TTCTGACCATAAACACCCGCACAGCATAAAAA
CCCAATAAATTGAGCGCGATTTTT
CAGAGGCTTAATGCCAATTTTTGTATATTTTG
AATCAAGTCCACCCTCTCAAAATCAACAACTTATGTGCTGATTACGCC
TAGTGATGTTAAACGAATGGTTTGTTTTTCAA
TATCGCGTGCTTCAAAGCGGGGTTCAAAGAAACCACCAGATTATCATT
TGCATCAAAAAGATTACAACAGGTGCTGAGACTCATATTC
TAGCCGAAAGCAATAGAGCGTCTTCAGCCATACGCGCCTGTCTGTCCA
ATTATAGTAAAAATCAATCATTAC
GCAAACTCAGAGGAAGTATTTCGGAACGCAAAACCAGCGC
GGAAACCGTATTACGCCGCGAGGCAAGGCTTATCGTAGGA
GCGGATTGACCGATTCTCCGGCGGGATCTTTTCATG
TCAGAGATTAGAGAGTTAGCTCAA
AGACTCCTAGGAAACGGAAGCCTTTACAATTTACCAATCATGAACAAG
CAAAGACAAAAGGAAAAATAAGTTATTCTGAAACATGGCAAAGCGGAT
GAGGTCATGGCTTAGATTGCG
TTAGCAAACGTAGAAAAGATATAGGTTTTAGC
TAATGCTGACCTTTAAAATTATCATCCTCAAG
GCAGAAGATAAAACAGCAAAATCGATTCAACTAATGCCAT
CGCCTGCAAAAATCTAATACAGGCTGGCATCA
TATTCATTTCACAAAAGAAAAGATT
AACCTCAAAGGTGAGGAAAACTAACGGAACAA
CAGCAGCAAATGAACAGTGCCCTCAGAGCGAGAAGCC
CCAAGTTAATATACAGTTTACCAGACGACTAG
GGTCAGTTGTTATCTAGTCAATAAGCGAACGA
TACATCGGGAGGGATTCGCGCATAG
ACTAACAAATATCAAATAGAGATACATAACGC
GGAATTGAGGAAGGGCAAATC
TCAGATGAACCATATCAAAATGTT
ATAATACACAATTCGAAGTACGGTGCTGAATA
ACGTAAAACAGATTGCGTAGGCAAAA
TAGACTTTACAAATTTGAGGA
TAGAACCTCAGATGATTAAACAGT
TTAATTTTATTAAATCCTTTGCCCCTAATAGACATGATAA
GAGTAACAAGGAGCGGTTGCTCCTGACCGGAA

ATCAATATAATCCTGATATACTTCATAAAT
CTGATTATGAACGTTACATTGGATAGCGTCCA
GGCGATCGGCAGGCTGCTCACGTTGTCTTAAAC
GTGGTGCCTAGAACGTATAAACCTAAAACGAAGGAGATTTCCAAACGG
GAAAAGCCTAAATTGTACTAAAACAAACGGGT
TTAAAATTATCCCACGAGCGTAATAACATCACTATTACCGGTAGAATT
TAAGCAAATATTCCAAAAAC
TTAAGTTGGTAAAACGCAGAGCCACCCTTATTAGCGTCAG
AACGGATAACCTCACCGGCGAAACTACCGACAAATTTAGG
TGGCAGCCGCACATCCCCAATCGCCGGCTTAG
TTTCAGAGAAAGGGGGTCAACAGTTTCAGGTACAATAAACCACTCCAA
CAAAAATAATTCTTAACCAATTTCCATTACTCATCT
ACGACGTTGGTAACGCAATTTTCTGAATAATA
CAGAGGGGAGGCTTTTATTTTCAGCCTTT
CATAAATCCAGAAGCAAGCAAATCATACATACCATGATTA
TCCCCCTCGAATCGTCTGAATAATTTGC
ATACTGCGAAATGCTTGGCAATTCCGCGCCCATCGAGAACGAACCTCC
GCTTAATTGTCTGGAAGTTTCATTGTTGATTCTTTAG
GCGATTTTAAGAACTGAAATCTACATACCGAACGAACGATATTTAACA
TTGCCGCCCGGTTGTGAGCCTGTTAAGGCGTT
ACTATCATATTACGAGCTGATTGCCGAAT
AAGATCGCGACGACGAATACCGATTAAAGGCC
AAACCAAAATAGCGAGGTAATAGTAAAATTATGGAAGGGT
TCGCCATTTGCGGGCCGGAATTGCGTATGGGA
CTCCGTGGGCTCTCACGAATCGCCATTCTTAC
CAAAAGGAAACCCTCGTAACAGTAGTTTAACG
TAACATCCTGTACCAACGGTCAGTAAATTGGGAACGTAACCAAAAGGG
ACCAGTCCGTGGAGCCTAAAAACAGGGAATAAAGAGCCACAACGCCCT
TGAAAAGGAAGGCAAAGAATTAGCAATAAAGCACGCTG
CATTATTAAATACCACCGCAGAGGTTTGAATA
CCAATTCTCCTGTTTAGCTATATTGCGCGAGCAACAG
TATGACCCTTGTGAATATGGTTTATACCGAGCGTTTCTGC
GATTTAGGCAGGTAGAGATCACCA
GGGAAGAAGCTCATTATTTAATGCCGGGCGCTCGTAACCA
AGAGGGTATAAGAGCAAGACGTACCTGGAGTTCAT
AACGTCACGCGTTTTCATCCGTACCTGGAGTTCAT
AATGAAATCAAAGTTACCACGTACCTGGAGTTCAT
ATCAATAGTGACGGAAATTCGTACCTGGAGTTCAT
ACTGTAGCCAATGAAACCGCCAGCATTGACGTACCTGGAGTTCAT
CATTACCAGTGAATTATCTCTGAATTTACCGTACCTGGAGTTCAT
GTAAATATAAAATTCAACAGTGCCCGTATCGTACCTGGAGTTCAT
CATTAAAGTTAGCAAGGCCCGTACCTGGAGTTCAT
TTTCGGTCATAGCCCCACCGGAACCGCCGTACCTGGAGTTCAT
CCCTGAACGCAGCCTTTGTTTAACGTCAAAAACGTACCTGGAGTTCAT
AAAATAAATCCAGAGCCTAATTTGCGTACCTGGAGTTCAT
CACCCAGCAAATCAAGATTAGTTGCGTACCTGGAGTTCAT
ACGCAAATACCGAGTAAAAGAGTCTTTTTTTTTTTTTTT
AGGAACGGAGGCCGATTAAAGGGATTTTTTTTTTTTTTT
ATTGCCTGACTGGTGTGTTCATTTTTTTTTTTTTTT
CCCCGGTTAATCCGCCGGGCGTTTTTTTTTTTTTTT
GCACGTATCGCGTACTATGGTTGCTTTTTTTTTTTTTTT
TCAACCGTTCACTGCGCGCCTTTTTTTTTTTTTTT
AGAATGCCACTCAAACTATTTTTTTTTTTTTTT

TCCTTGAATTGACGCTTAATAAAAGGGTTTTTTTTTTTTTTT
CTGAGAGACCTTGCTGGAAATACCTACTTTTTTTTTTTTTTT
AAATCAGCTCATTTTGCGTCTGGTAAAGACTGTCACCCTTAACATTCCTAACTTCTCATA
CAGAATGGTCAAATCATAAATTAGATGAACGCGGTCAATTAACATTCCTAACTTCTCATA
CGGACTTGCGGTCCGTTTCGTAGCAACGGCTATAACATTCCTAACTTCTCATA
AAATCGGTAATAAATCAAGCATCACAATATCTTAACATTCCTAACTTCTCATA
AGCTGGCGGCCGGAAAAAAGGAGCCTTTAAACTAACATTCCTAACTTCTCATA
AAACAGCGCGGAATTTCCACGGAGTGAGAATATAACATTCCTAACTTCTCATA
CTTCTGGTGCATCGTACATCGCCCACGCAAATTAACATTCCTAACTTCTCATA
ATTCTACTCGCAAATGAAATATCTGTCAATAGTAACATTCCTAACTTCTCATA
CCCGTCGGTAATGGGACAGGGAGTAGTTGCGCTAACATTCCTAACTTCTCATA
TTTGAGGGACTCCAGCGGTGAATTAAAATCTCTAACATTCCTAACTTCTCATA
ATACATTTAATAGTAGCCCTCAATCCTTGCTGTAACATTCCTAACTTCTCATA
TTTAATCATGTAATACCGAGTAGTATTAACACTAACATTCCTAACTTCTCATA
GTAGATTTGCAACTAACAACTCGTAAAAGTTTTAACATTCCTAACTTCTCATA
TTTCATCACGCATTAACTACGAAGGCACCTGTTAACATTCCTAACTTCTCATA
GGCAAACGAAAAAAAGCGGTAACCGATATATTTAACATTCCTAACTTCTCATA
AGACGTTTTAAATATAGTTTGACTTAGAGCCTTAGGAGCTAACATTCCTAACTTCTCATA
TGCGCCGTAGAACCCCCAGTCACTAAATCGTCGCTACCATAACATTCCTAACTTCTCATA
TAAAAGAAACCTATTTTAACGGGTGATATAAGTATATACTAACATTCCTAACTTCTCATA
AATCCCGTGATCAAACCTCATTGTATCGGTTTTAACATTCCTAACTTCTCATA
CGGGAGCTGAAATGGAGGAAAAAAAGAGTCAATAGTTCATAACATTCCTAACTTCTCATA
TGCCGGGGAGATCTAGAGCAAACGTCGAAATCGAAACAATAACATTCCTAACTTCTCATA
TTCAACCGATGATACTTAAAGCCAGCCACCACCCTCAATTAACATTCCTAACTTCTCATA
GGGATTTAATCCTCAAGGAGTGTAAGGCCCGGAATAGGTTAACATTCCTAACTTCTCATA
AAAGGAGGCGAACTGTACGTGGCATTTCATTTGAATTTATAACATTCCTAACTTCTCATA
GCCAGCACCTTGATACCACCAGACATTCCACAGACAATGTAACATTCCTAACTTCTCATA
TAGCCCACAGAGCCGTTCACAAACCTATTTTCAGGGATATAACATTCCTAACTTCTCATA
AGATGGGCACATTAAACATCGGAACGAGGATCTAACATTCCTAACTTCTCATA
/5Biosg/TTTGGTAAAGTAATTTTATCAA
/5Biosg/TTTTCTTTCCTTATCGTTTTTA
/5Biosg/TTTCTCAGAACCGCCCGTAACA
/5Biosg/TTTTAGATAAGTCCATAATCGG
/5Biosg/TTTAGTTTCGTCACTCTTTCCA
/5Biosg/TTTCTCAGTACCAGGTACCGCC
/5Biosg/TTTCCCCAGCGATTATCATATG
/5Biosg/TTTGATAGCTTAGATTAAG
/5Biosg/TTTTTAGCCGGAACGAATCAGG
/5Biosg/TTTTGTGAGTGAATAACCT
/5Biosg/TTTGCTGGCTGACCTTTATGAT

Blue color indicates the ssDNA handle for 5 nm gold seeds; purple color indicates the biotinylated ssDNA connector.

DNA barrel with 21 nm by 16 nm by 30 nm cuboid dimensions for Y-shaped trimer DNA composite:

ACGAGAAATGCAATGCTTTAGAACCCTCATAT
TAAAGATTAAAGCTGCGTAATCTTGACAAGAAAGAGGACAATGCCGGA
TACATAAATTCTGGCCTATTTTTGACGCTGCGAGGGCGCT
ATTTTAAACACCAGAATTTTGCGGATAAAGCT
CTGAGTAATCTTCGCGTCCTCACAGTTGAGGATCCCCGGGATTTCAAC
TTAATTACGAAACAAATATTAGTCTACCAG
CCCAAATCCTTATCGCCATTAAAAGTTAATAAAACGACAT
AACATAGCTGTGAGTGAATAACCT
GGAAACAGTGCTTCTGACGACCAGCAATCGTCTAAACAGGTACGCCAG
CCTTAGAAACGCTGAGCGCTCATGGTAATATCGTGAGGCCTAACCGTT
CATAAGGGTAAATTGTAAGAGAATCGATGGCCAGGTTTCTAGCCAGCG
CATCAAGATCATTCAGTGAATAAG
TCGCCTGAAACCGAACCATTAGCTATTTTTGATTACCTGCTTGCTCGT
CTACCTTTGATAGCTTAGATTAAG
ACTTTGAACCGGATATTGAAAGGCCGGAGACACGGCGGGCTGCATCAG
TATCAAAATCATAGGTGTTGGGTTGTAGAAGAAACGGCAGCACCGTCG
AGTACAACAGAGGCAACCAGCATCCAACCAGCTTACGGCT
CAGAGGCATTAATTGAGGAAAAAGCTGCTCAT
AAATGCTGTAGTTAATTTTTTCGTGCCGTTCC
AAAATACGTTGAGGACCCTTCCTGAGTAACAA
ATATATTTATGCAAATTCATAACGTGCTGGTCTGGTCAGC
ACAGACAAAACAGAGACTACAGGGAACGTGCTTTCCTCGT
CTCTGTGGTGCTGCGGGTGCCTGTTGTGTAGG
CAGCAGCGGAGGCTTGTAGGTCACTCTGCCAG
AAATAAGATAAATTTATGCTGATTCTCGTCGC
CGGTCGCTAAAGACAGTGTGAGCGTAGCCAGC
CATAATTAAGCCAACGTTAAATTTAGACGCAG
CGACAATGGCTTTCGACAGCTTTCAGCGCCAT
CAGTATAACTAGAAAATACATCGAGCGGCCTT
ATCAGCTTACAACAACACCGTGCAGTTGGTGT
AGTAGGGCTTTTCGAGGTGAGAGACCATGTTT
CAAAAAAACAACTAAATCTTCGCTCAAGGCGA
TGAGAAAGTACCGGGGTCGAATTCAAGAAAGC
GAAAGGAAAGGCTCCACCAGGCAACGGCACCG
GAGGGTGGGTGCCCCCCGTTTTCACGGGCTTA
GACGACGAATAAGAGAGAATAACAGCCACGGG
CATAGTTAGCGTAACGTTTTGCTAACCGGAACACGGCCAGTGCCAAGC
ATCTAAAGGCCACCCTCAGAGCCGCCATCGATAGTAGCAC
TTCAGCTATATCCCATCAAACCAACGCTAACGCTATCTTAGAGTTAAG
ACTACAACAATAGGAACAGGTCAGAAGCGCAGTCACCGTCGAGGGAAG
CAAAGGCTGGCGCAGAGTGTACAGACCAGGCG
TAATCGTACCCTGCGGGTCATTGCAGGCGCTT
AAAAATAAATGCAGAATTATTTATCCCAACCTCAAGAATTCCGAAGCC
GCAAGCCCGCCTGTAGACCACCACCAGAACCGTTGCCTTTAGCGTTTG
TTACGAGCATTAAACCACTTGCGGGAGGTTTTCAATAATATAAGCAGA
GAACCGCCGTACTCAGGTCATACACTTGAGTATATGGTTTGACACCAC
TCGCACTCGATAATCAATGTCAATACCAAGCGCCGCGACCTGCTCCAT
GTAGCAATACTTCTTTGATTAGGGCTGGTAATGGGGTTTT
GTATCACCACCCTCAGAGAATGGAACGATTGGAAATCACCAGCAGCAC

AAGCAAGCCATTCCAAGAACGGGTATGTAGAATATCCTGA
CGCACTCAATAAAAGTATTAAGAGCAGAAACGAGAATGAC
GAGAGGGTGTCAGTGCTGGCTTTTGATTGAGGACCGACTT
GTGCCGTCAGAAGGATCCCCTGCCCCCGAAAGACTTCAAA
GCGGTATGAGCCGGGTTCCCTTACAGAGTCTG
GTTAATGCTAGGATTAGCGAACCATTTGATAA
CGACTGGTAGAACTGGATAAAGGTGGCAACAT
CAGTAAGCGAGGTTTAGCGGATAA
TATAATCACAGAACAATTGCCTGAATATAACTCAGCGTGGGAACGTGC
ATCTTATAAAGAAAAGACGGAATACCCGCGAC
GGTTGAGGCCCATGTACACCCTCA
CATAAACACACTGTTGAAACTAGCGGAGGTGTAAGAATACAAACGTTA
ATAAGAAACTAATATCGAGAATTAACTGAACA
CTCAGAGCCTTTTGTCGCAGTACAA
TACAGAGAATATAAAGGTACAGCGTAGACTTT
AATCCTGAGAAGTTAAATTGCAACATTATTTATGATTAATTAATTTTC
CCATCTTTTCAGCGCATTAGACGGAGAGAGATAACGACAG
TCGTTAACGGCATCAGGCGCAGTGTCTAGCTGACCATCAA
TAGAACCGCAGATTCATTCTGACCTCATACCTTTTTTAAT
CCACACCCGCCGCTCACGTAAGAAATAGCCCTAAAACGAGTACCTTAT
TTCTGACCATAAACACCCGCACAGCATAAAAA
CCCAATAAATTGAGCGCGATTTTT
CAGAGGCTTAATGCCAATTTTTGTATATTTTG
AATCAAGTCCACCCTCTCAAAATCAACAACTTATGTGCTGATTACGCC
TAGTGATGTTAAACGAATGGTTTGTTTTTCAA
TATCGCGTGCTTCAAAGCGGGGTTCAAAGAAACCACCAGATTATCATT
TGCATCAAAAAGATTACAACAGGTGCTGAGACTCATATTC
TAGCCGAAAGCAATAGAGCGTCTTCAGCCATACGCGCCTGTCTGTCCA
ATTATAGTAAAAATCAATCATTAC
GCAAACTCAGAGGAAGTATTTCGGAACGCAAAACCAGCGC
GCGGATTGACCGATTCTCCGGCGGGATCTTTTCATG
TCAGAGATTAGAGAGTTAGCTCAA
AGACTCCTAGGAAACGGAAGCCTTTACAATTTACCAATCATGAACAAG
CAAAGACAAAAGGAAAAATAAGTTATTCTGAAACATGGCAAAGCGGAT
GAGGTCATGGCTTAGATTGCG
TTAGCAAACGTAGAAAAGATATAGGTTTTAGC
TAATGCTGACCTTTAAAATTATCATCCTCAAG
GCAGAAGATAAAACAGCAAAATCGATTCAACTAATGCCAT
CGCCTGCAAAAATCTAATACAGGCTGGCATCA
TATTCATTTCACAAAAGAAAAGATT
AACCTCAAAGGTGAGGAAAACTAACGGAACAA
CAGCAGCAAATGAACAGTGCCCTCAGAGCGAGAAGCC
CCAAGTTAATATACAGTTTACCAGACGACTAG
GGTCAGTTGTTATCTAGTCAATAAGCGAACGA
TACATCGGGAGGGATTCGCGCATAG
ACTAACAAATATCAAATAGAGATACATAACGC
GGAATTGAGGAAGGGCAAATC
TCAGATGAACCATATCAAAATGTT
ATAATACACAATTCGAAGTACGGTGCTGAATA
ACGTAAAACAGATTGCGTAGGCAAAA
TAGACTTTACAAATTTGAGGA
TAGAACCTCAGATGATTAAACAGT
TTAATTTTATTAAATCCTTTGCCCCTAATAGACATGATAA

GAGTAACAAGGAGCGGTTGCTCCTGACCGGAA
ATCAATATAATCCTGATATACTTCATAAAT
CTGATTATGAACGTTACATTGGATAGCGTCCA
GGCGATCGGCAGGCTGCTCACGTTGTCTTAAAC
GTGGTGCCTAGAACGTATAAACCTAAAACGAAGGAGATTTCCAAACGG
GAAAAGCCTAAATTGTACTAAAACAAACGGGT
TTAAAATTATCCCACGAGCGTAATAACATCACTATTACCGGTAGAATT
TAAGCAAATATTCCAAAAAC
TTAAGTTGGTAAAACGCAGAGCCACCCTTATTAGCGTCAG
AACGGATAACCTCACCGGCGAAACTACCGACAAATTTAGG
TGGCAGCCGCACATCCCCAATCGCCGGCTTAG
TTTCAGAGAAAGGGGGTCAACAGTTTCAGGTACAATAAACCACTCCAA
CAAAAATAATTCTTAACCAATTTCCATTACTCATCT
ACGACGTTGGTAACGCAATTTTCTGAATAATA
CAGAGGGGAGGCTTTTATTTTCAGCCTTT
CATAAATCCAGAAGCAAGCAAATCATACATACCATGATTA
TCCCCCTCGAATCGTCTGAATAATTTGC
ATACTGCGAAATGCTTGGCAATTCCGCGCCCATCGAGAACGAACCTCC
GCTTAATTGTCTGGAAGTTTCATTGTTGATTCTTTAG
GCGATTTTAAGAACTGAAATCTACATACCGAACGAACGATATTTAACA
TTGCCGCCCGGTTGTGAGCCTGTTAAGGCGTT
ACTATCATATTACGAGCTGATTGCCGAAT
AAGATCGCGACGACGAATACCGATTAAAGGCC
AAACCAAAATAGCGAGGTAATAGTAAAATTATGGAAGGGT
TCGCCATTTGCGGGCCGGAATTGCGTATGGGA
CTCCGTGGGCTCTCACGAATCGCCATTCTTAC
CAAAAGGAAACCCTCGTAACAGTAGTTTAACG
TAACATCCTGTACCAACGGTCAGTAAATTGGGAACGTAACCAAAAGGG
ACCAGTCCGTGGAGCCTAAAAACAGGGAATAAAGAGCCACAACGCCCT
TGAAAAGGAAGGCAAAGAATTAGCAATAAAGCACGCTG
CATTATTAAATACCACCGCAGAGGTTTGAATA
CCAATTCTCCTGTTTAGCTATATTGCGCGAGCAACAG
TATGACCCTTGTGAATATGGTTTATACCGAGCGTTTCTGC
GATTTAGGCAGGTAGAGATCACCA
GGGAAGAAGCTCATTATTTAATGCCGGGCGCTCGTAACCA
AACGTCACGCGTTTTCATCCGTACCTGGAGTTCAT
ATCAATAGTGACGGAAATTCGTACCTGGAGTTCAT
AGTACCAGGTACCGCCACCCGTACCTGGAGTTCAT
ACTGTAGCCAATGAAACCGCCAGCATTGACGTACCTGGAGTTCAT
CATTACCAGTGAATTATCTCTGAATTTACCGTACCTGGAGTTCAT
GTAAATATAAAATTCAACAGTGCCCGTATCGTACCTGGAGTTCAT
CATTAAAGTTAGCAAGGCCCGTACCTGGAGTTCAT
TTTCGGTCATAGCCCCACCGGAACCGCCGTACCTGGAGTTCAT
AGAACCGCCCGTAACACTGCGTACCTGGAGTTCAT
CCCTGAACGCAGCCTTTGTTTAACGTCAAAAACGTACCTGGAGTTCAT
AAAATAAATCCAGAGCCTAATTTGCGTACCTGGAGTTCAT
CACCCAGCAAATCAAGATTAGTTGCGTACCTGGAGTTCAT
ATAAGTCCATAATCGGCTGCGTACCTGGAGTTCAT
AAAGTAATTTTATCAACAACGTACCTGGAGTTCAT
TTCCTTATCGTTTTTATTTCGTACCTGGAGTTCAT
TTCGTCACTCTTTCCAGACCGTACCTGGAGTTCAT
ATTGCCTGACTGGTGTGTTCATTTTTTTTTTTTTTT
CCCCGGTTAATCCGCCGGGCGTTTTTTTTTTTTTTT

TCAACCGTTCACTGCGCGCCTTTTTTTTTTTTTTTT
AGAATGCCACTCAAACTATTTTTTTTTTTTTTTT
GCGATTATCATATGTATTTTTTTTTTTTTTTT
GCTGACCTTTATGATATTTTTTTTTTTTTTTT
TCCTTGAATTGACGCTTAATAAAAGGGTTTTTTTTTTTTTTT
CTGAGAGACCTTGCTGGAAATACCTACTTTTTTTTTTTTTTT
CGGAACGAATCAGGTCTTTTTTTTTTTTTTT
AAATCAGCTCATTTTGCGTCTGGTAAAGACTGTCACCCTTAACATTCCTAACTTCTCATA
CAGAATGGTCAAATCATAAATTAGATGAACGCGGTCAATTAACATTCCTAACTTCTCATA
CGGACTTGCGGTCCGTTTCGTAGCAACGGCTATAACATTCCTAACTTCTCATA
AAATCGGTAATAAATCAAGCATCACAATATCTTAACATTCCTAACTTCTCATA
AGCTGGCGGCCGGAAAAAAGGAGCCTTTAAACTAACATTCCTAACTTCTCATA
AAACAGCGCGGAATTTCCACGGAGTGAGAATATAACATTCCTAACTTCTCATA
CTTCTGGTGCATCGTACATCGCCCACGCAAATTAACATTCCTAACTTCTCATA
ATTCTACTCGCAAATGAAATATCTGTCAATAGTAACATTCCTAACTTCTCATA
CCCGTCGGTAATGGGACAGGGAGTAGTTGCGCTAACATTCCTAACTTCTCATA
TTTGAGGGACTCCAGCGGTGAATTAAAATCTCTAACATTCCTAACTTCTCATA
ATACATTTAATAGTAGCCCTCAATCCTTGCTGTAACATTCCTAACTTCTCATA
TTTAATCATGTAATACCGAGTAGTATTAACACTAACATTCCTAACTTCTCATA
GTAGATTTGCAACTAACAACTCGTAAAAGTTTTAACATTCCTAACTTCTCATA
TTTCATCACGCATTAACTACGAAGGCACCTGTTAACATTCCTAACTTCTCATA
GGCAAACGAAAAAAAGCGGTAACCGATATATTTAACATTCCTAACTTCTCATA
AGACGTTTTAAATATAGTTTGACTTAGAGCCTTAGGAGCTAACATTCCTAACTTCTCATA
TGCGCCGTAGAACCCCCAGTCACTAAATCGTCGCTACCATAACATTCCTAACTTCTCATA
TAAAAGAAACCTATTTTAACGGGTGATATAAGTATATACTAACATTCCTAACTTCTCATA
AATCCCGTGATCAAACCTCATTGTATCGGTTTTAACATTCCTAACTTCTCATA
CGGGAGCTGAAATGGAGGAAAAAAAGAGTCAATAGTTCATAACATTCCTAACTTCTCATA
TGCCGGGGAGATCTAGAGCAAACGTCGAAATCGAAACAATAACATTCCTAACTTCTCATA
TTCAACCGATGATACTTAAAGCCAGCCACCACCCTCAATTAACATTCCTAACTTCTCATA
GGGATTTAATCCTCAAGGAGTGTAAGGCCCGGAATAGGTTAACATTCCTAACTTCTCATA
AAAGGAGGCGAACTGTACGTGGCATTTCATTTGAATTTATAACATTCCTAACTTCTCATA
GCCAGCACCTTGATACCACCAGACATTCCACAGACAATGTAACATTCCTAACTTCTCATA
TAGCCCACAGAGCCGTTCACAAACCTATTTTCAGGGATATAACATTCCTAACTTCTCATA
AGATGGGCACATTAAACATCGGAACGAGGATCTAACATTCCTAACTTCTCATA
GCACGTATCGCGTACTATGGTTGCACACCACAAAAAAACC (monomer 1)
AGGAACGGAGGCCGATTAAAGGGAATCTAAACCACCAACT (monomer 1)
ACGCAAATACCGAGTAAAAGAGTCCTCTTTCCCTTTTAAC (monomer 1)
AAGTAGTAAAGAGAGAGAAGGAAACCGTATTACGCCGCGAGGCAAGGCTTATCGTAGGA (monomer 1)
TTTGTTGTGGTTGAGTAACAATGAAATCAAAGTTA (monomer 1)
GGTAGAGTGATGAAAAGTCAGAGGGTATAAGAGCA (monomer 1)

GCACGTATCGCGTACTATGGTTGCCAACTAAAAACTCACA (monomer 2)
AGGAACGGAGGCCGATTAAAGGGAATCCAAACTTCACCTC (monomer 2)
ACGCAAATACCGAGTAAAAGAGTCTTTTTCCTTACACTCA (monomer 2)
GGTTTTTTTGTGGTGTGAAGGAAACCGTATTACGCCGCGAGGCAAGGCTTATCGT AGGA (monomer 2)
AGTTGGTGGTTTAGATAACAATGAAATCAAAGTTA (monomer 2)
GTTAAAAGGGAAAGAGGTCAGAGGGTATAAGAGCA (monomer 2)
GCACGTATCGCGTACTATGGTTGCTCTCTCTTTACTACTT (monomer 3)
AGGAACGGAGGCCGATTAAAGGGAACTCAACCACAACAAA (monomer 3)
ACGCAAATACCGAGTAAAAGAGTCTTTTCATCACTCTACC (monomer 3)
TGTGAGTTTTTAGTTGGAAGGAAACCGTATTACGCCGCGAGGCAAGGCTTATCGT AGGA (monomer 3)
GAGGTGAAGTTTGGATAACAATGAAATCAAAGTTA (monomer 3)
TGAGTGTAAGGAAAAAGTCAGAGGGTATAAGAGCA (monomer 3)

Blue color indicates the ssDNA handle for 5 nm gold seeds; red and purple colors indicate the ssDNA connectors and anti-connectors at each monomer.

References and Notes

1. P. P. Pompa, L. Martiradonna, A. D. Torre, F. D. Sala, L. Manna, M. De Vittorio, F. Calabi, R. Cingolani, R. Rinaldi, Metal-enhanced fluorescence of colloidal nanocrystals with nanoscale control. *Nat. Nanotechnol.* **1**, 126–130 (2006). Medline doi:10.1038/nnano.2006.93

2. F. Wang, C. Li, H. Chen, R. Jiang, L. D. Sun, Q. Li, J. Wang, J. C. Yu, C. H. Yan, Plasmonic harvesting of light energy for Suzuki coupling reactions. *J. Am. Chem. Soc.* **135**, 5588–5601 (2013). Medline doi:10.1021/ja310501y

3. A. V. Kildishev, A. Boltasseva, V. M. Shalaev, Planar photonics with metasurfaces. *Science* **339**, 1232009 (2013). Medline doi:10.1126/science.1232009

4. A. L. Koh, A. I. Fernández-Domínguez, D. W. McComb, S. A. Maier, J. K. W. Yang, High-resolution mapping of electron-beam-excited plasmon modes in lithographically defined gold nanostructures. *Nano Lett.* **11**, 1323–1330 (2011). Medline doi:10.1021/nl104410t

5. Y. Sun, Y. Xia, Shape-controlled synthesis of gold and silver nanoparticles. *Science* **298**, 2176–2179 (2002). Medline doi:10.1126/science.1077229

6. Y. Xia, Y. Xiong, B. Lim, S. E. Skrabalak, Shape-controlled synthesis of metal nanocrystals: Simple chemistry meets complex physics? *Angew. Chem. Int. Ed.* **48**, 60–103 (2009). Medline doi:10.1002/anie.200802248

7. T. Ming, W. Feng, Q. Tang, F. Wang, L. Sun, J. Wang, C. Yan, Growth of tetrahexahedral gold nanocrystals with high-index facets. *J. Am. Chem. Soc.* **131**, 16350–16351 (2009). Medline doi:10.1021/ja907549n

8. N. Ma, E. H. Sargent, S. O. Kelley, One-step DNA-programmed growth of luminescent and biofunctionalized nanocrystals. *Nat. Nanotechnol.* **4**, 121–125 (2009). Medline doi:10.1038/nnano.2008.373

9. S. E. Lohse, C. J. Murphy, Applications of colloidal inorganic nanoparticles: From medicine to energy. *J. Am. Chem. Soc.* **134**, 15607–15620 (2012). Medline doi:10.1021/ja307589n

10. Z. Wang, L. Tang, L. H. Tan, J. Li, Y. Lu, Discovery of the DNA “genetic code” for abiological gold nanoparticle morphologies. *Angew. Chem. Int. Ed.* **51**, 9078–9082 (2012). Medline doi:10.1002/anie.201203716

11. L. Ruan, H. Ramezani-Dakhel, C. Y. Chiu, E. Zhu, Y. Li, H. Heinz, Y. Huang, Tailoring molecular specificity toward a crystal facet: A lesson from biorecognition toward Pt111. *Nano Lett.* **13**, 840–846 (2013). Medline doi:10.1021/nl400022g

12. A. Puzder, A. J. Williamson, N. Zaitseva, G. Galli, L. Manna, A. P. Alivisatos, The effect of organic ligand binding on the growth of CdSe nanoparticles probed by ab initio calculations. *Nano Lett.* **4**, 2361–2365 (2004). doi:10.1021/nl0485861

13. J. Yu, M. L. Becker, G. A. Carri, A molecular dynamics simulation of the stability-limited growth mechanism of peptide-mediated gold-nanoparticle synthesis. *Small* **6**, 2242–2245 (2010). Medline doi:10.1002/smll.201000889

14. C. R. Bealing, W. J. Baumgardner, J. J. Choi, T. Hanrath, R. G. Hennig, Predicting nanocrystal shape through consideration of surface-ligand interactions. *ACS Nano* **6**, 2118–2127 (2012). Medline doi:10.1021/nn3000466

15. N. C. Seeman, DNA in a material world. *Nature* **421**, 427–431 (2003). Medline doi:10.1038/nature01406

16. J. H. Chen, N. C. Seeman, Synthesis from DNA of a molecule with the connectivity of a cube. *Nature* **350**, 631–633 (1991). Medline doi:10.1038/350631a0

17. E. Winfree, F. Liu, L. A. Wenzler, N. C. Seeman, Design and self-assembly of two-dimensional DNA crystals. *Nature* **394**, 539–544 (1998). Medline doi:10.1038/28998

18. W. M. Shih, J. D. Quispe, G. F. Joyce, A 1.7-kilobase single-stranded DNA that folds into a nanoscale octahedron. *Nature* **427**, 618–621 (2004). Medline doi:10.1038/nature02307

19. P. W. K. Rothemund, Folding DNA to create nanoscale shapes and patterns. *Nature* **440**, 297–302 (2006). Medline doi:10.1038/nature04586

20. P. Yin, R. F. Hariadi, S. Sahu, H. M. Choi, S. H. Park, T. H. Labean, J. H. Reif, Programming DNA tube circumferences. *Science* **321**, 824–826 (2008). Medline doi:10.1126/science.1157312

21. Y. He, T. Ye, M. Su, C. Zhang, A. E. Ribbe, W. Jiang, C. Mao, Hierarchical self-assembly of DNA into symmetric supramolecular polyhedra. *Nature* **452**, 198–201 (2008). Medline doi:10.1038/nature06597

22. S. M. Douglas, H. Dietz, T. Liedl, B. Högberg, F. Graf, W. M. Shih, Self-assembly of DNA into nanoscale three-dimensional shapes. *Nature* **459**, 414–418 (2009). Medline doi:10.1038/nature08016

23. H. Dietz, S. M. Douglas, W. M. Shih, Folding DNA into twisted and curved nanoscale shapes. *Science* **325**, 725–730 (2009). Medline doi:10.1126/science.1174251

24. D. Han, S. Pal, J. Nangreave, Z. Deng, Y. Liu, H. Yan, DNA origami with complex curvatures in three-dimensional space. *Science* **332**, 342–346 (2011). Medline doi:10.1126/science.1202998

25. B. Wei, M. Dai, P. Yin, Complex shapes self-assembled from single-stranded DNA tiles. *Nature* **485**, 623–626 (2012). Medline doi:10.1038/nature11075

26. Y. Ke, L. L. Ong, W. M. Shih, P. Yin, Three-dimensional structures self-assembled from DNA bricks. *Science* **338**, 1177–1183 (2012). Medline doi:10.1126/science.1227268

27. D. Han, S. Pal, Y. Yang, S. Jiang, J. Nangreave, Y. Liu, H. Yan, DNA gridiron nanostructures based on four-arm junctions. *Science* **339**, 1412–1415 (2013). Medline doi:10.1126/science.1232252

28. R. Iinuma, Y. Ke, R. Jungmann, T. Schlichthaerle, J. B. Woehrstein, P. Yin, Polyhedra self-assembled from DNA tripods and characterized with 3D DNA-PAINT. *Science* **344**, 65–69 (2014). Medline doi:10.1126/science.1250944

29. See supplementary materials on *Science* Online.

30. S. M. Douglas, A. H. Marblestone, S. Teerapittayanon, A. Vazquez, G. M. Church, W. M. Shih, Rapid prototyping of three-dimensional DNA-origami shapes with caDNAno. *Nucleic Acids Res.* **37**, 5001–5006 (2009). Medline doi:10.1093/nar/gkp436

31. C. E. Castro, F. Kilchherr, D. N. Kim, E. L. Shiao, T. Wauer, P. Wortmann, M. Bathe, H. Dietz, A primer to scaffolded DNA origami. *Nat. Methods* **8**, 221–229 (2011). Medline doi:10.1038/nmeth.1570

32. D. N. Kim, F. Kilchherr, H. Dietz, M. Bathe, Quantitative prediction of 3D solution shape and flexibility of nucleic acid nanostructures. *Nucleic Acids Res.* **40**, 2862–2868 (2012). Medline doi:10.1093/nar/gkr1173

33. Y. Ke, S. M. Douglas, M. Liu, J. Sharma, A. Cheng, A. Leung, Y. Liu, W. M. Shih, H. Yan, Multilayer DNA origami packed on a square lattice. *J. Am. Chem. Soc.* **131**, 15903–15908 (2009). Medline doi:10.1021/ja906381y

34. J. P. Michel, I. L. Ivanovska, M. M. Gibbons, W. S. Klug, C. M. Knobler, G. J. Wuite, C. F. Schmidt, Nanoindentation studies of full and empty viral capsids and the effects of capsid protein mutations on elasticity and strength. *Proc. Natl. Acad. Sci. U.S.A.* **103**, 6184–6189 (2006). Medline doi:10.1073/pnas.0601744103

35. M. B. Dickerson, K. H. Sandhage, R. R. Naik, Protein- and peptide-directed syntheses of inorganic materials. *Chem. Rev.* **108**, 4935–4978 (2008). Medline doi:10.1021/cr8002328

36. Z. Zhao, E. L. Jacovetty, Y. Liu, H. Yan, Encapsulation of gold nanoparticles in a DNA origami cage. *Angew. Chem. Int. Ed.* **50**, 2041–2044 (2011). Medline doi:10.1002/anie.201006818

37. D. Zanchet, C. M. Micheel, W. J. Parak, D. Gerion, A. P. Alivisatos, Electrophoretic isolation of discrete Au nanocrystal/DNA conjugates. *Nano Lett.* **1**, 32–35 (2001). doi:10.1021/nl005508e

38. F. R. Fan, D. Y. Liu, Y. F. Wu, S. Duan, Z. X. Xie, Z. Y. Jiang, Z. Q. Tian, Epitaxial growth of heterogeneous metal nanocrystals: From gold nano-octahedra to palladium and silver nanocubes. *J. Am. Chem. Soc.* **130**, 6949–6951 (2008). Medline doi:10.1021/ja801566d

39. F. Wang, C. Li, L. D. Sun, H. Wu, T. Ming, J. Wang, J. C. Yu, C. H. Yan, Heteroepitaxial growth of high-index-faceted palladium nanoshells and their catalytic performance. *J. Am. Chem. Soc.* **133**, 1106–1111 (2011). Medline doi:10.1021/ja1095733

40. R. Ghosh Chaudhuri, S. Paria, Core/shell nanoparticles: Classes, properties, synthesis mechanisms, characterization, and applications. *Chem. Rev.* **112**, 2373–2433 (2012). Medline doi:10.1021/cr100449n

41. G. Maurin-Pasturel, J. Long, Y. Guari, F. Godiard, M. G. Willinger, C. Guerin, J. Larionova, Nanosized heterostructures of Au@Prussian blue analogues: Towards multifunctionality

at the nanoscale. *Angew. Chem. Int. Ed.* **53**, 3872–3876 (2014). Medline doi:10.1002/anie.201310443

42. J. A. Scholl, A. L. Koh, J. A. Dionne, Quantum plasmon resonances of individual metallic nanoparticles. *Nature* **483**, 421–427 (2012). Medline doi:10.1038/nature10904

43. J. Nelayah, M. Kociak, O. Stéphan, F. J. García de Abajo, M. Tencé, L. Henrard, D. Taverna, I. Pastoriza-Santos, L. M. Liz-Marzán, C. Colliex, Mapping surface plasmons on a single metallic nanoparticle. *Nat. Phys.* **3**, 348–353 (2007). doi:10.1038/nphys575

44. V. Myroshnychenko, J. Nelayah, G. Adamo, N. Geuquet, J. Rodríguez-Fernández, I. Pastoriza-Santos, K. F. MacDonald, L. Henrard, L. M. Liz-Marzán, N. I. Zheludev, M. Kociak, F. J. García de Abajo, Plasmon spectroscopy and imaging of individual gold nanodecahedra: A combined optical microscopy, cathodoluminescence, and electron energy-loss spectroscopy study. *Nano Lett.* **12**, 4172–4180 (2012). Medline doi:10.1021/nl301742h

45. L. Berti, G. A. Burley, Nucleic acid and nucleotide-mediated synthesis of inorganic nanoparticles. *Nat. Nanotechnol.* **3**, 81–87 (2008). Medline doi:10.1038/nnano.2007.460

46. S. J. Tan, M. J. Campolongo, D. Luo, W. Cheng, Building plasmonic nanostructures with DNA. *Nat. Nanotechnol.* **6**, 268–276 (2011). Medline doi:10.1038/nnano.2011.49

47. C. Gao, Q. Zhang, Z. Lu, Y. Yin, Templated synthesis of metal nanorods in silica nanotubes. *J. Am. Chem. Soc.* **133**, 19706–19709 (2011). Medline doi:10.1021/ja209647d

48. E. Braun, Y. Eichen, U. Sivan, G. Ben-Yoseph, DNA-templated assembly and electrode attachment of a conducting silver wire. *Nature* **391**, 775–778 (1998). Medline doi:10.1038/35826

49. H. Yan, S. H. Park, G. Finkelstein, J. H. Reif, T. H. LaBean, DNA-templated self-assembly of protein arrays and highly conductive nanowires. *Science* **301**, 1882–1884 (2003). Medline doi:10.1126/science.1089389

50. J. Liu, Y. Geng, E. Pound, S. Gyawali, J. R. Ashton, J. Hickey, A. T. Woolley, J. N. Harb, Metallization of branched DNA origami for nanoelectronic circuit fabrication. *ACS Nano* **5**, 2240–2247 (2011). Medline doi:10.1021/nn1035075

51. R. Schreiber, S. Kempter, S. Holler, V. Schüller, D. Schiffels, S. S. Simmel, P. C. Nickels, T. Liedl, DNA origami-templated growth of arbitrarily shaped metal nanoparticles. *Small* **7**, 1795–1799 (2011). Medline doi:10.1002/smll.201100465

52. Z. Jin, W. Sun, Y. Ke, C. J. Shih, G. L. Paulus, Q. Hua Wang, B. Mu, P. Yin, M. S. Strano, Metallized DNA nanolithography for encoding and transferring spatial information for graphene patterning. *Nat. Commun.* **4**, 1663 (2013). Medline doi:10.1038/ncomms2690

53. M. Pilo-Pais, S. Goldberg, E. Samano, T. H. Labean, G. Finkelstein, Connecting the nanodots: Programmable nanofabrication of fused metal shapes on DNA templates. *Nano Lett.* **11**, 3489–3492 (2011). Medline doi:10.1021/nl202066c

54. A. Kuzyk, R. Schreiber, Z. Fan, G. Pardatscher, E. M. Roller, A. Högele, F. C. Simmel, A. O. Govorov, T. Liedl, DNA-based self-assembly of chiral plasmonic nanostructures with tailored optical response. *Nature* **483**, 311–314 (2012). Medline doi:10.1038/nature10889

55. E. C. Samano, M. Pilo-Pais, S. Goldberg, B. N. Vogen, G. Finkelstein, T. H. LaBean, Self-assembling DNA templates for programmed artificial biomineralization. *Soft Matter* **7**, 3240–3245 (2011). doi:10.1039/c0sm01318h

56. M. Fischler, U. Simon, H. Nir, Y. Eichen, G. A. Burley, J. Gierlich, P. M. Gramlich, T. Carell, Formation of bimetallic Ag-Au nanowires by metallization of artificial DNA duplexes. *Small* **3**, 1049–1055 (2007). Medline doi:10.1002/smll.200600534

57. H. Zhang, J. Chao, D. Pan, H. Liu, Q. Huang, C. Fan, Folding super-sized DNA origami with scaffold strands from long-range PCR. *Chem. Commun.* **48**, 6405–6407 (2012). Medline doi:10.1039/c2cc32204h

58. S. Woo, P. W. K. Rothemund, Programmable molecular recognition based on the geometry of DNA nanostructures. *Nat. Chem.* **3**, 620–627 (2011). Medline doi:10.1038/nchem.1070

59. M. Sarikaya, C. Tamerler, A. K. Y. Jen, K. Schulten, F. Baneyx, Molecular biomimetics: Nanotechnology through biology. *Nat. Mater.* **2**, 577–585 (2003). Medline doi:10.1038/nmat964

60. J.-P. J. Sobczak, T. G. Martin, T. Gerling, H. Dietz, Rapid folding of DNA into nanoscale shapes at constant temperature. *Science* **338**, 1458–1461 (2012). Medline doi:10.1126/science.1229919

61. S. P. Surwade, F. Zhou, B. Wei, W. Sun, A. Powell, C. O'Donnell, P. Yin, H. Liu, Nanoscale growth and patterning of inorganic oxides using DNA nanostructure templates. *J. Am. Chem. Soc.* **135**, 6778–6781 (2013). Medline doi:10.1021/ja401785h

62. M. Bathe, A finite element framework for computation of protein normal modes and mechanical response. *Proteins* **70**, 1595–1609 (2008). Medline doi:10.1002/prot.21708

63. B. Brooks, D. Janežič, M. Karplus, Harmonic analysis of large systems. I. methodology. *J. Comput. Chem.* **16**, 1522–1542 (1995). doi:10.1002/jcc.540161209

64. J. Sharma, R. Chhabra, C. S. Andersen, K. V. Gothelf, H. Yan, Y. Liu, Toward reliable gold nanoparticle patterning on self-assembled DNA nanoscaffold. *J. Am. Chem. Soc.* **130**, 7820–7821 (2008). Medline doi:10.1021/ja802853r

65. U. Hohenester, A. Trügler, MNPBEM a matlab toolbox for the simulation of plasmonic nanoparticles. *Comput. Phys. Commun.* **183**, 370–381 (2012). doi:10.1016/j.cpc.2011.09.009

66. U. Hohenester, Simulating electron energy loss spectroscopy with the MNPBEM toolbox. *Comput. Phys. Commun.* **185**, 1177–1187 (2014). doi:10.1016/j.cpc.2013.12.010

67. E. Boulais, R. Lachaine, M. Meunier, Plasma mediated off-resonance plasmonic enhanced ultrafast laser-induced nanocavitation. *Nano Lett.* **12**, 4763–4769 (2012). Medline doi:10.1021/nl302200w

68. E. Boulais, R. Lachaine, M. Meunier, Plasma-mediated nanocavitation and photothermal effects in ultrafast laser irradiation of gold nanorods in water. *J. Phys. Chem. C* **117**, 9386–9396 (2013). doi:10.1021/jp312475h

69. C. Desgranges, J. Delhommelle, Molecular dynamics simulation of the nucleation and growth of gold nanoparticles. *J. Phys. Chem. C* **113**, 3607–3611 (2009). doi:10.1021/jp8101546

70. M. Mariscal, J. Velázquez-Salazar, M. Yacaman, Growth mechanism of nanoparticles: Theoretical calculations and experimental results. *CrystEngComm* **14**, 544–549 (2012). doi:10.1039/c1ce05602f

71. L. Chuntonov, G. Haran, Maximal Raman optical activity in hybrid single molecule-plasmonic nanostructures with multiple dipolar resonances. *Nano Lett.* **13**, 1285–1290 (2013). Medline doi:10.1021/nl400046z

72. H. Liang, D. Rossouw, H. Zhao, S. K. Cushing, H. Shi, A. Korinek, H. Xu, F. Rosei, W. Wang, N. Wu, G. A. Botton, D. Ma, Asymmetric silver “nanocarrot” structures: Solution synthesis and their asymmetric plasmonic resonances. *J. Am. Chem. Soc.* **135**, 9616–9619 (2013). Medline doi:10.1021/ja404345s

73. O. D. Miller, C. W. Hsu, M. T. Reid, W. Qiu, B. G. DeLacy, J. D. Joannopoulos, M. Soljačić, S. G. Johnson, Fundamental limits to extinction by metallic nanoparticles. *Phys. Rev. Lett.* **112**, 123903 (2014). Medline doi:10.1103/PhysRevLett.112.123903

74. V. V. Thacker, L. O. Herrmann, D. O. Sigle, T. Zhang, T. Liedl, J. J. Baumberg, U. F. Keyser, DNA origami based assembly of gold nanoparticle dimers for surface-enhanced Raman scattering. *Nat. Commun.* **5**, 3448 (2014). Medline doi:10.1038/ncomms4448

75. E. D. Palik, *Handbook of Optical Constants of Solids III* (Academic Press, New York, 1998).

76. G. Mie, Beiträge zur Optik trüber Medien, speziell kolloidaler Metallösungen. *Ann. Physik* **330**, 377–445 (1908). doi:10.1002/andp.19083300302

77. M. A. Yurkin, A. G. Hoekstra, The discrete dipole approximation: An overview and recent developments. *J. Quant. Spectrosc. Radiat.Transf.* **106**, 558–589 (2007).

78. J. D. Jackson, *Classical Electrodynamics* (Wiley, New York, ed. 3, 1999).

79. P. B. Johnson, R. W. Christy, Optical constants of the noble metals. *Phys. Rev. B* **6**, 4370–4379 (1972). doi:10.1103/PhysRevB.6.4370

80. M. I. Stockman, Nanoplasmonics: Past, present, and glimpse into future. *Opt. Express* **19**, 22029–22106 (2011). Medline doi:10.1364/OE.19.022029

81. B. J. Wiley, S. H. Im, Z. Y. Li, J. McLellan, A. Siekkinen, Y. Xia, Maneuvering the surface plasmon resonance of silver nanostructures through shape-controlled synthesis. *J. Phys. Chem. B* **110**, 15666–15675 (2006). Medline doi:10.1021/jp0608628

82. D. K. Lim, K. S. Jeon, J. H. Hwang, H. Kim, S. Kwon, Y. D. Suh, J. M. Nam, Highly uniform and reproducible surface-enhanced Raman scattering from DNA-tailorable nanoparticles with 1-nm interior gap. *Nat. Nanotechnol.* **6**, 452–460 (2011). Medline doi:10.1038/nnano.2011.79

83. J. H. Lee, G. H. Kim, J. M. Nam, Directional synthesis and assembly of bimetallic nanosnowmen with DNA. *J. Am. Chem. Soc.* **134**, 5456–5459 (2012). Medline doi:10.1021/ja2121525

84. G. M. Church, Y. Gao, S. Kosuri, Next-generation digital information storage in DNA. *Science* **337**, 1628–1628 (2012). Medline doi:10.1126/science.1226355